CHAPTER 2

EXPERIMENTAL, RESULTS AND DISCUSSION

2.1 Instruments, Apparatus and Chemicals

2.1.1 Instruments and Apparatus

1. Peristaltic pump : four-channels (MC-MS/CA4/6) ; Ismatec, Switzerland.
2. Aquarium air pump [5] : Nissel, Japan.
3. Rotary injection valve : home-made low cost with two injection loops [5].
4. Rotary injection valve : Ismatec, Switzerland.
5. Three way valve : for medical purposes (shown in Appendix A); Connecta®, Sweden.
6. Colorimeter : (green LED) Ismatec Ltd., Switzerland.
7. UV-VIS Spectrophotometer : UV-265, Shimadzu, Japan.
8. Spectrofluorometric detector : Jasco, Model 821-FP, Japan.
9. F-2000 Fluorescence spectrophotometer : HITACHI, Japan.
10. Chart recorder : Mckee-Pedersen Instruments Danville, Calif., MPI 1027B, U.S.A.
11. Flow through cell (1 cm) : Hellma, Germany.
12. Glass bead column (GBC), as previously described [68].
13. Cadmium reduction column : (shown in Appendix B).
14. C18 SPE column (shown in Appendix C) : packed with LiChrolut®RP-18, E.Merck, Germany.
15. Three way connection (shown in Appendix D).

2.1.2 Chemicals

Most of them are analytical reagent grade (except that specified) and used without further purification. The chemicals are listed as follows.

1. Polyvinylalcohol : [-C_2H_4O-], (M.W.≈ 14,000) ; BDH, England.
2. Rhodamine B : [$C_{28}H_{31}ClN_2O_3$] ; Sigma, U.S.A.
3. Potassium dihydrogen phosphate : [KH_2PO_4] ; Univar, Australia.
4. Ammonium heptamolybdate : [$(NH_4)_6Mo_7O_{24}.4H_2O$] ; Sigma, U.S.A.
5. Kaolin : [SiO_2~46 %, Al_2O_3~39 %], (particle size = 0.1-4 μm) ; Fluka, Switzerland.
6. Adenosine 5'-triphophate, disodium salt hydrate : (M.W. = 551.15) ; Sigma, U.S.A.
7. Phytic acid, dodecasodium salt hydrate : (M.W. = 857.88) ; Aldrich, U.S.A.
8. Sodium tripolyphophate hexahydrate : [$Na_5P_3O_{10}.6H_2O$] ; Sigma, U.S.A.
9. Sodium pyrophosphate decahydrate : [$Na_4P_2O_7.10H_2O$] ; Sigma, U.S.A.
10. Sulfuric acid : [H_2SO_4] ; E.Merck, Germany.
11. Sulfanilamide : [$C_6H_8N_2O_2S$] ; Fluka, Switzerland.
12. N-(1-naphthyl)-ethylenediamine dihydrochloride(NED) : [$C_{12}H_{14}N_2.2HCl.CH_3OH$] ; Fluka, Switzerland.

13. Phosphoric acid : [H_3PO_4] ; Carlo Erba, Italy.
14. Sodium nitrite : [$NaNO_2$] ; E.Merck, Germany.
15. Potassium nitrate : [KNO_3] ; E.Merck, Germany.
16. Ammonium chloride : [NH_4Cl] ; Fluka, Switzerland.
17. Sodium hydroxide : [NaOH] ; E.Merck, Germany.
18. Copper sulfate : [$CuSO_4$] ; Fluka, Switzerland.
19. Hydrochloric acid : [HCl] ; E.Merck, Germany.
20. Acetone : [C_3H_6O] ; Baker , U.S.A.
21. Disodium ethylenediaminetetraacetic acid dihydrate : [$C_{10}H_{14}N_2O_8Na_2.2H_2O$] ; E.Merck, Germany.
22. Chromium chloride : [$CrCl_3$] ; E.Merck, Germany.
23. Potassium dichromate : [$K_2Cr_2O_7$] ; M&B, England.
24. 1,5-Diphenylcarbazide : [$C_{13}H_{14}N_4O$] ; E.Merck, Germany.
25. Ceric(IV) ammonium sulfate : [$Ce(NH_4)_4(SO_4)_4$] ; Fluka, Switzerland.
26. Nitric acid : [HNO_3] ; E.Merck, Germany.
27. Methanol : [CH_3OH] ; Baker , U.S.A.
28. LiChrolut®RP-18 :E.Merck, Germany.
29. Murexide : [$C_8H_8N_6O_6$] ; Fluka, Switzerland,
30. Ethylenediamine : [$NH_2CH_2CH_2NH_2$] ; Fluka, Switzerland.
31. Calmagite : [$C_{17}H_{14}N_2O_5S$] ; BDH, England.
32. Boric acid : [H_3BO_3] ; Fluka, Switzerland.
33. Magnesium chloride hexahydrate : [$MgCl_2.6H_2O$] ; E.Merck, Germany.
34. Ethylenediaminetetracetic acid : [$C_{10}H_{16}N_2O_8$] ; Fluka, Switzerland.
35. Calcium carbonate : [$CaCO_3$] ; Fluka, Switzerland.
36. Cadmium coarse granules : (particle size = 0.3-1.5 mm) ; E.Merck, Germany.

2.2 Solutions

Deionized water was used for all solutions.

1. Phosphate Standard Solutions

100 ml of stock phosphate solution (1000 mg PO_4^{3-}/l) was prepared by dissolving 0.1433 g of dried (at 110 °C ,1.5 h.) KH_2PO_4 in deionized water. The stock solution was kept in a refrigerator for preservation.

Working standard solutions were freshly prepared by diluting the stock solution.

2. Nitrite Standard Solutions

100 ml of stock nitrite solution (1000 mg NO_2^-/l) was prepared by dissolving 0.150 g of dried (at 110 °C ,1.5 h.) $NaNO_2$ in deionized water. This solution should be prepared weekly and kept in a refrigerator for preservation.

Working standard solutions were freshly prepared by diluting the stock solution.

3. Nitrate Standard Solutions

100 ml of stock nitrate solution (1000 mg NO_3^-/l) was prepared by dissolving 0.163 g of dried (at 110 °C ,1.5 h.) KNO_3 in deionized water. This solution was stable for at least one month and kept in a refrigerator for preservation.

Working standard solutions were freshly prepared by diluting the stock solution.

4. Chromium(III) Standard Solutions

100 ml of stock chromium(III) solution (1000 mg Cr^{3+}/l) was prepared by dissolving 0.3048 g of dried (at 110 °C ,1.5 h.) $CrCl_3$ in deionized water.

Working standard solutions were freshly prepared by diluting the stock solution with 0.025 M H_2SO_4.

5. Chromium(VI) Standard Solutions

100 ml of stock chromium(VI) solution (1000 mg Cr^{6+}/l) was prepared by dissolving 0.2829 g of dried (at 110 °C ,1.5 h.) $K_2Cr_2O_7$ in deionized water.

Working standard solutions were freshly prepared by diluting the stock solution with 0.025 M H_2SO_4.

6. Calcium Standard Solutions

1000 ml of stock calcium solution (1000 mg Ca^{2+}/l) was prepared by dissolving 2.5021 g of dried (at 110 °C ,1.5 h.) $CaCO_3$ in 600 ml of deionized water. 0.1 M HCl carefully was added (to dissolved the calcium carbonate). The solution diluted to the mark with water.

Working standard solutions were freshly prepared by diluting the stock solution.

7. Rhodamine B Solution

100 ml of stock Rhodamine B (RB) solution (0.25 % (w/v)) was prepared by dissolving 0.025 g of RB in 50 ml of deionized water. This solution was filtered through a membrane filter (0.45 μm pore size) and diluted to mark.

8. Ammonium Molybdate Solution

500 ml of stock ammonium molybdate solution (10% (w/v)) was prepared by dissolving 50.0 g of $(NH_4)_6Mo_7O_{24}.4H_2O$ in 50-60 °C of deionized water, cooled, filtered through a membrane filter (0.45 μm pore size) and diluted to mark.

9. Polyvinyl Alcohol Solution

500 ml of stock polyvinyl alcohol (PVA) solution (0.5 % (w/v)) was prepared by dissolving 2.5 g of PVA in 300 ml of deionized water. This solution was filtered through a membrane filter (0.45 μm pore size) and diluted to mark.

10. Sodium Hydroxide Solution

100 ml of stock sodium hydroxide solution (15 M) was prepared by dissolving 60 g of NaOH in deionized water.

11. Ammonium Chloride Buffer

1000 ml of ammonium chloride buffer (pH = 8.5) was prepared by dissolving 13.0 g of NH_4Cl and 1.7 g of $Na_2EDTA.2H_2O$ in deionized water, then adjusted to the pH 8.5 with 15 M NaOH and diluted to mark.

12. Regeneration Solution for Cd-Column

500 ml of regeneration solution was prepared by dissolving 0.85 g of $Na_2EDTA.2H_2O$ in 400 ml of 0.1 M HCl and diluted to mark with 0.1 M HCl.

13. 1,5-Diphenylcarbazide Solution

1000 ml of 1,5-diphenylcarbazide solution (0.1 % w/v) was prepared by dissolving 1 g of 1,5-diphenylcarbazide in 40 ml of acetone. And then the solution added to a 900 ml of 1 M HNO_3, diluted to mark with 1 M HNO_3 and filtered. This solution should be prepared daily and degased before used.

14. Ceric(IV) Ammonuim Sulfate Solution

500 ml of $Ce(NH_4)_4(SO_4)_4$ solution (1.2 % w/v) was prepared by dissolving 6 g of $Ce(NH_4)_4(SO_4)_4$ in 300 ml of 0.3 M H_2SO_4, filtered and diluted to mark with 0.3 M H_2SO_4.

15. Murexide Solution

100 ml of murexide stock solution (0.1 % (w/v)) was prepared by dissolving 0.1 g of murexide in 80 ml of deionized water, diluted to mark and filtered. This solution should be prepared daily.

16. Ethylenediamine Buffer

1000 ml of ethylenediamine buffer (pH 11.0) was prepared by dissolved 200 ml of 2 M ethylenediamine buffer in 800 ml of deionized water, adjusted the pH to 11.0±0.1 with 6 M hydrochloric acid and diluted to mark.

17. Boric/Borate Buffer

1000 ml of boric/borate buffer (pH 10.0) was prepared by dissolving 3.59 g of sodium hydroxide and 6.18 g of boric acid in 800 ml of deionized water, adjusted the pH to 10.0 with 15 M sodium hydroxide or 1 M hydrochlolic acid and diluted to mark.

18. Calmagite Stock Solution

500 ml of calmagite stock solution (0.15 % (w/v)) was prepared by dissolving 0.75 g of calmagite in 300 ml of deionized water, stirred for one and a half hours, and diluted to mark. The solution was filtered through filter paper.

19. Magnesium Chloride Solution

250 ml of magnesium chloride stock solution (0.5 % (w/v)) was prepared by dissolving 1.25 g of magnesium chloride in boric/borate buffer (pH = 10).

20. Disodium Ethylenediaminetetraacetic Acid Solution

250 ml of stock solution (1.0 % (w/v)) was prepared by dissolving 2.5 g of $Na_2EDTA.2H_2O$ in boric/borate buffer (pH = 10).

21. Working Calmagite Reagent Solution

A working calmagite reagent solution was prepared by mixing the Na_2EDTA stock solution (36 ml) with the magnesium solution (80 ml) and the boric/borate buffer solution (700 ml). The calmagite stock solution (120 ml) was added to the mixture and made volume with boric/borate buffer (pH = 10) to 1L. Finally the $Na_2EDTA.2H_2O$ stock solution was further added dropwise with stirring until color of the mixture turned "royal blue".

2.3 Determination of Phosphate by Flow Injection Fluorimetric Method

Various FIA procedures by different techniques for phosphate have been reported as previously described in 1.2.2.

This investigation concerns a flow injection fluorimetric method for the determination of phosphate which is based on the principle that the fluorescence of Rhodamine B (RB) is quenched by the formation of the ion associate (or non-fluorescent ternary complex), thereby providing foundation for a fluorescence-quenching method. The molar ratio of molybdophosphate to RB in the ion associate was determined to be 1:3 in previous works [19-20].

2.3.1 Preliminary Studies of the Fluorescence Spectra Scanning

Preliminary investigations for determination phosphorus as phosphate were carried out by measurement of absorption and emission spectra due to molybdophosphate-RB ion association type.

Wavelength for fluorescence intensity was measured in a direction perpendicular to the incident light using a HITACHI F-2000 fluorescence spectrophotometer with a 1 cm light path quartz cell. The fluorescence spectra was recorded in the range of 400-700 nm at 240 nm/min scan speed, 2 sec response, 10 nm bandpass and 4 nm intervals of incident light between 400 and 700 nm.

The fluorescence spectra of RB and the ion association are shown in Figure 2.1. The adopted maximum wavelengths were 560 nm for absorption (λ_{ex}) and 580 nm for emission (λ_{em}) because the intensity at 560 and 580 nm decreased with addition of molybdate and phosphate. So the fluorescence quenching at 580 nm was observed with an increase in the concentration of phosphate.

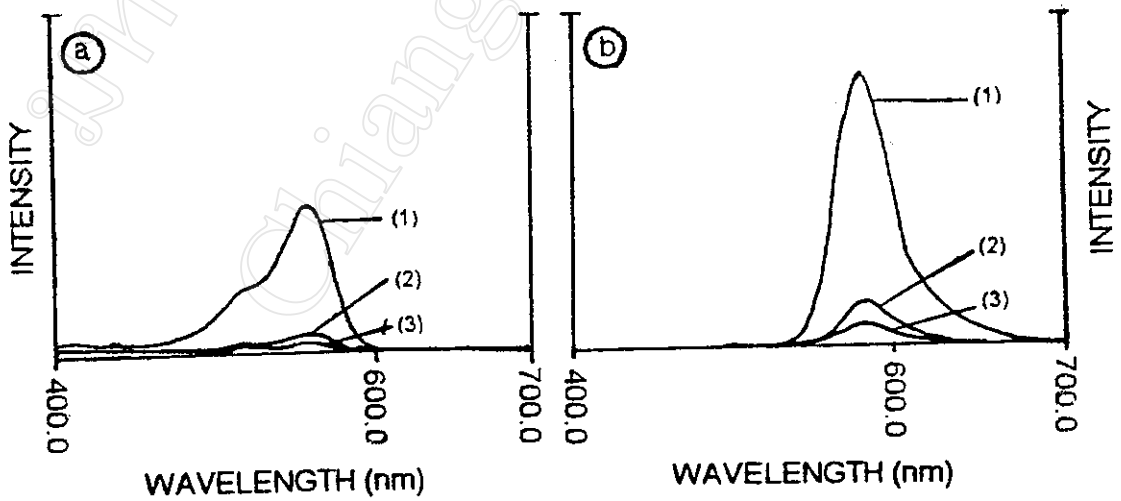

Figure 2.1 Fluorescence spectra of RB and ion associate formed between molybdophosphate and RB. Spectra : (a) absorption and (b) emission : (1) the RB solution (0.8×10^{-4} % (w/v) RB + 0.1 M H_2SO_4 + 8×10^{-3} % (w/v) PVA), (2) 0.25 % (w/v) molybdate in the RB solution and (3) 20 μg PO_4^{3-}/l together with molybdate (0.25 % (w/v)) in the RB solution.

2.3.2 Manifold

The simple flow diagram of the system shown in Figure 2.2 was modified from the ones for sea and natural water reported by Motomizu et.al [19] Fusheng et.al [18], respectively.

In the system (Figure 2.2), carrier and pink-reagent stream were pumped through tygon tubes (i.d.= 0.8 mm). A phosphate-sample solution was injected into the carrier stream by means of an injection valve, and mixed with pink-reagent stream in reaction coil and blue-products were transported to the flow cell cassette of spectrofluorometric detector (Jasco 821-FP). The spectrofluorometer parameters were : λ_{ex} : 560 nm, λ_{em} : 580 nm, excitation band width : 8 nm, emission band width : 30 nm, gain : ×1, measurement range : 1 and response : fast.

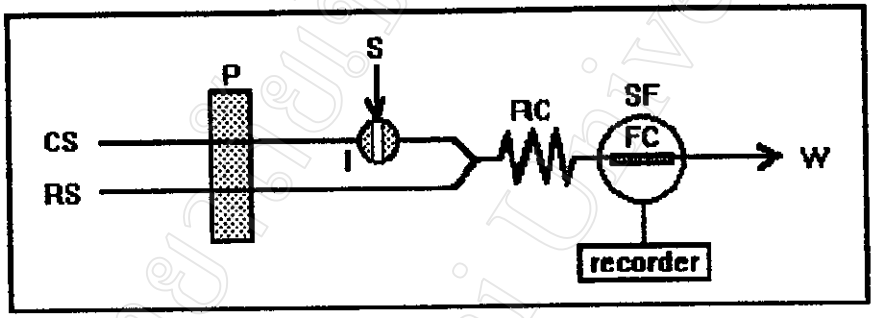

Figure 2.2 Flow diagram of phosphate fluorimetric determination ; CS : carrier solution (H_2O), RS : reagent solution (ammonium molybdate + H_2SO_4 + RB + PVA), P : peristaltic pump, I : injection valve, S : sample, RC : reaction coil, FC : flow cell cassette (quartz cell), SF : spectrofluorometric detector (Jasco 821-FP) and W : waste.

2.3.3 Optimization of Flow Injection Determination of Phosphate

Preliminary conditions were set as following :

Parameter	This work	Reference [19]
ammonium molybdate	2 % (w/v)	0.11 M
Rhodamine B (RB)	3×10^{-4} % (w/v)	6.2×10^{-4} M
polyvinyl alcohol (PVA)	0.05 % (w/v)	0.05 % (w/v)
flow rate of carrier stream (CS) and reagent stream (RS)	1.0 ml/min	0.5 ml/min
sample volume (teflon tube)	423 µl	200 µl
reaction coil length (teflon tube,i.d. = 0.8 mm)	100 cm	200 cm
flow cell cassette	quartz cell	flow cell (18 µl)
excitation wavelength	560 nm	560 nm
emission wavelength	580 nm	580 nm
excitation and emission band widths	8 nm and 30 nm	-
gain	×1	-
measurement range	1	-
response	fast	-
sensitivity of recorder	25 mV	-
chart speed of recorder	0.2 cm/min	-

2.3.3.1 Effect of H_2SO_4 Concentration

Using the manifold shown in Figure 2.2. A blank and a series of standard phosphate solutions were injected into the system using the conditions described above but with different H_2SO_4 concentration. The results are shown in Table 2.1 and Figure 2.3. The results indicate that 0.6 M H_2SO_4 gives the largest difference in quenching of the fluorimetric peak height but it caused base line drift because the ion association complex formed readily absorbed on the inner wall of tubing and the flow cell cassette. However, 0.8 M of H_2SO_4 is considered for further investigation as giving acceptable sensitivity or peak height and stability of the base line.

Table 2.1 Effect of H_2SO_4 concentration on peak height ; mean of triplicate injections.

PO_4^{3-} (µg/l)	Peak height (mV) $[H_2SO_4]$ (M)			
	0.4	0.6	0.8	1.0
0	0	0	0	0
10	0.2	0.3	0.3	0.2
20	0.6	0.6	0.5	0.5
40	1.1	1.5	1.3	0.8
60	1.8	2.3	2.0	1.6
80	2.6	3.3	2.6	2.1
100	3.2	4.3	3.8	2.7
150	5.5	8.6	7.3	6.7
200	7.9	12.7	11.0	9.7

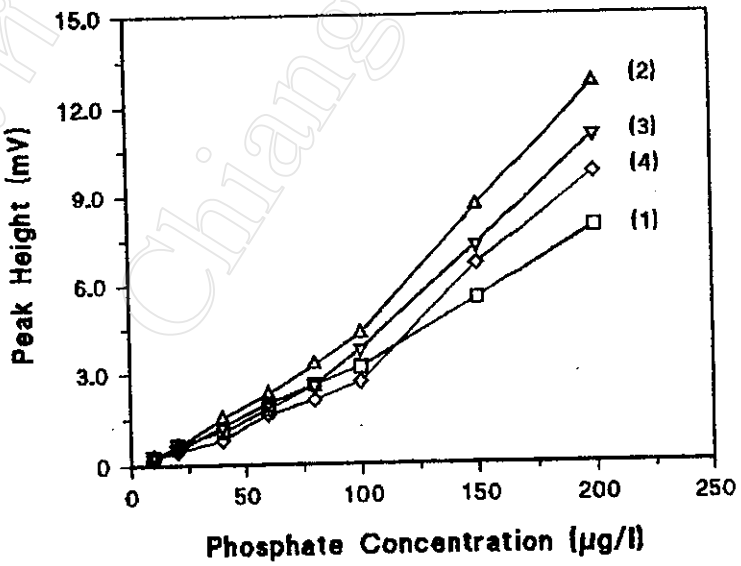

Figure 2.3 Effect of H_2SO_4 concentration on peak height ; (1) 0.4, (2) 0.6, (3) 0.8 and (4) 1.0 M H_2SO_4.

2.3.3.2 Effect of Ammonium Molybdate Concentration

Using the conditions described in 2.3.3.1, a blank and a series of standard phosphate solutions were injected into the system with various concentrations of ammonium molybdate. The results are shown in Table 2.2 and Figure 2.4. The concentration of 2 % (w/v) was chosen as giving the highest peak height.

Table 2.2 Effect of ammonium molybdate concentration on peak height ; mean of triplicate injections.

PO_4^{3-} (µg/l)	Peak height (mV)			
	Ammonium molybdate (% w/v)			
	0.5	1	2	4
0	0	0	0	0
10	0.1	0.1	0.3	0.1
20	0.2	0.3	0.6	0.3
40	0.4	0.9	1.1	0.7
60	0.5	1.5	1.7	1.2
80	0.8	1.8	2.3	1.8
100	1.1	2.6	2.9	2.4
150	1.3	5.1	5.7	4.8
200	1.9	7.9	9.1	7.3

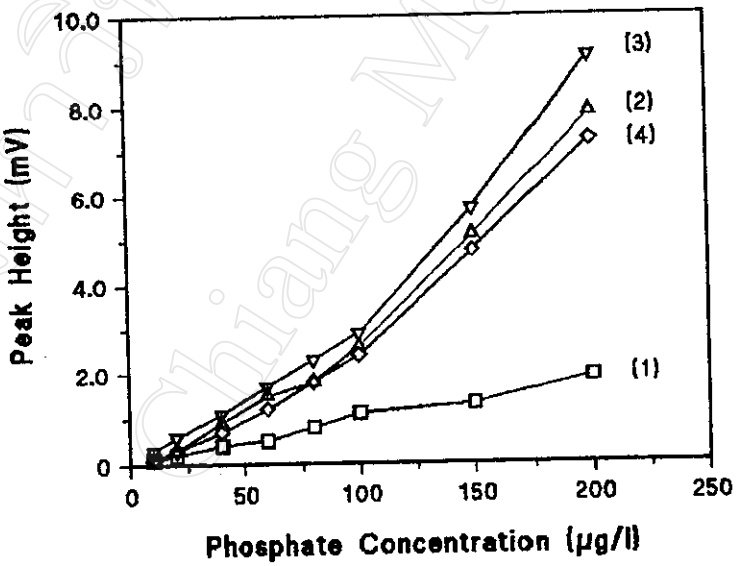

Figure 2.4 Effect of ammonium molybdate concentration on peak height ; Ammonium molybdate concentrations : (1) 0.5, (2) 1, (3) 2 and (4) 4 % (w/v).

2.3.3.3 Effect of Rhodamine B Concentration

Using the conditions described in 2.3.3.2, a blank and a series of standard phosphate solutions were injected into the system with various concentrations of RB. The results are shown in Table 2.3 and Figure 2.5. It was found that an increase in the concentration of RB, the base line became noisy. However, peak heights became higher when the concentration of RB increased. RB solution of 3×10^{-4} % (w/v) was chosen to give a good compromise between sensitivity and base line stability. The linear range of calibration curve is extended to 100 µg PO_4^{3-}/l.

Table 2.3 Effect of RB concentration on peak height ; mean of triplicate injections.

PO_4^{3-} (µg/l)	Peak height (mV) [RB] (% w/v)				
	0.5×10^{-4}	1×10^{-4}	3×10^{-4}	5×10^{-4}	7×10^{-4}
0	0	0	0	0	0
10	0.1	0.1	0.1	0.5	0.6
20	0.2	0.2	0.4	0.9	1.3
40	0.3	0.5	0.9	1.6	3.1
60	0.4	0.7	1.4	3.5	5.1
80	0.6	1.1	2.1	5.4	7.7
100	0.7	1.3	2.7	7.1	11.1
125	0.8	1.8	3.9	10.0	13.5
150	1.0	2.4	5.4	12.4	16.1
175	1.2	2.9	6.7	14.5	19.0
200	1.4	3.6	8.5	17.5	-

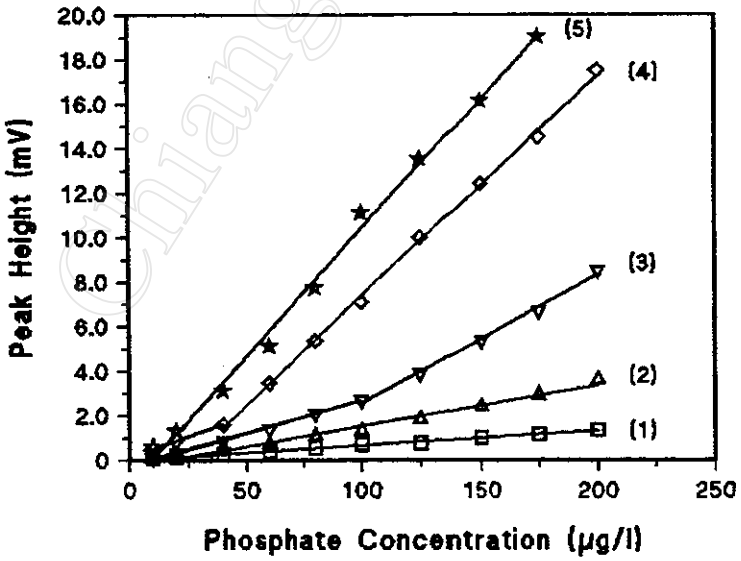

Figure 2.5 Effect of RB concentration on peak height; RB concentrations: (1) 0.5×10^{-4}, (2) 1×10^{-4}, (3) 3×10^{-4}, (4) 5×10^{-4} and (5) 7×10^{-4} % (w/v).

2.3.3.4 Effect of PVA Concentration

Using the conditions described in 2.3.3.3, a blank and a series of standard phosphate solutions were injected into the system with various concentrations of PVA. The results are shown in Table 2.4 and Figure 2.6. It was found that an increase in concentrations of PVA, the peak height decreased. However, PVA of low concentration should be added to prevent the aggregates or precipitates and adsorption of the ion associate compounds (formed by RB and molybdophosphate) on the inner wall of tubing and the flow cell cassette. A concentration of 0.005 % (w/v) PVA was chosen as a compromise.

Table 2.4 Effect of PVA concentration on peak height ; mean of triplicate injections.

PO_4^{3-} (µg/l)	Peak height (mV) [PVA] (% w/v)					
	0	0.005	0.01	0.03	0.05	0.07
0	0	0	0	0	0	0
10	1.7	0.6	0.4	0.4	0.3	0.3
20	3.3	1.9	1.2	1.0	0.7	0.6
40	6.8	4.3	3.2	1.9	1.7	1.4
60	10.1	6.8	5.7	3.6	2.8	2.8
80	13.2	9.6	7.7	5.6	4.8	4.2
100	16.1	12.0	9.9	7.5	6.6	5.9

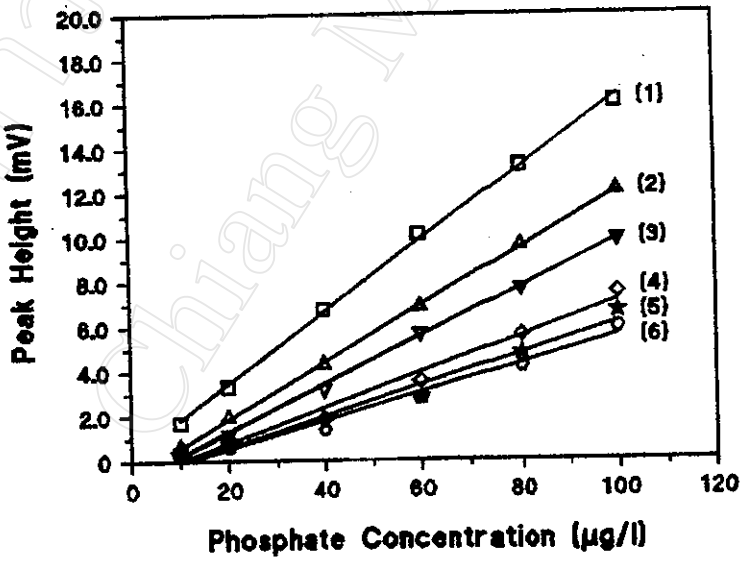

Figure 2.6 Effect of PVA concentration on peak height ; PVA concentrations : (1) 0, (2) 0.005, (3) 0.01, (4) 0.03, (5) 0.05 and (6) 0.07 % (w/v).

2.3.3.5 Effect of Flow Rate of the two Streams (CS and RS)

The effect of flow rates of CS and of RS were studied. Using the conditions described in 2.3.3.4, a blank and a series of standard phosphate solutions were injected into the system. The results are shown in Table 2.5 and Figure 2.7. All, the calibration curves studied were linear up to 100 μg PO_4^{3-}/l at a flow rate of 0.5-1.5 ml/min. A flow rate of 1.0 ml/min was chosen as giving the highest peak height and slope.

Table 2.5 Effect of flow rates of CS and RS on peak height ; mean of triplicate injections.

PO_4^{3-} (μg/l)	Peak height (mV) Flow rate (ml/min)			
	0.5	0.7	1.0	1.5
0	0	0	0	0
10	0.7	0.6	1.1	0.7
20	1.5	1.8	2.5	1.7
40	3.8	4.6	4.9	3.5
60	6.1	6.9	7.8	5.5
80	8.2	8.8	10.3	7.3
100	10.2	11.0	13.0	9.4
slope	0.108	0.115	0.132	0.096

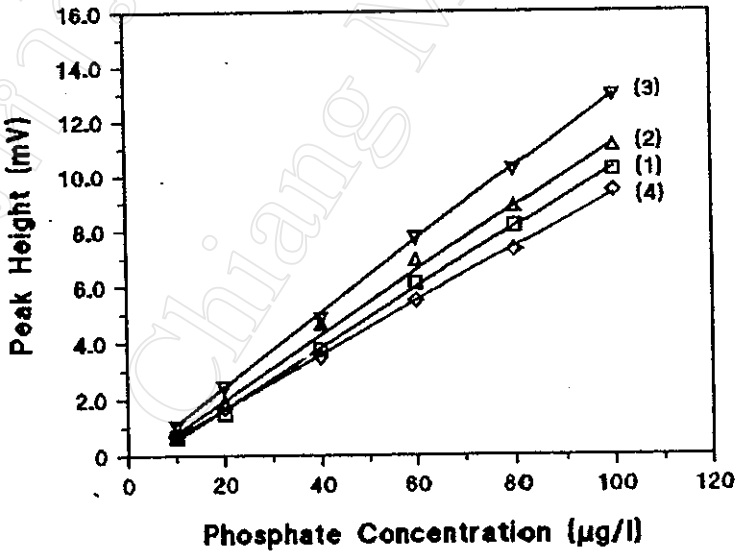

Figure 2.7 Effect of flow rate of the two streams on peak height ; Flow rates : (1) 0.5, (2) 0.7, (3) 1.0 and (4) 1.5 ml/min.

2.3.3.6 Effect of Reaction Coil Length

The effect of reaction coil length (teflon tubing, i.d.=0.8 mm) was studied. Using the conditions described in 2.3.3.5, a blank and a series of standard phosphate solutions were injected into the system. The results are shown in Table 2.6 and Figure 2.8. The results indicate that the peak height decreased when the length of the reaction coil increased. Therefore, a reaction coil length of 100 cm was considered as giving the highest peak height and slope.

Table 2.6 Effect of reaction coil length on peak height ; mean of triplicate injections.

PO_4^{3-} (µg/l)	Peak height (mV) Reaction coil length (cm)				
	50	100	150	200	300
0	0	0	0	0	0
10	0.9	1.1	1.1	1.0	0.8
20	2.2	2.3	2.3	2.2	1.6
40	4.7	4.8	4.5	4.1	3.2
60	7.3	7.5	6.8	6.3	4.5
80	9.4	9.8	8.8	8.3	6.1
100	11.8	12.1	11.1	10.2	7.8
slope	0.121	0.123	0.110	0.102	0.077

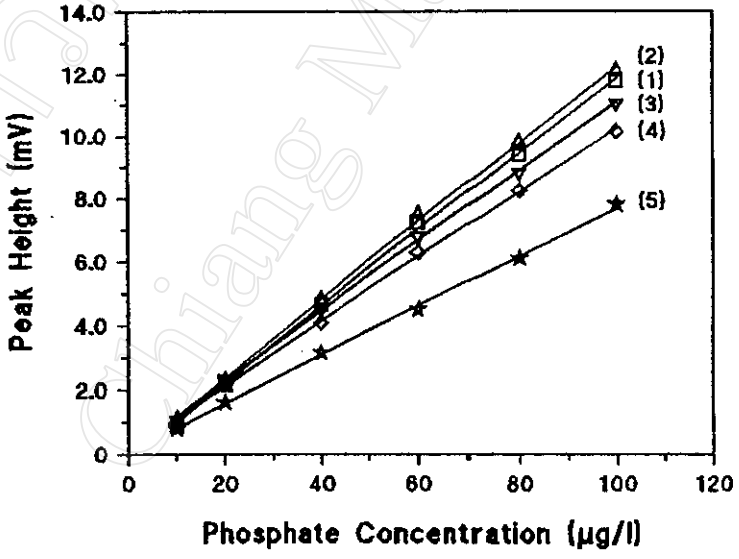

Figure 2.8 Effect of reaction coil length on peak height ; Reaction coil lengths : (1) 50, (2) 100, (3) 150 and (4) 200 cm.

2.3.3.7 Effect of Sample Volume

The effect of sample volume was studied by varying length of the sample loop (i.d.=0.5 mm). Using the conditions described in 2.3.3.6, a blank and a series of standard phosphate solutions were injected into the system. The results are shown in Table 2.7 and Figure 2.9. A range of sample volume of 423-523 µl were chosen as giving the highest peak height (% RSD = 3.02-6.30) and slope.

[**Note** : The determination of dead volume (or internal volume; Sd = 123 µl) of the injection valve was studied (Appendix E)].

Table 2.7 Effect of sample volume on peak height ; mean of triplicate injections.

PO_4^{3-} (µg/l)	Peak height (mV)					
	Sample volume (µl)					
	123	223	323	423	523	623
0	0	0	0	0	0	0
10	0.6	0.7	0.8	1.4	1.1	0.5
20	1.3	1.6	1.9	2.8	2.4	1.2
40	2.6	3.3	3.8	5.3	4.7	2.8
60	3.6	5.0	5.7	7.9	7.0	4.5
80	5.1	6.6	7.5	10.2	9.2	6.5
100	6.2	8.2	9.3	12.4	11.4	8.1
y=a(x)+b	y=0.062(x) -0.013	y=0.084(x) -0.118	y=0.094(x) -0.044	y=0.122(x) +0.341	y=0.114(x) +0.098	y=0.086(x) -0.497
r^2	0.999	0.999	0.999	0.999	0.999	0.998
% RSD	2.2	9.0	6.3	5.0	3.0	7.8

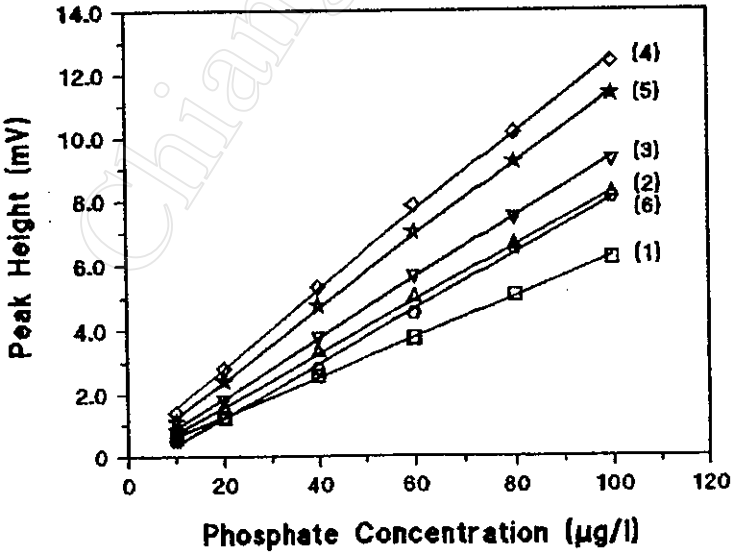

Figure 2.9 Effect of sample volume on peak height ; Sample volumes : (1) 123, (2) 223, (3) 323, (4) 423, (5) 523 and (6) 623 µl.

2.3.3.8 Summary of Condition Used

The recommended FIA manifold is depicted in Figure 2.2 and the optimum conditions are summarized in Table 2.8.

Table 2.8 Conditions used for the determination of phosphate

carrier solution (CS)	water
reagent solution (RS)	2 % (w/v) ammonium molybdate + 0.8 M H_2SO_4 + 3×10^{-4} % (w/v) RB + 0.005 % (w/v) PVA
flow rate of each solution	1.0 ml/min
sample volume	423 µl
reaction coil length (i.d. = 0.8 mm)	100 cm
flow cell cassette	quartz cell
wavelength	λ_{ex} = 560 nm, λ_{em} = 580 nm
band width	excitation = 8 nm, emission = 30 nm
gain	×1
measurement range	1
response	fast
sensitivity of recorder	25 mV
chart speed of recorder	0.2 cm/min

2.3.3.9 Calibration Curve and Detection Limit

Using the optimum FIA system described in 2.3.3.8. The calibration curve and detection limit of the condition used were studied. The results are shown in Table 2.9, Figure 2.10 and Figure 2.11. The results were obtained in the linear range of 5-100 µg PO_4^{3-}/l and the detection limit of 5 µg PO_4^{3-}/l [described in Appendix J] and the sample throughput of 36-40 injections/h. From the results, different values were observed by comparing to the reported ones by Motomizu et.al. [19]. It was found that the range = 3-300 µg PO_4^{3-}/l, the detection limit = 3 µg PO_4^{3-}/l, % RSD = 1.2 and the sample throughput = 15 injections/h.

Table 2.9 Calibration curve for phosphate.

PO_4^{3-} (µg/l)	Peak height (mV)			Mean (mV)
0	0			0
5	0.3	0.3	0.3	0.3
10	0.8	0.8	0.8	0.8
20	1.7	1.6	1.6	1.6
40	4.0	4.0	4.0	4.0
60	6.2	6.3	6.4	6.3
80	8.5	8.5	8.5	8.5
100	10.4	10.5	10.4	10.4

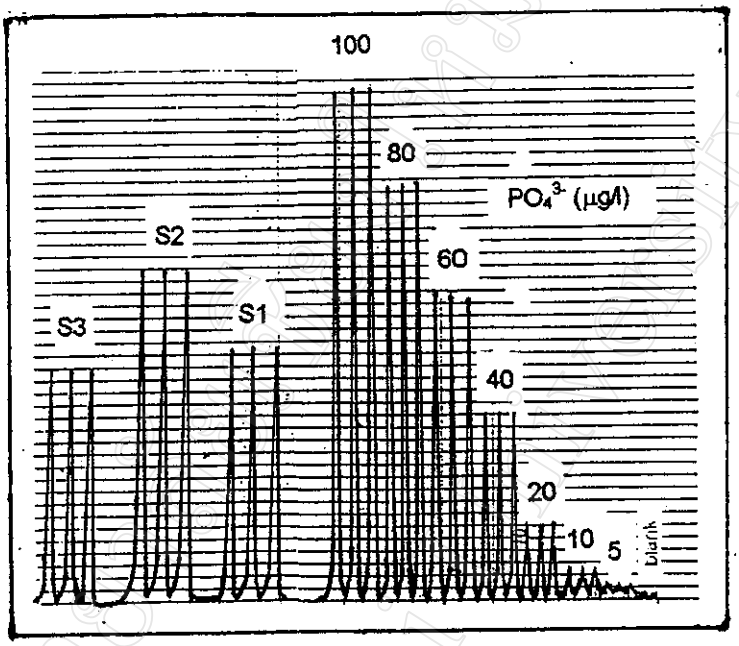

Figure 2.10 FIA signals for the determination of phosphate. S_1, S_2 and S_3 : real samples 1, 2 and 3 respectively.

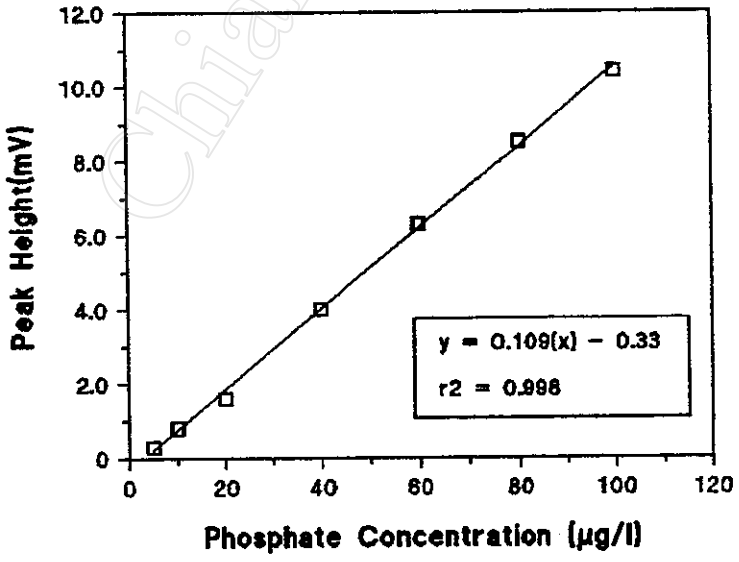

Figure 2.11 Calibration curve for phosphate (n = 3).

2.3.3.10 Precision

Using the optimum FIA conditions described in 2.3.3.8. The precision of the condition used was determined by repeating injection of 80 µg PO_4^{3-}/l of standard phosphate solution for 12 replicates. The results are shown in Table 2.10. The relative standard deviation (RSD) is 1.3 %.

Table 2.10 Precision study using 80 µg PO_4^{3-} /l , n = 12.

Peak height (mV)				Mean (x)	S.D.	% RSD
8.1	8.1	8.2	8.0	8.0	0.1	1.3
8.0	8.0	7.9	7.8			
8.0	7.9	8.1	7.9			

2.3.3.11 Interference Studies

The effect of interfering ions including condensed phosphates (pyro- and poly-) and organic phosphates was studied. Using the optimum condition described in 2.3.3.8, a blank and 50 µg/l of standard phosphate solutions containing various other interferences concentration were injected. The results obtained are shown in Table 2.11 and summarized in Table 2.12. As can be seen, most cations and anions commonly found in natural water did not interfere. Arsenic (VI) causes positive errors at higher amount of 0.1 mg/l due to that it may react with molybdate to form the heteropoly acid. Iron (II) caused positive errors too at the amounts of higher than 1 mg/l. Tin (II) and aluminium (III) interfere at concentrations of higher than 0.1 and 0.8 mg/l, respectively. ATP, phytic acid and tripolyphosphate ($P_3O_{10}^{5-}$) interfere at the concentrations of more than 1 mg/l each ; that causes positive errors. Of these interferences may be due to sodium ion in the compounds used for the study. However, in natural water, the concentrations of these interferent species are very much lower.

Table 2.11 Effect of interferent for phosphate concentration of 50 µg/l ; mean of triplicate injections.

Ion	Added as	Concentration added (mg/l)	Peak height (mV)	PO_4^{3-} found (µg/l)	% relative error
none	-	-	5.7	50.0	-
Na^+	NaCl	10	5.7	50.0	0
		50	5.8	50.4	0.8
		100	5.9	52.2	4.4
		500	7.7	68.1	36.2

Table 2.11 (Continued)

Ion	Added as	Concentration added (mg/l)	Peak height (mV)	PO_4^{3-} found (µg/l)	% relative error
K^+	KCl	10	5.6	49.6	-0.8
		50	5.7	50.0	0
		100	5.6	49.8	-0.4
		250	5.6	49.8	-0.4
		500	5.7	50.0	0
Mg^{2+}	$MgCl_2$	10	5.7	50.0	0
		50	5.7	50.0	0
		100	5.7	50.0	0
		250	5.6	49.6	-0.8
		500	5.7	50.0	0
Ca^{2+}	$CaCl_2$	10	5.7	50.0	0
		50	5.7	50.0	0
		100	5.7	50.0	0
		250	5.8	51.3	2.6
		500	6.4	56.5	13.0
Ba^{2+}	$BaCl_2$	10	5.7	50.0	0
		50	5.7	50.0	0
		100	5.7	50.0	0
		250	5.7	52.6	5.2
		500	6.6	58.4	16.8
Cr^{3+}	$CrCl_3$	10	5.6	49.6	-0.8
		50	5.8	51.3	2.6
		100	6.0	52.6	5.2
		500	9.3	58.4	16.8
Mn^{2+}	$MnSO_4$	5	5.7	50.0	0
		10	5.7	50.0	0
		50	5.7	50.0	0
		100	5.8	50.9	1.8
		250	6.6	58.2	16.4
		500	7.9	69.0	38.0
Fe^{2+}	$FeSO_4$	1	5.7	50.0	0
		5	5.1	44.8	-10.4
		10	4.7	41.4	-17.2
		50	2.5	22.9	-54.2
		100	2.0	18.1	-63.8
Fe^{3+}	$FeCl_3$	5	5.7	50.0	0
		10	6.0	53.0	6.0
		50	7.3	63.8	27.6
		100	8.2	71.6	43.2
Co^{2+}	$Co(NH_3)_2$	10	5.7	50.0	0
		50	5.6	49.2	-1.6
		100	5.6	49.6	-0.8
		250	5.6	49.8	-0.4
		500	5.6	49.2	-1.6
Ni^{2+}	$Ni(NO_3)_2$	10	5.7	50.0	0
		50	5.7	50.0	0
		100	5.7	50.0	0
		250	5.6	49.8	-0.4
		500	5.7	50.0	0

Table 2.11 (Continued)

Ion	Added as	Concentration added (mg/l)	Peak height (mV)	PO_4^{3-} found (µg/l)	% relative error
Cu^{2+}	$CuSO_4$	50	5.7	50.0	0
		100	5.7	50.4	0.8
		250	5.7	50.0	0
		500	5.7	50.0	0
Zn^{2+}	$ZnSO_4$	5	5.7	50.0	0
		10	5.6	49.2	-1.6
		50	5.6	49.2	-1.6
		100	5.7	50.0	0
		250	5.7	50.0	0
		500	5.7	50.0	0
Cd^{2+}	$CdCl_2$	10	5.7	50.0	0
		50	5.7	50.0	0
		100	5.7	50.4	0.8
		250	5.7	50.0	0
		500	5.7	50.4	0.8
Sn^{2+}	$SnCl_2$	0.1	5.7	50.0	0
		0.2	4.6	37.9	-24.2
		1	2.3	18.1	-63.8
		5	1.0	9.9	-80.2
		10	0.5	5.6	-88.8
Pb^{2+}	$Pb(NO_3)_2$	10	5.7	50.0	0
		50	5.6	49.2	-1.6
		100	5.7	50.0	0
		250	5.7	50.4	0.8
		500	5.7	50.0	0
Al^{3+}	$Al(NO_3)_3$	0.8	5.7	50.0	0
		1	5.0	40.1	-19.8
		5	2.7	24.6	-50.8
		10	2.6	23.7	-52.6
		100	2.4	22.0	-56.0
		250	1.9	17.5	-65.0
NO_2^-	$NaNO_2$	5	5.7	50.0	0
		10	5.8	51.1	2.2
		50	6.0	52.8	5.6
		100	6.1	53.9	7.8
		250	6.2	54.8	9.6
NO_3^-	KNO_3	10	5.7	50.0	0
		50	5.7	50.0	0
		100	5.7	50.0	0
		250	5.7	50.4	0.8
		500	6.7	56.5	13.0
HCO_3^-	$NaHCO_3$	10	5.7	50.0	0
		50	5.7	50.0	0
		100	5.7	50.4	0.8
		250	6.0	53.0	6.0
		500	6.5	56.9	13.8

Table 2.11 (Continued)

Ion	Added as	Concentration added (mg/l)	Peak height (mV)	PO_4^{3-} found (µg/l)	% relative error
CO_3^{2-}	Na_2CO_3	5	5.7	50.0	0
		10	5.7	50.0	0
		100	6.0	52.8	5.6
		250	6.8	59.5	19.0
		500	8.2	72.0	44.0
SO_4^{2-}	K_2SO_4	10	5.6	49.8	-0.4
		50	5.7	50.0	0
		100	5.6	49.8	-0.4
		250	5.7	50.0	0
		500	5.7	50.4	-0.8
SiO_3^{2-}	Na_2SiO_3	5	5.7	50.0	0
		10	6.0	52.6	5.2
		50	8.0	70.3	40.6
		100	10.0	87.9	75.8
F^-	KF	5	5.7	50.0	0
		10	5.7	50.6	1.2
		50	6.3	55.6	11.2
		100	7.0	61.7	23.4
		250	9.0	78.5	57.0
		500	12.5	109.1	118.2
Cl^-	KCl	10	5.7	50.0	0
		50	5.7	50.4	0.8
		250	5.7	50.0	0
		500	5.7	50.0	0
Br^-	NaBr	10	5.7	50.0	0
		50	5.7	50.0	0
		100	5.6	49.2	-1.6
		250	5.7	50.0	0
		500	5.7	50.0	0
I^-	NaI	10	5.7	50.0	0
		50	5.7	50.0	0
		100	5.6	49.8	-0.4
		250	5.9	52.2	4.4
		500	6.4	56.5	13.0
SCN^-	KSCN	10	5.7	50.0	0
		100	5.7	50.4	0.8
		250	5.8	50.9	1.8
		500	5.7	50.0	0
ClO_4^-	$NaClO_4$	10	5.7	50.0	0
		100	5.7	50.0	0
		250	5.9	51.7	3.4
		500	5.9	51.7	3.4
VO_3^-	NH_4VO_3	5	5.7	50.0	0
		10	5.8	51.3	2.6
		50	6.6	58.2	16.4
		100	7.4	64.9	29.8

Table 2.11 (Continued)

Ion	Added as	Concentration added (mg/l)	Peak height (mV)	PO_4^{3-} found (µg/l)	% relative error
As^{5-}	Na_3AsO_4	0.1	5.7	50.0	0
		0.2	6.3	55.2	10.4
		0.5	7.4	67.9	35.6
		1	9.5	83.4	66.8
		5	14.4	125.2	150.4
		10	19.6	170.3	240.6
$P_3O_{10}^{5-}$	$Na_5P_3O_{10}$	0.5	5.7	50.0	0
		1	5.7	50.0	0
		2.5	6.3	53.0	6.7
		5	6.5	57.3	14.6
		10	7.4	62.5	25.0
		50	13.0	113.1	126.2
$P_2O_7^{4-}$	$Na_4P_2O_7$	5	5.7	50.0	0
		10	5.7	50.0	0
		50	7.8	68.5	37.0
		100	10.1	88.4	76.8
-	Phytic acid	0.5	5.7	50.0	0
		1	6.0	53.0	6.0
		2.5	6.5	54.7	9.4
		5	7.2	60.9	21.8
		10	8.4	71.4	42.8
-	ATP	0.5	5.7	50.0	0
		1	6.2	54.5	9.0
		2.5	6.6	55.6	11.2
		5	7.2	60.8	21.6
		10	8.0	70.3	40.6

Table 2.12 Summary of the interference effect for phosphate determination.

Interferent ions	*Tolerable concentration ratio (mg/l) of [ion] / $[PO_4^{3-}]$
K^+, Mg^+, Co^{2+}, Ni^{2+}, Pb^{2+}, Cu^{2+}, Zn^{2+}, Cd^{2+}, SO_4^{2-}, Cl^-, Br^-, SCN^-, ClO_4^-	≥ 10,000
Ca^{2+}, Ba^{2+}, NO_3^-, I^-	5,000
Na^+, Cr^{3+}, Mn^{2+}, HCO_3^-, CO_3^{2-}	2,000
Fe^{3+}, NO_2^-, VO_3^-, SiO_3^{2-}, $P_2O_7^{4-}$	200
Fe^{2+}, $P_3O_{10}^{5-}$, phytic acid, ATP	20
Al^{3+}	16
Sn^{2+}, As^{5+}	2

* A concentration of an ion is referred to interfere when causing a relative error of more than ±5 % with respect to the signal of the phosphate alone [18].

2.3.3.12 The Effect of Suspended Solids (SS)

Fluorescence of phosphate measurements at low concentrations are therefore more often found to be blank-limited. Since this limitation arises from the nature of the sample or from the treatment prior to measurement. The most serious effect comes from impurities which are themselves fluorescent and emit radiation which has a similar wavelength to that emitted by the analyte.The problem is made worse if both the excitation and emission wavelengths are similar which makes discrimination by careful selection of wavelengths difficult. Another type of impurity is one which is present as suspended particles which scatter radiation at the excitation wavelength. If the intensity of the scattered radiation is very high in comparison with that of the fluorescence it will give rise to a high stray light level which will swamp the analytical signal.

The assessment of the effect of SS was studied. Using the optimum condition described in 2.3.3.8. Kaolin was used as a model for suspended solids. A blank and a series of standard phosphate solutions that with and without the various concentrations of kaolin (0.1-4 μm particle size) were injected. The results are shown in Table 2.13 and Figure 2.12. The results indicate that kaolin as SS causes higher signal and less reproducibility (cf. % RSD). Hence natural water samples should be filtered before injection.

Table 2.13 Effect of SS (kaolin) on peak height ; mean of triplicate injections.

PO_4^{3-} (μg/l)	Peak height (mV)						
	Kaolin (μg/l)						
	0	5	10	50	100	150	200
10	1.1	1.4	1.8	4.6	7.6	10.0	12.2
20	2.1	2.1	2.8	5.5	8.2	10.5	12.8
40	3.7	3.9	4.6	7.2	9.8	11.9	13.8
60	5.5	5.8	6.1	8.5	11.1	13.0	14.8
80	7.3	7.4	8.0	10.4	12.2	14.2	15.8
100	9.1	9.4	9.9	11.9	13.6	15.2	16.6
y=a(x)+b	y=0.088(x)+ 0.24	y=0.089(x)+ 0.39	y=0.089(x) +0.96	y=0.081(x)+ 3.85	y=0.067(x)+ 6.98	y=0.059(x)+ 9.43	y=0.049(x)+ 11.80
r^2	0.999	0.999	0.999	0.999	0.997	0.998	0.998
% RSD	7.9	17.3	26.5	60.6	76.2	82.5	86.6

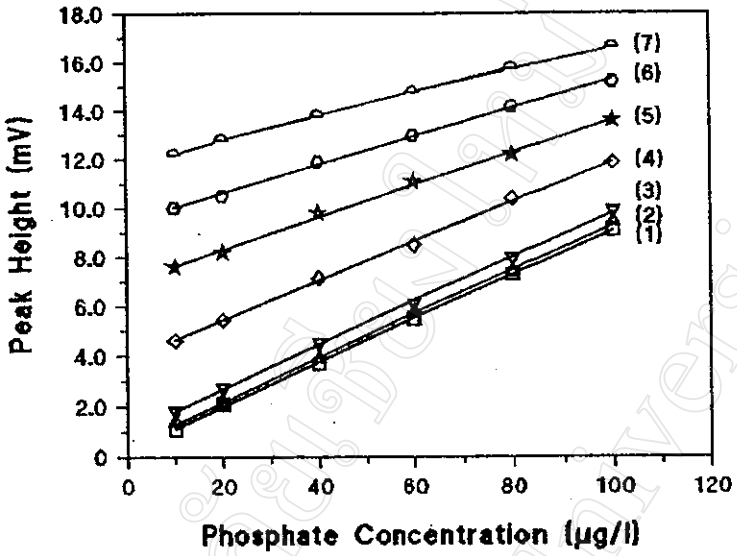

Figure 2.12 Effect of SS on peak height ; Kaolin concentrations : (1) 0, (2) 5, (3) 10, (4) 50, (5) 100, (6) 150 and (7) 200 mg/l.

2.3.3.13 Determination of Phosphate in Natural Water Sample

The optimized system was applied to the determination of phosphate in natural water samples. The samples were filtered through 0.45 µm milipore membrane filter. A comparative determination of phosphate of the conventional-FIA (conventional spectrophotometric-FIA method) [60] was also carried out. The results are shown in Table 2.14 and Figure 2.13. The different between the means and the precisions obtained from the fluorimetric-FIA and the conventional-FIA were evaluated by t-test [59]. The calculated t-test value is 0.55. The critical value of t-test is 2.04 (where t has 21 degrees of freedoms) at the confidence interval of 95% and since the calculated value of t-test is less than the critical value. These resultes from the two recommended methods are not sinificantly different for the mean phosphate concentration at confidence interval of 95%.

Table 2.14 Determination of phosphate in natural water.

Sample No.	** SS (mg/l)	Phosphate found (µg/l)	
		*** Fluorimetric-FIA method	**** Conventional-FIA method
1	-	43	43
2	-	8	12
3	-	33	35
4	-	30	31
5	-	43	40
6*	60	125	130
7*	32	14	22
8*	41	84	87
9*	30	69	71
10*	42	91	115
11	-	36	40
12	-	41	43
13	-	29	31
14	-	104	105
15	-	342	340
16	-	245	247
17	-	24	24
18	-	147	151
19	-	68	68
20	-	367	371
21	-	92	92
22	-	78	80

* Unfiltered sample No. 1, 2, 3, 4 and 5, respectively.

** SS suspended solids refers to the suspended matter that is retained on a 0.45 µm milipore filter paper (dried at 104 ^{o}C).

*** The results were obtained by triplicate injections.

**** Determination by conventional-FIA method with ammonium molybdate and reduction by recommended method stannous chloride and hydrazine sulfate. [60]

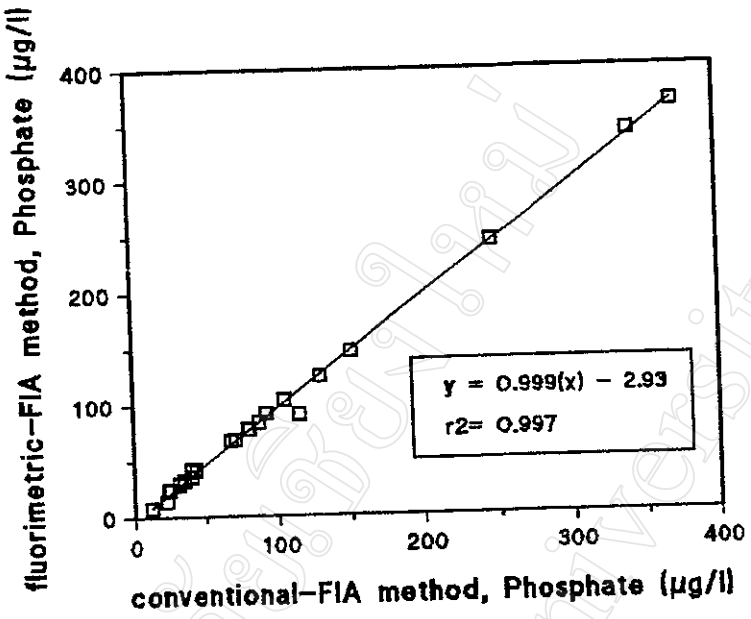

Figure 2.13 Comparison of phosphate concentrations in natural water samples determining by the conventional-FIA method and fluorimetric-FIA methods.

2.3.3.14 Standard Addition FIA

Using the optimized condition in 2.3.3.8, a series of standard phosphate solutions containing 0, 20, 40, 60 and 80 µg/l was transferred into five 50 ml volumetric flasks and to each were added with 10 ml of the sample solution. Each solution was injected into the FIA system. The results are shown in Table 2.15 and Figure 2.14. It was found that the mean of % recovery value was 105 with a relative standard deviation (RSD) of 5 % (n=6).

Table 2.15 The phosphate contents found by using FIA standard addition method ; mean of triplicate injections.

Sample No.	Added as	Peak height (mV)					Concentration found (µg/l)	% recovery
		0	20	40	60	80		
1	* sample No.5	0.8	2.8	4.7	6.6	8.3	45.7	106
2	* sample No.10	1.5	3.4	5.3	7.0	8.5	91.5	101
3	* sample No.14	1.1	3.0	4.8	6.6	8.5	105.0	101
4	standard 10 (µg/l) PO_4^{3-}	1.0	2.7	4.5	6.3	7.9	11.5	115
5	standard 25 (µg/l) PO_4^{3-}	2.3	4.0	5.8	7.6	9.3	25.9	104
6	standard 40 (µg/l) PO_4^{3-}	3.5	5.2	6.9	8.5	10.3	41.7	104
								X = 105 % RSD = 5

* Sample No. from Table 2.14.

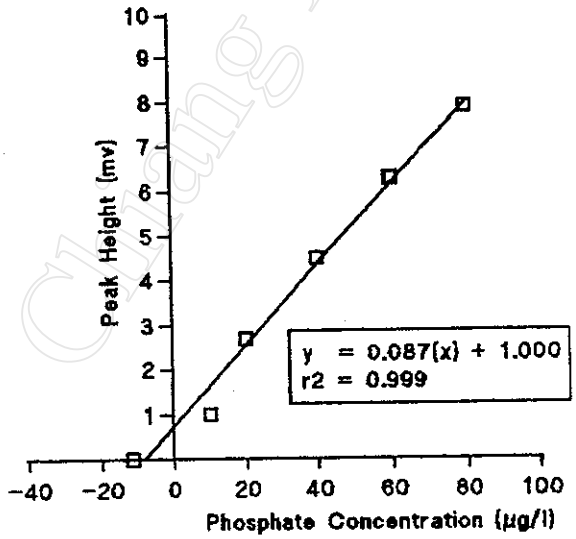

Figure 2.14 Standard addition curve of the FIA phosphate determination (data of the sample No.4 in Table 2.15).

2.4 Flow Injection Determination of Nitrite and Nitrate

Flow injection procedure for nitrite based on the formation by the diazotization /coupling as described earlier (in 1.3.1).

2.4.1 Absorption Spectrum

The absorption spectrum of the solution containing nitrite with coloring reagent (0.1 % (w/v) N-(1-naphthyl)-ethylenediamine (NED) + 1 % (w/v) sulfanilamide + 10 % (v/v) H_3PO_4) was studied. Absorption spectrum was recorded (400-650 nm) (Figure 2.15). The maximum absorption wavelength of wine red complex is 535 nm.

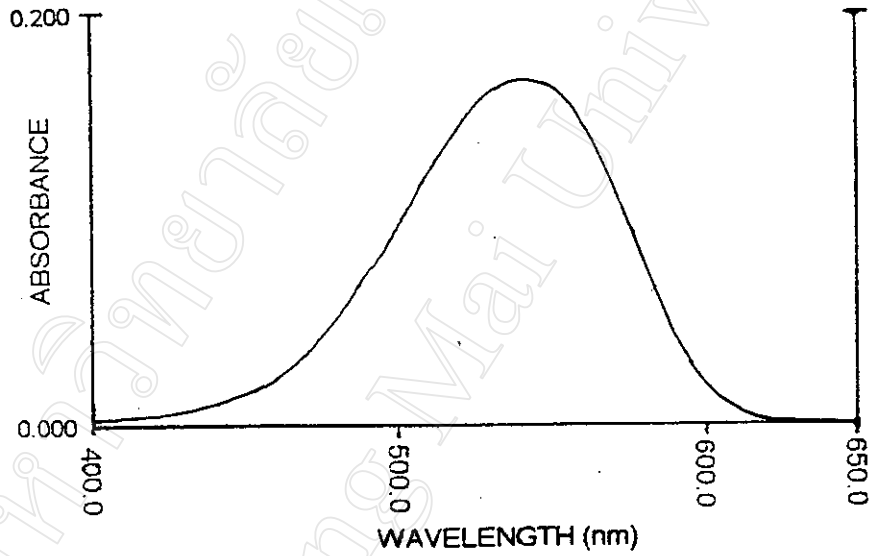

Figure 2.15 Absorption spectrum of the azo dye product of nitrite with reagent (versus reagent blank).

2.4.2 Manifold

The flow diagram of the system shown in Figure 2.16 was modified from the previous reports for simultaneous determination of nitrite and nitrate by Anderson [27], Gine et.al [28] and Van Staden [30].

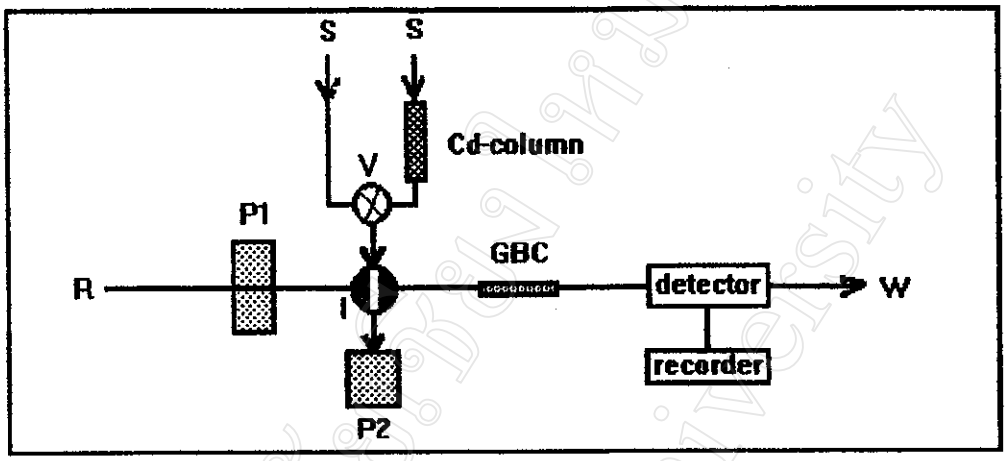

Figure 2.16 Flow diagram ; R : colouring reagent (sulfanilamide and NED in phosphoric acid solution), S : sample , I: injection valve, P1: peristaltic pump, P2: aquarium pump , GBC : glass bead column , V: three way valve , W: waste ,and Cd-column (Copperized cadmium column or cadmium reduction column).

A sample was injected into a colouring reagent by passing through a line without the cadmium reduction column (described in Appendix B). Nitrite reacts with the colouring reagent and a wine red colour-product was continuously monitored at 535 nm and recorded with a chart recorder. Nitrate can be determined by passing through a copperized cadmium column and reduced to nitrite. Then, the total nitrite (reduced nitrite plus original nitrite) was injected into the system. Nitrate alone can be determined from the difference of the total nitrite and the original nitrite. The chemical reactions are involved [25] :

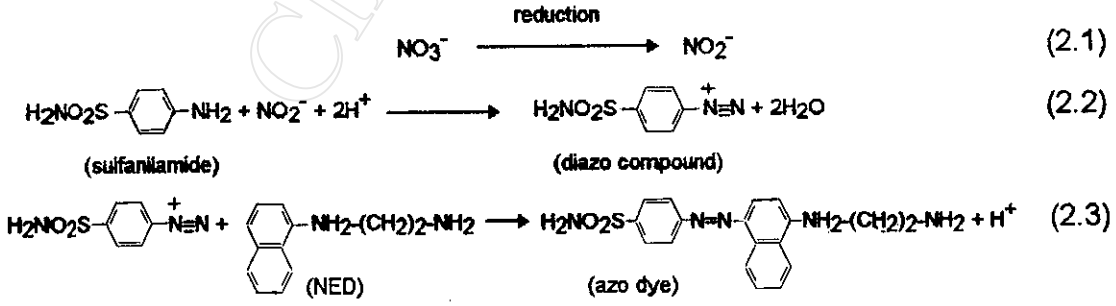

2.4.3 Optimization of Flow Injection Determination of Nitrite

Preliminary conditions were used as following :

concentration of sulfanilamide	1	% w/v
concentration of H_3PO_4	10	% v/v
flow rate of coloring reagent	5.0	ml/min
sample volume	110	µl
GBC length (i.d.= 0.35 cm)	5	cm
flow through cell volume	80	µl (path length 1 cm)
LED color of colorimeter detector	green	
sensitivity of recorder	50	mV
chart speed of recorder	1.0	cm/min

2.4.3.1 Effect of NED Concentration

Using the manifold as shown in Figure 2.16 of which the Cd-column was closed, a blank and 50 µg/l of standard NO_2^- solution were injected. Various concentrations of NED were varied. The results are shown in Table 2.16. The results indicate that 0.1 %(w/v) NED should be the most appropriate concentration as giving the highest peak height.

Table 2.16 Effect of NED concentration on peak height ; mean of triplicate injections.

NED (% w/v)	Peak height (mV)		
	Blank	NO_2^- (50 µg/l)	Corrected for blank
0.05	12.2	12.4	0.2
0.10	10.7	12.6	1.9
0.15	10.8	12.3	1.6

2.4.3.2 Effect of Sulfanilamide Concentration

Using the conditions described in 2.4.3.1, a blank and 50 µg/l of standard NO_2^- solution were injected. Concentrations of sulfanilamide were varied. The results are shown in Table 2.17. The results indicate that 0.5 % (w/v) sulfanilamide yielded the highest peak height.

Table 2.17 Effect of sulfanilamide concentration on peak height ; mean of triplicate injections.

Sulfanilamide (% w/v)	Peak height (mV)		
	Blank	NO_2^- (50 µg/l)	Corrected for blank
0.5	10.7	14.4	3.7
1.0	14.2	17.1	2.9
1.5	17.5	20.7	3.2

2.4.3.3 Effect of H_3PO_4 Acid Solution Concentration

Using the conditions described in 2.4.3.2, a blank and 50 µg/l of standard NO_2^- solution were injected. Different concentrations of H_3PO_4 acid solutions were tried. The results are shown in Table 2.18. The results indicate that 2.5 %(v/v) H_3PO_4 acid solution produced the highest peak height.

Table 2.18 Effect of H_3PO_4 acid solution concentration on peak height ; mean of triplicate injections.

H_3PO_4 (% v/v)	Peak height (mV)		
	Blank	NO_2^- (50 µg/l)	Corrected for blank
2.5	2.6	7.4	4.8
5.0	5.3	8.9	3.6
10.0	12.4	15.8	3.4

2.4.3.4 Effect of Flow Rate of Reagent Stream

The effect of various flow rates of reagent stream was studied. Using the conditions described in 2.4.3.3, a blank and 50 µg/l of standard NO_2^- solution were injected. The results and the curves obtained are shown in Table 2.19 and Figure 2.17. The results indicate that a flow rate of 3.0 ml/min produced the highest peak height but high blank peaks were observed and sample throughputs were less. The flow rate of 8.0 ml/min should be used as it yielded acceptable peak height and high sample throughputs.

Table 2.19 Effect of flow rate of reagent stream on peak height ; mean of triplicate injections.

Flow rate (ml/min)	Peak height (mV)		
	Blank	NO_2^- (50 µg/l)	Corrected for blank
3.0	13.4	17.3	3.9
5.0	3.7	7.3	3.6
6.5	7.1	10.0	2.9
8.0	7.2	10.9	3.7
8.5	9.1	11.9	2.8
9.5	8.7	11.3	2.6

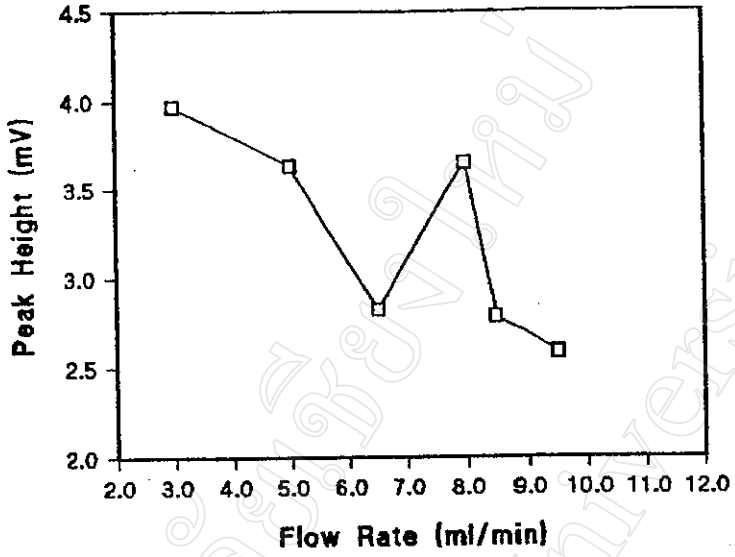

Figure 2.17 Effect of flow rate of reagent stream on peak height.

2.4.3.5 Effect of GBC Length

The effect of GBC length (i.d.= 0.35 cm) was studied. Using the conditions described in 2.4.3.4, a blank and 50 µg/l of standard NO_2^- solution were injected into the reagent stream. The results are shown in Table 2.20. The results indicate that 11 cm GBC should be used as yielding the higher peaks.

Table 2.20 Effect of GBC length on peak height ; mean of triplicate injections.

GBC length (cm)	Peak height (mV)		
	blank	NO_2^- (50 µg/l)	corrected for blank
5	6.7	11.2	4.5
11	1.3	6.0	4.7

2.4.3.6 Effect of Sample Volume

The effect of sample volume was studied. Using the conditions described in 2.4.3.5, a blank and 50 µg/l of standard NO_2^- solution were injected into a reagent stream. The results are shown in Table 2.21. The results indicate that a sample volume of 110 µl should be appropriate as giving the highest peak height.

Table 2.21 Effect of sample volume on peak height ; mean of triplicate injections.

Sample volume (µl)	Peak height (mV)		
	blank	NO_2^- (50 µg/l)	corrected for blank
40	1.7	1.9	0.2
90	2.6	5.3	2.7
110	1.4	6.0	4.6

2.4.3.7 Summary of Condition Used

The recommended FIA manifold is depicted in Figure 2.16 and the optimum conditions are summarized in Table 2.22.

Table 2.22 Conditions used for the determination of nitrite

concentration of coloring reagent (R)	0.1 % (w/v) NED + 0.5 % (w/v) sulfanilamide + 2.5 % (v/v) H_3PO_4
flow rate of coloring reagent	8.0 ml/min
sample volume	110 µl
GBC length (i.d.= 0.35 cm)	11 cm
flow through cell volume	80 µl (path length 1 cm)
LED color of colorimeter detector	green
sensitivity of recorder	50 mV
chart speed of recorder	1.0 cm/min

2.4.3.8 Calibration Curve and Detection Limit

Using the optimum FIA condition described in 2.4.3.7. The calibration curve and detection limit of the condition used were studied. The results are shown in Table 2.23, Figure 2.18 and Figure 2.19. Linearity was obtained in the range of 10-300 µg/l, the detection limit was 9 µg/l (described in Appendix J) and the sample throughput was 180 injections/h.

Table 2.23 Calibration curve for nitrite ; mean of triplicate injections.

NO_2^- (µg/l)	Peak height (mV)			Mean (mV)	Peak height corrected for blank (mV)
blank	4.2	4.3	4.4	4.3	-
10	5.0	4.5	4.4	4.6	0.3
20	5.0	5.5	5.5	5.3	1.0
50	7.5	7.5	7.7	7.6	3.3
100	11.4	11.3	11.2	11.3	7.0
200	19.3	18.9	18.9	19.0	14.7
300	26.8	25.8	26.8	26.5	22.2

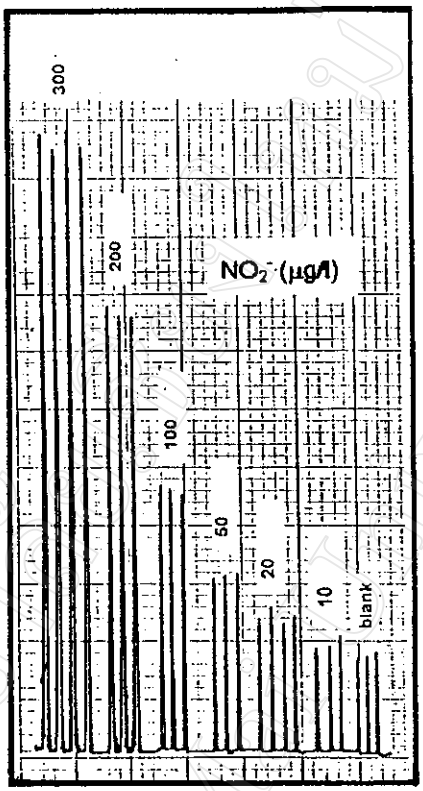

Figure 2.18 FIA signals of nitrite standards.

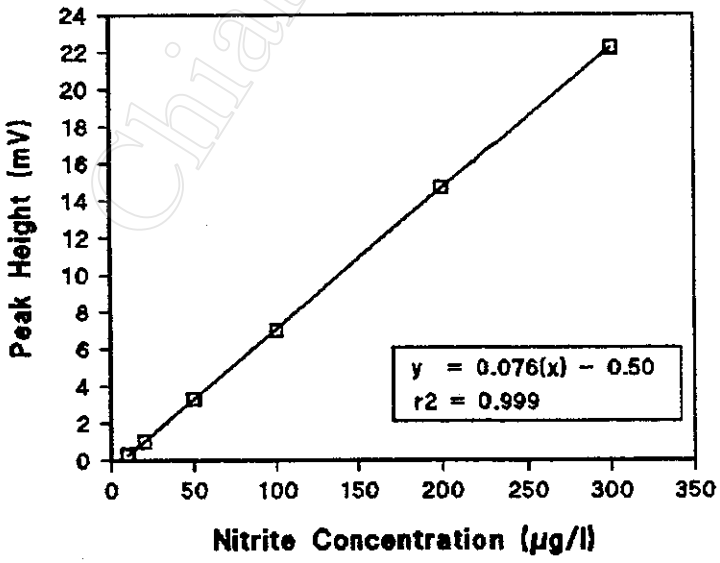

Figure 2.19 Calibration curve for nitrite standards (n=3).

2.4.3.9 Precision

The precision of the condition used was determined by repeating injection of 50 µg/l of standard NO_2^- solution for 15 replicates. The results are shown in Table 2.24. The relative standard deviation (RSD) is 1.2 %.

Table 2.24 Precision study of 50 µg NO_2^-/l, n=15.

Peak height (mV)			Mean (X)	SD	% RSD
8.0	8.1	8.1	8.1	0.1	1.2
8.2	8.2	8.1			
8.1	8.2	8.2			
8.0	8.3	8.0			
8.1	8.2	8.1			

2.4.3.10 Interference Studies

The effect of interfering ions was studied. Using the optimum conditions described in 2.4.3.7, a blank and 0.05 mg/l of standard NO_2^- solution containing various other ions were injected. The results (Table 2.25) indicate that all of the ions investigated upto the concentration ratio (mg/l of the ions to 0.05 mg/l of NO_2^-) 10,000 still did not interfere.

Table 2.25 Effect of interfering ions for nitrite concentration of 0.05 mg/l ; mean of triplicate injections.

Ion	Added as	Concentration added (mg/l)	Peak height (mV)	% relative error
none	-	-	8.8	-
Ca^{2+}	$CaCl_2$	50	8.8	0
		200	9.0	+2.3
		500	9.0	+2.3
Mg^{2+}	$MgCl_2$	50	8.8	0
		200	8.8	0
		500	8.8	0
Mn^{2+}	$MnSO_4$	50	8.8	0
		200	8.8	0
		500	9.0	+2.3
Zn^{2+}	$ZnSO_4$	50	8.8	0
		200	8.8	0
		500	8.9	+1.1
Cu^{2+}	$CuSO_4$	50	8.8	0
		200	8.8	0
		500	8.8	0
Fe^{2+}	$FeSO_4$	50	8.8	0
		200	9.1	+3.4
		500	9.2	+4.5

Table 2.25 (Continued)

Ion	Added as	Concentration (mg/l)	Peak height (mV)	% relative error
PO_4^{3-}	Na_2HPO_4	50	8.8	0
		200	8.8	0
		500	8.8	0
CO_3^{2-}	Na_2CO_3	50	8.8	0
		200	8.8	0
		500	8.8	0
SO_4^{2-}	$CaSO_4$	50	8.8	0
		200	8.9	+1.1
		500	8.8	+0.7
NO_3^-	KNO_3	50	8.8	0
		200	8.8	0
		500	8.8	0
F^-	NaF	50	8.8	0
		200	8.8	0
		500	8.8	0
Cl^-	NaCl	50	8.8	0
		200	8.7	-1.1
		500	8.8	0

2.4.4 Sequential Flow Injection Determination of Nitrite and Nitrate

Preliminary conditions for this study (by using the manifold in Figure 2.16) were as following :

concentration of coloring reagent (R)	0.1 % (w/v) NED + 0.5 % (w/v) sulfanilamide+2.5 % (v/v) H_3PO_4
flow rate of coloring reagent	8.0 ml/min
flow rate passing through Cd-column	5.5 ml/min
sample volume	110 µl
GBC length (i.d.= 0.35 cm)	11 cm
flow through cell volume	80 µl (path length 1 cm)
LED color of colorimeter detector	green
sensitivity of recorder	50 mV
chart speed of recorder	1.0 cm/min
cadmium granule size	distribution size (ϕ < 0.4 cm)

2.4.4.1 Effect of Cd-Column Length

The effect of various Cd-column lengths (i.d.= 0.35 cm, cadmium granule size < 9 mesh) was studied. Using the manifold shown in Figure 2.16 and the conditions as above. A blank, 20, 50, and 70 µg/l of standard nitrite and nitrate solutions were injected through a Cd-column. The results are shown in Table 2.26. The results indicate that the 15 cm of Cd-column should be the most appropriate length as giving the highest percentage efficiency (% Efficiency ; described in Appendix F).

Table 2.26 Effect of Cd-column length on peak height ; mean of triplicate injections.

Cd-column length (cm)	NO_2^-			NO_3^-			% Efficiency
	(µg/l)	Peak height (mV)	Peak height corrected for blank (mV)	(µg/l)	Peak height (mV)	Peak height corrected for blank (mV)	
5	blank	5.2	-	blank	5.2	-	-
	20	6.4	1.2	20	5.9	0.7	79
	50	8.4	3.2	50	6.3	1.1	46
	70	10.3	5.1	70	5.7	0.5	13
10	blank	5.2	-	blank	5.2	-	-
	20	6.5	1.3	20	6.0	0.8	83
	50	8.1	2.9	50	6.3	1.1	51
	70	10.4	5.2	70	6.9	1.7	44
15	blank	5.3	-	blank	5.3	-	-
	20	6.6	1.3	20	6.2	0.9	93
	50	8.2	2.9	50	7.1	1.8	84
	70	10.1	4.8	70	8.2	2.9	82

2.4.4.2 Effect of Cadmium Granule Size

The effect of cadmium granule size was studied. Using the conditions described in 2.4.4.1, a blank and a series of standard nitrite solutions were injected through a Cd-column. The results are shown in Table 2.27 and Figure 2.20. It was found that small sizes (ϕ < 16 mesh) of cadmium granule were chosen as giving the highest slope and a lower blanks.

Table 2.27 Effect of cadmium granule size on peak height ; mean of triplicate injections.

NO_3^- (µg/l)	Cadmium granule sizes					
	* Small (<16 mesh)		** Medium (16-9 mesh)		*** Large (>9 mesh)	
	Peak height (mV)	Peak height corrected for blank (mV)	Peak height (mV)	Peak height corrected for blank (mV)	Peak height (mV)	Peak height corrected for blank (mV)
blank	6.9	-	7.1	-	7.7	-
50	7.4	0.5	7.3	0.3	7.9	0.2
100	8.6	1.7	8.2	1.1	8.5	0.8
200	10.0	3.1	9.6	2.5	9.6	1.9
300	12.4	5.5	11.3	4.2	11.6	3.3
y=a(x)+b	y = 0.019(x) - 0.43		y = 0.015 (x) - 0.48		y = 0.012(x) - 0.44	
r^2	0.988		0.998		0.997	

* < 16 mesh : diameter of cadmium granule size is < 0.833 mm.
** 16-9 mesh : diameter of cadmium granule size is 0.833-1.651 mm.
*** > 9 mesh : diameter of cadmium granule size is > 1.651 mm.

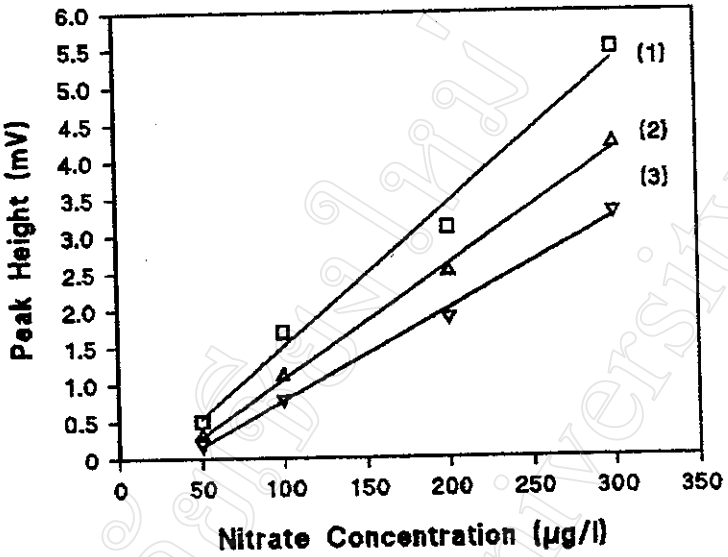

Figure 2.20 Effect of cadmium granule size on peak height ; Cadmium granule sizes : (1) small (<16 mesh), (2) medium (16-9 mesh) and (3) large (<9 mesh).

2.4.4.3 Effect of Flow Rate Passing Through Cd-Column

The effect of various flow rates passing through Cd-column was studied. Using the conditions described in 2.4.4.2, a blank and 300 µg/l of standard nitrate solutions were injected through a Cd-column. The results are shown in Table 2.28 and Figure 2.21. The results indicate that the peak height decreased when the flow rate increased and a range of 1.0-3.0 ml/min gave the highest peak heights. However, 3.0 ml/min was chosen as giving acceptable peak height and higher sample throughput.

Table 2.28 Effect of flow rate passing through Cd-column on peak height ; mean of triplicate injections.

Flow rate (ml/min)	Peak height (mV)		
	Blank	NO_3^- (300 µg/l)	Peak height corrected for blank
1.0	6.7	18.5	11.8
2.0	7.4	18.3	10.9
2.5	7.4	18.3	10.9
3.0	6.8	18.3	11.5
4.5	7.4	14.8	7.4
6.0	6.6	14.3	7.7
7.0	7.3	12.1	4.8
9.1	7.7	10.5	2.8
12.4	7.8	13.2	5.4

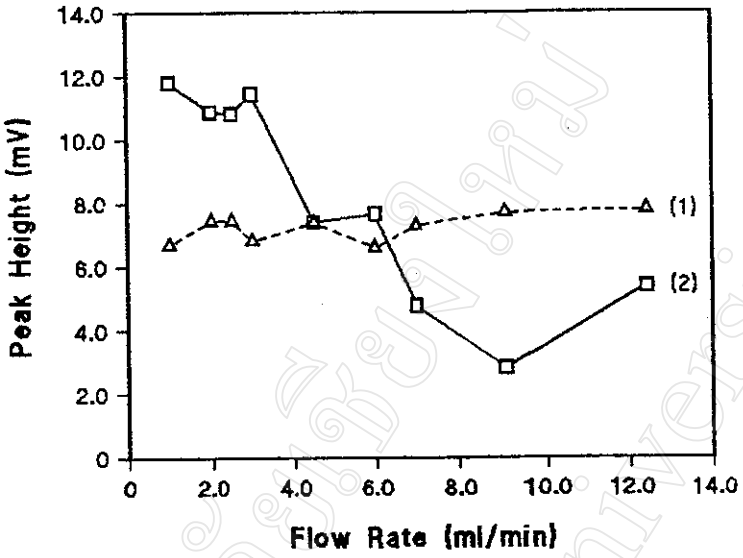

Figure 2.21 Effect of flow rate passing through Cd-column on peak height ; (1) blank and (2) 300 NO_3^- µg/l.

2.4.4.4 Regenerating the Cd-Column

The effect of various regenerating time of the Cd-column was studied (show in Appendix G). Using the condition described in 2.4.4.3, a blank and 150 µg/l of standard nitrate solutions were injected through a Cd-column. The results in Table 2.29 indicate that when a new Cd-column was used, the signals for 150 µg/l of standard nitrate remained constant for the first 30-40 peaks and the relative standard deviations (% RSD) were in the range of 13.4-4.8 %. After that, the peak heights decreased. 10 min of regenerating time was chosen.

Table 2.29 Effect of regenerating time and precision of the Cd-column on peak height ; mean of the first 30 replicate injections.

Regenerating time (min)	Number of peaks remaining reproducible	Peak height (mV)		
		* Blank	NO_3^- (150 µg/l)	Corrected for blank
New Cd-column	upto 35 (%RSD=3.4, n=35)	7.1	11.2	4.1
5	upto 29 (%RSD=3.6, n=29)	5.7	10.0	4.3
10	upto 34 (%RSD=3.5, n=34)	5.6	9.8	4.2
15	upto 47 (%RSD=4.8, n=47)	5.4	9.3	3.9

* Blank peak height for mean of triplicate injections.

Efficiency of the column regeneration was studied (in Appendix G). Using the conditions described above, a blank and 70 μg/l of standard nitrate solution passes through the column before injection. Repeating injections were made until the charge of the out-put signals, i.e. decreasing peak heights were observed (comparing to the mean heights of the nitrate peaks ($X \pm 3\sigma$)). Regeneration of the column was made by passing the regenerating solution through the column (10 min, flow rate = 3.0 min/ml). After the column had been regenerated, repeating injections were again made. It was found that column efficiency decreased each time (Table 2.30).

Table 2.30 Effect of regenerating efficiency and precision of the Cd-column on peak height ; mean of the first 30 replicate injections of nitrate.

Regeneration	Number of NO_3^- peaks attained reproducible signals	Peak height (mV)			* % Column efficiency
		Blank	NO_3^- (70 μg/l)	Corrected for blank	
New Cd-column	upto 76 (%RSD=4.5,n=76)	6.3	8.3	2.0	75
1st	upto 80 (%RSD=4.8,n=80)	6.2	8.0	1.8	68
2nd	upto 43 (%RSD=7.7,n=43)	6.4	7.7	1.3	49
3rd	upto 40 (%RDS=6.8,n=40)	6.5	7.7	1.2	45

* % Column efficiency described in Appendix F, the peak height (corrected for blank) of 70 μg NO_2^-/l is 3.6 mV (mean of triplicate injections).

2.4.4.5 Summary of Conditions Used

The recommended FIA manifold is depicted in Figure 2.16 and the optimum conditions are summarized in Table 2.31.

Table 2.31 Condition used for the determination of nitrite and nitrate

concentration of cloring reagent (R)	0.1 % (w/v) NED + 0.5 % (w/v) sulfanilamide + 2.5 % (v/v) H_3PO_4
flow rate of coloring reagent	8.0 ml/min
flow rate passing through Cd-column	3.0 ml/min
sample volume	110 μl
GBC length (i.d.= 0.35 cm)	11 cm
flow through cell volume	80 μl (path length 1 cm)
LED color of colorimeter detector	green
sensitivity of recorder	50 mV
chart speed of recorder	1.0 ml/min
Cd-column length (i.d.= 0.35 cm)	15 cm
cadmium granule size	small (ϕ < 16 mesh)
regenerating time of Cd-column	10 min

2.4.4.6 Calibration Curve and Detection Limit

Using the optimum FIA system described in Figure 2.4.4.5, a calibration curve constructed and detection limit of the condition used were studied. The results are shown in Table 2.32, Figure 2.22 and Figure 2.23. Linearity was obtained in the range of 50-300 μg/l and the detection limit is 36 μg NO_3^-/l. The % efficiency of nitrate calibration curve compared with nitrite calibration curve (in 2.4.3.8) is 59 % (described in Appendix F).

Table 2.32 Calibration curve for nitrate ; mean of triplicate injections.

NO_3^- (μg/l)	Peak height (mV)			Mean (mV)	Peak height corrected for blank (mV)
blank	6.8	7.0	6.9	6.9	-
50	7.7	7.6	7.9	7.7	0.8
100	9.7	9.6	9.9	9.7	2.8
200	13.1	12.9	13.1	13.0	6.1
300	16.2	16.3	16.7	16.4	9.5

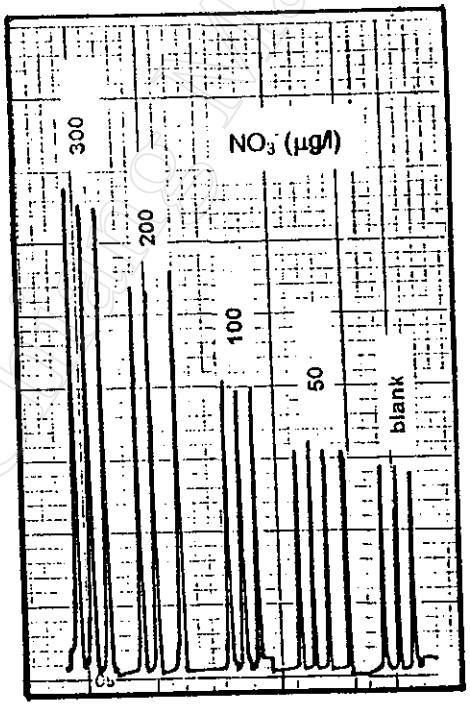

Figure 2.22 FIA signals of nitrate standards.

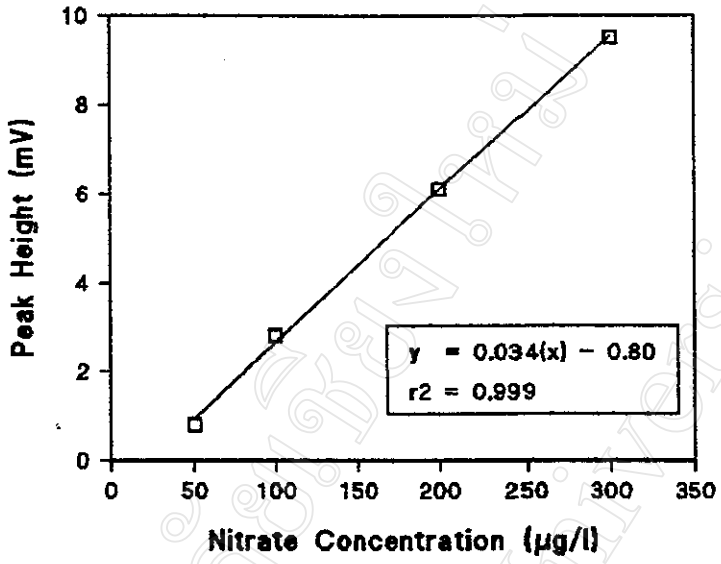

Figure 2.23 Calibration curve of nitrate standards (n=3).

2.4.4.7 Interference Studies

The effect of interfering ions was studied. Using the optimum conditions described in 2.4.4.5, a blank, 200 and 100 µg/l of standard nitrate solutions containing various other interfering cations and anions were injected through the Cd-column. The results obtained are shown in Table 2.33(a) , 2.33(b) and summarized in Table 2.34. Manganese, zinc and phosphate ions at a concentration above 50 mg/l interfere the nitrate determination. Zinc, phosphate, fluoride and chloride ions result negative errors.

Table 2.33(a) Effect of interference cations for nitrate concentration of 200 µg/l.

Ion	Added as	Concentration added (mg/l)	* Peak height (mV)	% relative error
none	-	-	6.3	-
Mg^{2+}	$MgCl_2$	50	6.3	0
		200	6.4	+1.6
		500	6.2	-1.6
Ca^{2+}	$CaCl_2$	50	6.3	0
		200	6.4	+1.6
		500	6.9	+9.5
Mn^{2+}	$MnSO_4$	5	6.3	0
		50	6.3	0
		200	9.6	+52.4
		500	11.6	+88.9

Table 2.33(a) (Continued)

Ion	Added as	Concentration added (mg/l)	* Peak height (mV)	% relative error
Fe^{2+}	$FeSO_4$	50	6.3	0
		200	6.5	+3.2
		500	7.0	+11.1
Co^{2+}	$Co(NH_3)_2$	5	6.3	0
		50	6.3	0
		200	6.3	0
		500	6.3	0
Cu^{2+}	$CuSO_4$	50	6.4	+1.6
		200	6.3	0
		500	6.3	0
Zn^{2+}	$ZnSO_4$	50	6.3	0
		200	5.0	-20.6
		500	2.2	-65.1
Cd^{2+}	$CdCl_2$	5	6.3	0
		50	6.3	0
		200	6.2	-1.6
		500	6.4	+1.6

* Peak height corrected for blank (blank = 7.3 mV).

Table 2.33(b) Effect of interfering anions for nitrate concentration of 100 μg/l.

Ion	Added as	Concentration added (mg/l)	* Peak height (mV)	% relative error
none	-	-	3.0	-
CO_3^{2-}	Na_2CO_3	50	3.0	0
		200	3.0	0
		500	2.9	-3.3
SO_4^{2-}	$CaSO_4$	50	3.0	0
		200	2.9	-3.3
		500	3.1	+3.3
PO_4^{2-}	Na_2HPO_4	50	3.0	0
		200	2.3	-23.3
		500	1.8	-40.0
F^-	NaF	50	3.0	0
		200	2.9	-3.3
		500	2.8	-6.7
Cl^-	NaCl	50	3.0	0
		200	2.9	-3.3
		500	2.8	-6.7

* Peak height corrected for blank (blank = 5.7 mV).

Table 2.34 Summary of the interference effect for nitrate determination.

Interference Ions	* Tolerable concentration ratio (mg/l) of [ion] / [NO_3^-]
Mg^{2+}, Co^{2+}, Cu^{2+}, Cd^{2+}, CO_3^{2-}, SO_4^{2-}	≥ 2,500
Fe^{2+}, Ca^{2+}, F^-, Cl^-	1,000
Mn^{2+}, Zn^{2+}, PO_4^{3-}	250

* A concentration of anion is referred to interfere when causing a relative error of more than ± 5 % with respect to the signal of the nitrate alone [18].

2.4.4.8 Effect of Cd-Column for Nitrite Determination

The effect of Cd-column for the nitrite determination was studied. Using the FIA system conditions described in 2.4.4.5, a blank and a series of standard nitrite solutions were injected into a reagent stream with and without Cd-column. The results are shown in Table 2.35 and Figure 2.24. It was found that the system without Cd-column gave higher peak heights than the one with Cd-column. This may be due to the higher degree of dispersion occuring in the system using Cd-column. However, both result the practically the same slope of calibration curve.

Table 2.35 Effect of Cd-column for nitrite determination; mean of triplicate injections.

NO_2^- (µg/l)	Without Cd-column		With Cd-column	
	Peak height (mV)	Peak height corrected for blank (mV)	Peak height (mV)	Peak height corrected for blank (mV)
blank	5.4	-	4.5	-
50	8.8	3.4	7.0	2.5
100	12.1	6.7	10.2	5.7
150	14.9	9.5	12.9	8.4
200	18.8	13.4	16.7	12.2
250	21.7	16.3	19.4	14.9
300	25.8	20.4	22.8	18.3
y=a(x)+b	y=0.067(x)-0.15		y=0.063(x)-0.71	
r^2	0.997		0.998	

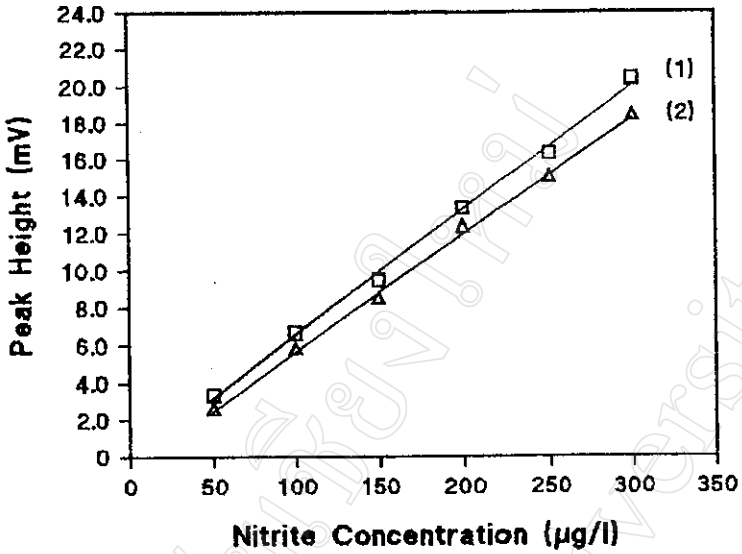

Figure 2.24 Effect of Cd-column for nitrite determination ; The nitrite calibration curves : (1) without Cd-column (2) with Cd-column.

2.4.4.9 A Study for Nitrite and Nitrate Mixture

The proposed FIA condition described in 2.4.4.5 was applied to determine nitrite and nitrate in a mixture. The out-put signals obtained when using a Cd-column would be due to the sum of nitrite and nitrate while the one without Cd-column would belong to the nitrite only. Results are summarized in Table 2.36. A calibration curve for the nitrate by using Cd-column was : $y = 0.037(x) - 1.65$; $r^2 = 0.997$ while the one for (without Cd-column) was : $y = 0.074(x) - 0.17$; $r^2 = 0.998$.

Table 2.36 A study for nitrite and nitrate mixture on peak height ; mean of triplicate injections.

Concentration found (µg/l)		Peak height (mV)				Concentration found (µg/l)		% recovery	
		Without Cd-column		With Cd-column					
NO_2^-	NO_3^-	mean	corrected for blank	mean	corrected for blank	NO_2^-	NO_3^-	NO_2^-	NO_3^-
50	0	9.2	3.2	-	-	46	-	92	-
100	0	13.1	7.0	-	-	97	-	97	-
150	0	17.4	11.3	-	-	155	-	103	-
50	0	-	-	10.3	3.7	52	-	104	-
100	0	-	-	12.2	5.6	78	-	78	-
150	0	-	-	15.0	8.4	116	-	77	-
50	100	9.1	3.1	12.4	5.8	44	117	88	117
100	100	12.6	6.6	14.8	8.2	91	89	91	89
150	150	17.5	11.4	20.3	13.7	156	107	104	71
0	150	5.8	-0.3	11.9	5.3	-	188	-	125
0	200	5.7	-0.4	12.2	5.6	-	196	-	98
								x=93	x=100
								% RSD=11	% RSD=22

2.4.4.10 Determination of Nitrite and Nitrate in a Water Sample

The optimised FIA system was applied to the determination of nitrite and nitrate in a water sample. A sample of drinking water (Dew Drop Brand) was applied with various concentrations of nitrite. Results (in Table 2.37) indicated recoveries of 90-103 %

Table 2.37 FIA determination of nitrite in spiked water sample.

No.	NO_2^- (µg/l)		% recovery
	Spiking	* Found	
1	0	N.D.	-
2	20	18	90
3	35	32	91
4	40	39	98
5	200	206	103
6	250	257	103
7	100	99	99
			% RSD = 6

* mean of triplicate injections.

2.5 Determination of Chromium

The determination of chromium is based on the reaction of 1,5-diphenylcarbazide (DPC) which reacts with Cr(VI) in an acid solution to form the red-volet complex according to [62,63,65] :

$$2CrO_4^{2-} + 3H_4L + 8H^+ \rightleftharpoons 3H_2L + 2Cr^{3+} + 8H_2O \quad (2.4)$$

$$Cr^{3+} + 2H_2L \rightleftharpoons [Cr(III)(HL)_2]^+ + 2H^+ \quad (2.5)$$

$$2CrO_4^{2-} + 3H_2L + 8H^+ \rightleftharpoons [Cr(III)(HL)_2]^+ + Cr^{3+} + H_2L + 8H_2O \quad (2.6)$$

(red-violet complex)

where H_4L is the DPC and H_2L is the 1,5-diphenylcarbazone.

Oxidation with Ce(IV) for conversion of Cr(III) to Cr(VI) is useful to the determination of total chromium [4].

$$Cr^{3+} + 3Ce^{4+} \rightleftharpoons Cr^{6+} + 3Ce^{3+} \quad (2.7)$$

This also allows Cr(III) to be determine by difference.

In this work on FIA method, in which the above-mentioned reaction was investigated. The sequential determination of Cr(VI) and Cr(III) was attempted using the normal mode. The on-line preconcentration step using a C18 solid phase extraction column is proposed to remove the major ions as well as to concentrate $[Cr(III)(HL)_2]^+$ complex.

2.5.1 Absorption Spectra of Metal-DPC Complexes

An absorption spectrum (400-600 nm) of an aqueous solution containing Cr (VI) (5 mg/l), DPC (0.2 % w/v) and H_2SO_4 (0.2 M) was recorded (Figure 2.25(a)). Maximum absorption is at 540 nm with molar absorptivity of 2.0×10^4 $cm^{-1}M^{-1}$. A spectrum of the Cr-complex in methanol was also recorded (Figure 2.25(b)). A methanol solution of the complex was obtained by the methanol elution from the C18 column (see detail in section 2.5.2). The maximum absorption of the complex in methanol solution is the same as the one in aqueous solution.

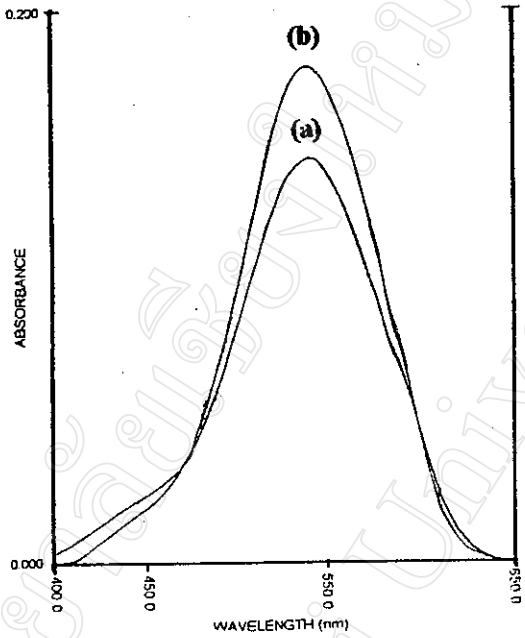

Figure 2.25 Absorption spectra of Cr(VI)-DPC-complex : (a) versus aqueous reagent solution (0.2 % w/v DPC + 0.2 M H_2SO_4) and (b) versus methanol (see text for detail).

Table 2.38 Molar absorptivity study of chromium(VI)-DPC complex.

Cr^{6+}	Absorbance
blank	0
0.4	0.181
0.6	0.226
0.8	0.262
1.0	0.296
* ε	2.0×10^{4} $cm^{-1}M^{-1}$

* The calculation of molar absorptivity (ε) is in Appendix H.

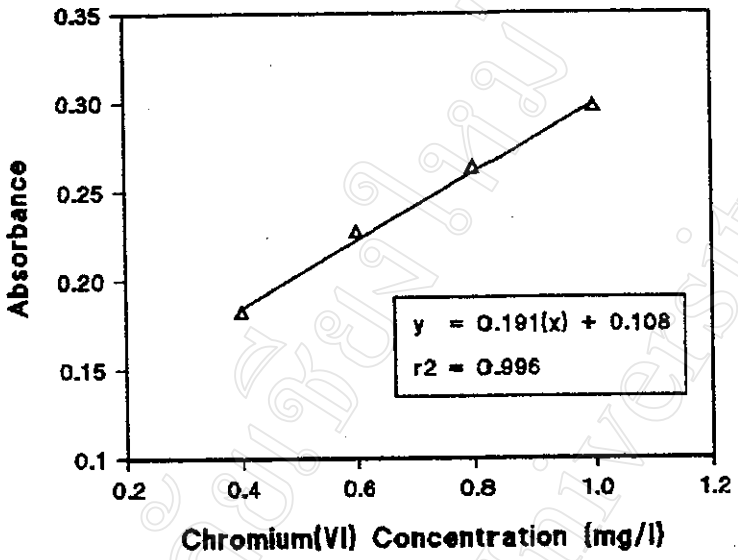

Figure 2.26 Curve of a molar absorptivity study of chromium complex (versus aqueous reagent solution ((0.2 % w/v DPC + 0.2 M H_2SO_4) as a reference).

Due to that Ce(IV) was planned to use as an oxidizing agent to convert Cr(III) to Cr(VI), absorption spectra of the Ce(VI) and its complexes with DPC were studied. A set of spectra were recorded.

1). The color reagent blank (0.1 % w/v DPC + 0.5 M HNO_3 + 0.15 M H_2SO_4)
2). Ce(IV) solution (0.6 % w/v $Ce(NH_4)_4(SO_4)_4$ + 0.15 M H_2SO_4)
3). 0.6 % w/v Ce(IV) in the color reagent
4). 1.0 mg/l of Cr(VI) in the color reagent
5). 1.0 mg/l of Cr(VI) and 0.6 % w/v Ce(IV) in the color reagent
6). 1.0 mg/l of Cr(III) and 0.6 % w/v Ce(IV) in the color reagent
7). 1.0 mg/l of Cr(III) in the color reagent

It can be seen that aqueous Ce(IV) solution absorbs very weak at 540 nm but Ce-DPC complex absorption maximum is at 563 nm.

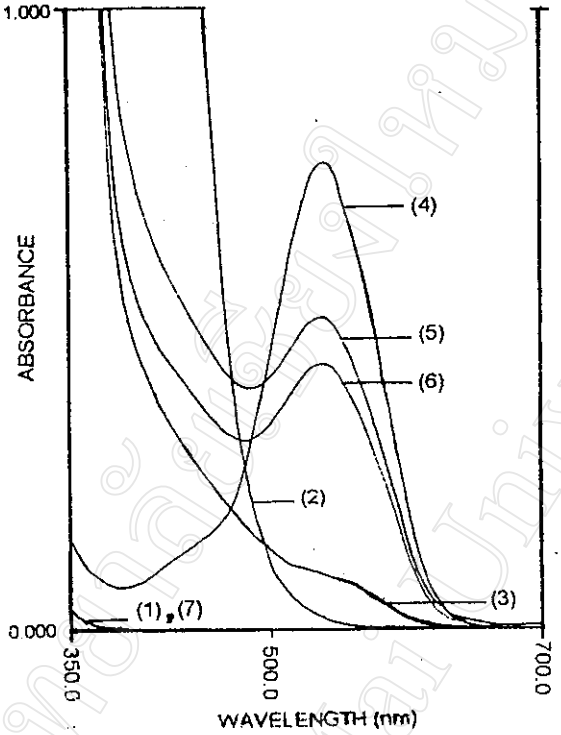

Figure 2.27 Absorption spectra (versus H_2O as a reference) of :
(1) the color reagent blank (0.1 % w/v DPC + 0.5 M HNO_3 + 0.15 M H_2SO_4),
(2) Ce(IV) solution (0.6 %w/v $Ce(NH_4)_4(SO_4)_4$ + 0.15 M H_2SO_4),
(3) 0.6 % w/v Ce(IV) in the color reagent,
(4) 1.0 mg/l of Cr(VI) in the color reagent,
(5) 1.0 mg/l of Cr(VI) and 0.6 % w/v Ce(IV) in the color reagent,
(6) 1.0 mg/l of Cr(III) and 0.6 % w/v Ce(IV) in the color reagent and
(7) 1.0 mg/l of Cr(III) in the color reagent.

2.5.2 Manifold

The flow diagrams of the system are shown in Figure 2.28.

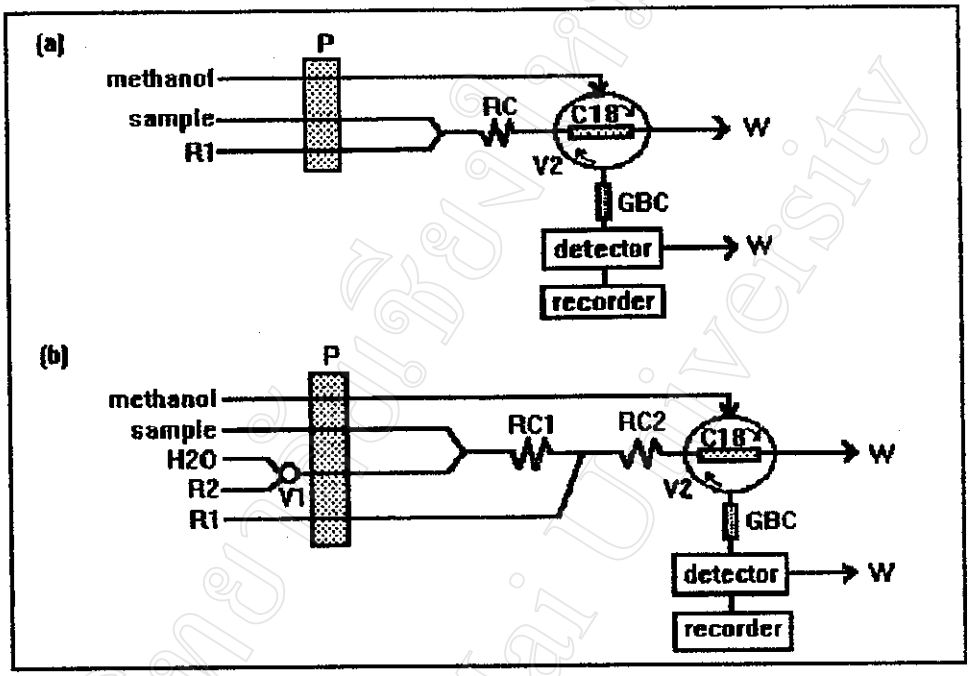

Figure 2.28 Flow diagrams of the system designed for ; (a) determination of Cr(VI) (b) sequential determination of Cr(VI) and Cr(III) ; P : peristaltic pump, RC : reaction coil, R1 : reagent solution (DPC in acid solution), R2 : oxidizing reagent solution (Ce (IV) in sulfuric solution), GBC : glass bead column, V1 : three way valve (in Appendix A), V2 : rotary injection valve, C18 SPE column (see in Appendix C) on V2 and W : waste.

A simple flow system (Figure 2.28(a)) was used for the determination of Cr(VI). The sample was continuously pumped to merge with the reagent stream (R1). The red-violet Cr-DPC complex retained on the C18 SPE column was eluted with methanol by changing the positions of the column of the injection valve V2 [5,67,68]. The eluted product flow further through glass bead column to the flow-through detector (540 nm).

Figure 2.28(b) shows the flow system which was modified from the system previously described (Figure 2.28(a)) for the sequential determination of Cr(VI) and Cr(III).

Cr(VI) alone in the mixture was determined first by merging the sample with water stream controlled by the valve V1. Then the merged stream was further merged with the reagent stream (R1). The red-violet complex was retained on C18 SPE column and was eluted similarly to the above flow system. In stead of water, switching the volume V1, the Ce(IV) reagent (R2) flow to merge with the sample containing Cr(VI) and Cr(III). The Cr(III) was then oxidized. The total Cr(VI) (the Cr(VI) originally containing in the sample plus the oxidized Cr(III)) in the stream would merged with the DPC reagent stream (R1). Cr(VI) and Cr(III) could be then determined.

2.5.3 Optimization of FI Determination of Chromium(VI)

The manifold in Figure 2.28(a) was used.

Preliminary conditions were first tried as following :

reagent R1	0.01% (w/v) DPC + 0.2 M H_2SO_4
C18 SPE column length	3 cm (i.d. = 1.5 mm)
loading time on C18 SPE column	1 min
flow through cell volume	30 µl (path length = 1 cm)
RC length (before injection valve)	150 cm (i.d. = 0.5 mm)
GBC length (after injection valve)	10 cm (i.d. = 0.35 cm)
LED colour of colorimeter detector	green
sensitivity of recorder	1000 mV
chart speed of recorder	0.5 cm/min

2.5.3.1 Effect of Flow Rates of Methanol , Sample and R1 Streams

The effects of flow rates of methanol, sample and R1 streams were studied. Using the manifold shown in Figure 2.28(a), a blank, 0.1 and 1.0 mg/l of standard Cr(VI) solutions were continuously flow and merged with the R1 reagent stream (0.01% (w/v) DPC in 0.2 M H_2SO_4) and passing through the C18 SPE column for 1 min and then eluted with methanol. The results are shown in Table 2.39 and Figure 2.29. The results indicate that the flow rates of 2.8 to 3.9 ml/min yielded a single peak, higher flow rates increased back pressure and leakage or burst were observed. The flow rate of 3.9 ml/min should be used as giving a single peak and acceptable peak height.

Table 2.39 Effect of flow rates of methanol , sample and R1 stream on peak height, mean of duplicate injections.

Flow rate (ml/min)	peak height (mV)			peak height corrected	
	blank	0.1 mg Cr^{6+}/l	1.0 mg Cr^{6+}/l	0.1 mg Cr^{6+}/l	1.0 mg Cr^{6+}/l
1.6	27.8	83.3	420.6	55.5	392.8
2.2	55.6	83.3	429.6	27.7	374.0
2.8	57.5	103.2	452.4	45.7	394.9
3.3	67.5	99.2	456.4	31.7	388.9
3.9	71.4	103.2	508.0	31.8	437.0

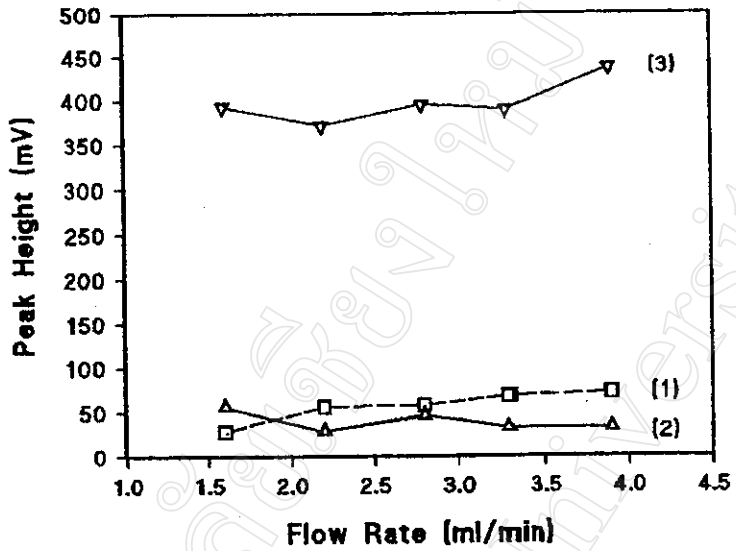

Figure 2.29 Effect of flow rate on peak height for ; (1) blank (deionized water), (2) 0.1 and (3) 1.0 mg Cr^{6+}/l.

2.5.3.2 Effect of DPC Concentration

Using the conditions described in 2.5.3.1, various concentrations of DPC were tried. The results are shown in Table 2.40 and Figure 2.30. It was found that decrease in the concentration of DPC, the peak heights and slope increased. The DPC concentration of 0.01% (w/v) was chosen as giving an acceptable peak heights and slope.

Table 2.40 Effect of DPC concentration on peak height; mean of triplicate injections.

Cr^{6+} (mg/l)	Peak height corrected for blank (mV)				
	DPC (% w/v)				
	0.005	0.01	0.05	0.10	0.15
blank	132.9	138.9	108.3	121.0	117.1
0.1	52.8	48.8	50.4	25.8	15.1
0.25	167.8	148.0	113.9	52.4	32.9
0.4	308.7	257.9	176.2	86.5	49.6
0.5	386.9	332.1	231.8	117.1	62.7
y=a(x)+b	y=847.32(x) -35.74	y=709.82(x) -25.12	y=446.82(x) +3.44	y=226.04(x) -0.19	y=117.89(x) +3.23
r^2	0.998	0.999	0.996	0.988	0.999

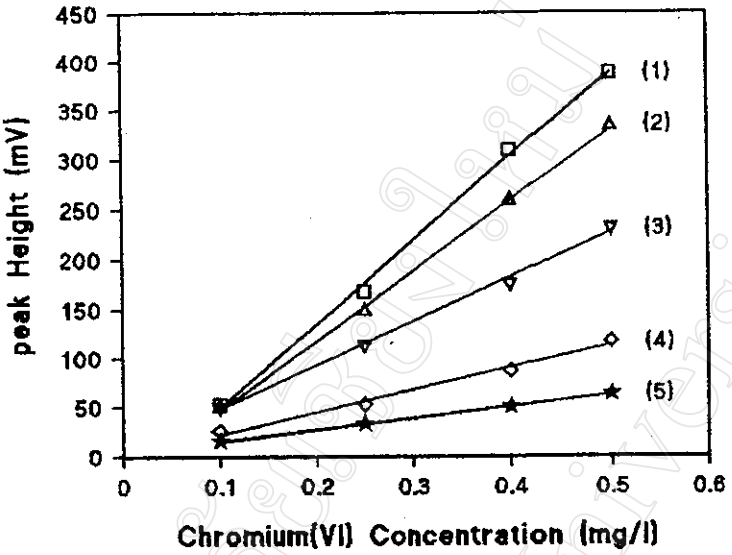

Figure 2.30 Effect of DPC concentration on peak height; DPC concentrations: (1) 0.005, (2) 0.01, (3) 0.05, (4) 0.10 and (5) 0.15% (w/v).

2.5.3.3 Effect of Acid Concentration of DPC Solution

Using the conditions described in 2.5.3.2, a blank and 0.1 mg/l of standard Cr(VI) solution were tried with various acid concentrations of H_2SO_4 and HNO_3 media. The results are shown in Table 2.41, Table 2.42 and Figure 2.31. The results indicate that HNO_3 media should be used as giving the highest peak heights. The HNO_3 concentrations of 0.8 to 1.7 M gave a higher peak height. 1.0 M HNO_3 was then used for further investigation.

Table 2.41 Effect of H_2SO_4 concentration in DPC solution on peak height; mean of triplicate injections.

H_2SO_4 (M)	Peak height (mV)		
	Blank	0.1 mg Cr^{6+}/l	Corrected for blank
0.2	178.6	215.5	36.9
0.4	152.0	210.3	58.3
0.6	137.7	205.2	67.5
0.8	136.1	217.1	81.0
1.0	144.1	219.4	75.3
1.2	132.1	202.4	70.3

Table 2.42 Effect of HNO_3 concentration in DPC solution on peak height; mean of triplicate injections.

HNO_3 (M)	Peak height (mV)		
	Blank	0.1 mg Cr^{6+}/l	Corrected for blank
0.1	125.8	152.4	26.6
0.2	134.9	219.4	84.5
0.3	136.1	240.1	104.0
0.4	137.7	252.8	115.1
0.5	141.7	254.0	112.3
0.6	132.9	250.0	117.1
0.8	145.6	273.8	128.2
1.0	146.8	285.7	138.9
1.3	138.9	276.6	137.7
1.5	145.6	284.5	138.9
1.7	142.9	277.8	134.9

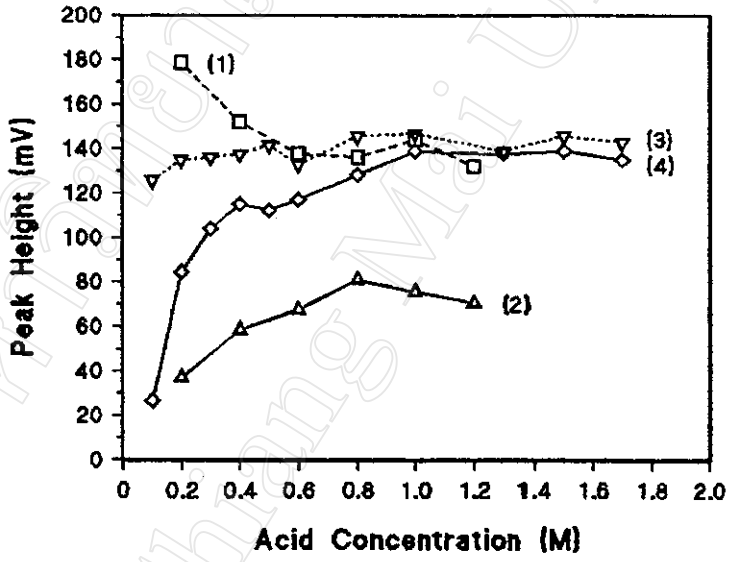

Figure 2.31 Effect of acid concentration on peak height for (1) blank, H_2SO_4 media , (2) 0.1 mg Cr^{6+}/l, H_2SO_4 media, (3) blank, HNO_3 media and (4) 0.1 mg Cr^{6+}/l, HNO_3 media.

2.5.3.4 Effect of the GBC Length

The effect of the GBC length was studied. Using the conditions described in 2.5.3.3, a blank and 1.0 mg/l of standard Cr(VI) were tried. The results are shown in Table 2.43 and Figure 2.32. The results indicate that 2.0 cm of GBC length should be used as giving an acceptable peak height, sharp peaks and high sample throughput.

Table 2.43 Effect of the GBC length on peak height; mean of triplicate injections.

GBC length (cm)	Cr^{6+} (mg/l)	Peak height (mV)	Peak height corrected for blank (mV)
2.0	blank	83.3	-
	1.0	422.6	339.3
5.0	blank	81.4	-
	1.0	390.9	309.5
10.0	blank	75.4	-
	1.0	418.7	343.3
15.0	blank	43.7	-
	1.0	297.6	253.9

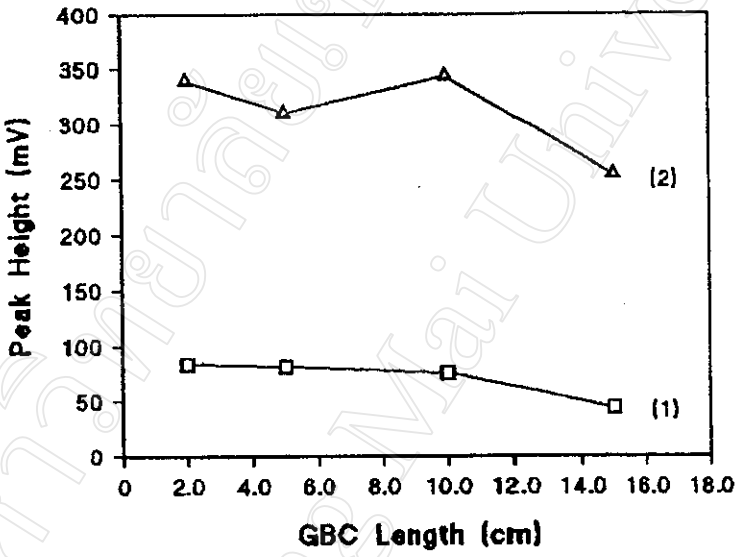

Figure 2.32 Effect of the GBC length on peak height for (1) blank and (2) 1.0 mg Cr^{6+}/l.

2.5.3.5 Effect of the RC Length

The effect of the RC length was studied. Using the conditions described in 2.5.3.4, a blank 0.1 and 1.0 mg/l of standard Cr(VI) solutions were used. The results are shown in Table 2.44 and Figure 2.33. The results indicate that 150 cm of RC length should be used as giving an acceptable peak height and blank peaks.

Table 2.44 Effect of the RC length on peak height; mean of duplicate injections.

RC length (cm)	peak height (mV)			peak height corrected	
	blank	0.1 mg Cr^{6+}/l	1.0 mg Cr^{6+}/l	0.1 mg Cr^{6+}/l	1.0 mg Cr^{6+}/l
50	59.5	91.3	448.4	31.8	388.9
100	51.6	105.2	504.0	53.6	452.4
150	61.5	97.2	527.8	35.7	466.3
200	59.5	79.4	504.0	19.9	444.5

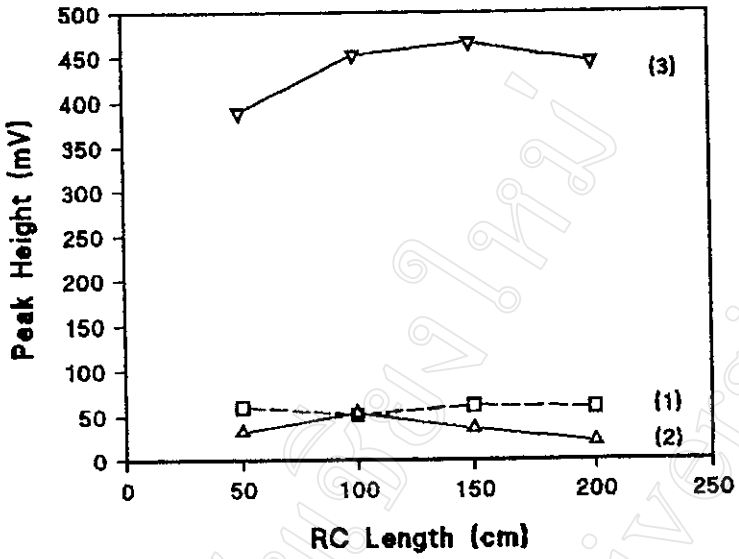

Figure 2.33 Effect of the RC length on peak height for (1) blank, (2) 0.1 and (3) 1.0 mg Cr^{6+}/l.

2.5.3.6 Summary of Conditions Used for Cr(VI) Determination

The recommended FIA manifold is depicted in Figure 2.28(a) and optimum conditions are summarized in Table 2.45.

Table 2.45 Condition used for the determination of chromium(VI)

reagent R1	0.01% (w/v) DPC + 1.0 M HNO_3
flow rate of methanol	3.9 ml/min
flow rate of R1	3.9 ml/min
flow rate of sample	3.9 ml/min
C18 column length	3 cm (i.d.= 1.5 mm)
loading time on C18 SPE column	1 min
flow through cell volume	30 µl (path length = 1 cm)
RC length (before injection valve)	150 cm (i.d.= 0.5 mm)
GBC length (after injection valve)	2 cm (i.d.= 0.35 cm)
LED color of colorimeter detector	green
sensitivity of recorder	1000 mV
chart speed of recorder	0.5 cm/min

2.5.3.7 Calibration Curve and Detection Limit

Using the optimum FIA system described in 2.5.3.6, loading time on C18 SPE column was either 40 or 60 sec. The results are shown in Table 2.46, Figure 2.34 and Figure 2.35. The results indicate that 60 sec of loading time should be used as giving higher slope of the calibration curve. Linearity was obtained in the range of 0.01 - 0.4 mg Cr^{6+}/l (detection limit = 0.02 mg Cr^{6+}/l , described in Appendix J) for the loading time of 60 sec and 0.01 - 0.4 mg Cr^{6+}/l (detection limit = 0.04 mg Cr^{6+}/l) for the loading time of 40 sec.

Table 2.46 Calibration curve for chromium(VI); mean of triplicate injections.

Cr^{6+} (mg/l)	Peak height corrected for blank (mV)	
	Loading time (sec)	
	40*	60**
0.01	7.9	3.2
0.02	14.7	14.7
0.05	34.5	48.8
0.08	66.7	93.3
0.10	94.4	127.0
0.15	168.7	211.5
0.20	248.8	292.5
0.40	540.9	624.2

* A blank : 170.6 mV.
** A blank : 166.7 mV.

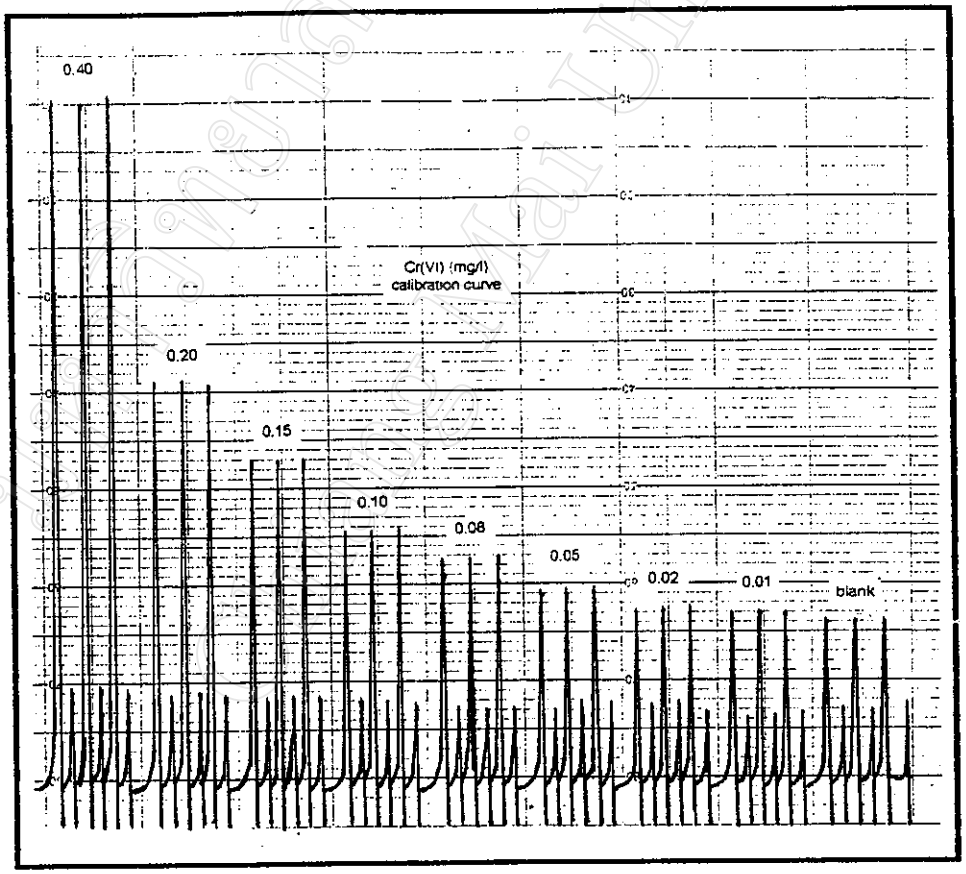

Figure 2.34 FIA signals for the determination of chromium(VI) using 60 sec loading time.

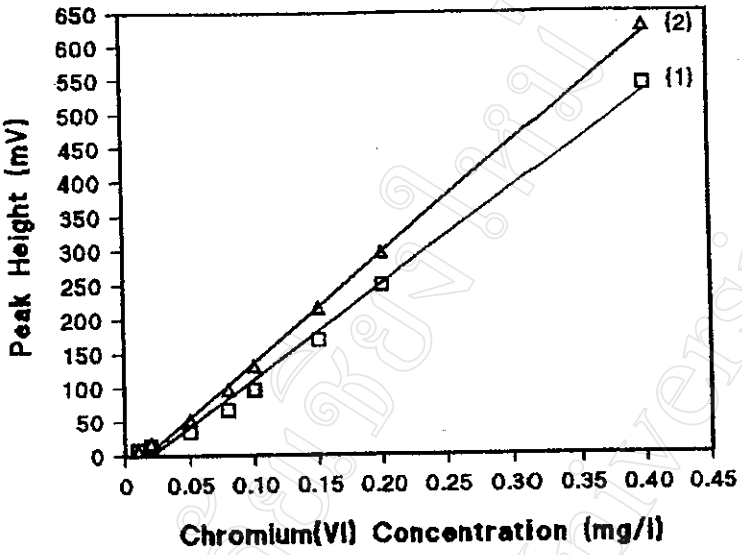

Figure 2.35 Effect of loading time on the calibration curve ; Loading time: (1) 40 sec [y = 1396.56(x) - 29.24, r^2 = 0.993] and (2) 60 sec [y = 1610.02(x) - 26.36, r^2 = 0.998].

2.5.3.8 Precision

Using the optimum FIA condition described in 2.5.3.6. The precision of the condition used was determined by repeat injecting 0.1 mg/l Cr(VI) standard solution for 20 replicates. The results are shown in Table 2.47. The relative standard deviation (RSD) was found to be 1.5 %.

Table 2.47 Precision study using 0.1 mg Cr^{6+}/l, n = 20.

* Peak height corrected for blank (mV)					Mean (x)	SD	%RSD
142.9	142.9	142.9	146.8	146.8	144.8	2.2	1.5
146.8	142.9	146.8	144.8	146.8			
142.9	138.9	144.8	144.8	142.9			
146.8	146.8	146.8	146.8	144.8			

* A blank : 154.8 mV.

2.5.3.9 Interference Studies

The effect of interfering ions was studied. Using the optimum conditions described in 2.5.3.6, a blank and 0.1 mg/l of standard Cr(VI) solutions containing various other interfering cations and anions were tried. The results obtained are shown in Table 2.48 and summarized in Table 2.49. The interfering ions were found to be sulfate, nitrite, cobalt(II) and iron(II). Iron(II) is a particular case since its shows a strong negative influence at approximately 5 times concentration higher than of Cr(VI) (a relative error less than ± 5%). This may be explained that iron(II) can easily reduce Cr(VI). Fortunately, high concentrations of iron (II) are usually not found in water sample.

Table 2.48 Effect of interference study for chromium(VI) concentration of 0.10 mg/l; mean of triplicate injections.

Ion	Added as	Concentration added (mg/l)	Peak height (mV)	% relative error
none	-	-	281.8	-
Na^+	NaCl	50	281.8	0
		100	285.7	+1.4
		500	288.1	+2.2
K^+	KCl	50	286.9	+1.8
		100	286.9	+1.8
		500	294.8	+4.6
Mg^{2+}	$MgCl_2$	50	281.8	0
		100	281.8	0
		500	292.5	+3.8
Ca^{2+}	$CaCO_3$	50	282.9	+0.4
		100	288.5	+2.4
		500	294.8	+4.6
Mn^{2+}	$MnSO_4$	50	282.5	+0.3
		100	288.5	+2.4
		500	294.8	+4.6
Co^{2}	$CoSO_4$	50	282.9	+0.4
		100	301.6	+7.0
		500	302.8	+7.5
Ni^{2+}	$NiSO_4$	50	281.8	0
		100	289.7	+2.8
		500	290.9	+3.2
Cu^{2+}	$CuSO_4$	50	281.8	0
		100	284.5	+1.0
		500	292.5	+3.8
Zn^{2+}	$ZnSO_4$	50	289.7	+2.8
		100	293.7	+4.2
		500	297.6	+5.6
Cd^{2+}	$CdSO_4$	50	282.9	+0.4
		100	285.7	+1.4
		500	288.5	+2.4
Pb^{2+}	$Pb(CH_3COO)_2$	50	293.7	+4.2
		100	273.8	-2.8
		500	272.6	-3.3

Table 2.48 (Continued)

Ion	Added as	Concentration added (mg/l)	Peak height (mvo)	% relative error
Fe^{2+}	$FeSO_4.(NH_4)_2SO_4$	0.5	278.6	- 1.1
		1	222.2	- 21.1
		5	192.5	- 31.7
		10	146.8	- 47.9
Fe^{3+}	$Fe(NO_3)_3$	40	282.9	+ 0.4
		50	284.5	+ 1.0
		100	321.4	+ 14.1
Cr^{3+}	$CrCl_3$	50	276.6	- 1.8
		100	280.6	- 0.4
		500	286.9	+ 1.8
Al^{3+}	$Al(NO_3)_3$	50	279.8	- 0.7
		100	284.9	+ 1.1
		500	286.9	+ 1.8
Cl^-	NaCl	50	281.8	0
		100	278.6	- 1.1
		500	282.9	+ 0.4
NO_2^-	$NaNO_2$	5	276.6	- 1.8
		10	269.8	- 4.2
		20	261.9	- 7.1
		100	185.3	- 34.2
NO_3^-	KNO_3	50	275.0	- 2.4
		100	285.7	+ 1.4
		500	275.8	- 2.1
SO_4^{2-}	$CaSO_4$	50	282.9	+ 0.4
		100	267.1	- 5.2
		500	263.1	- 6.6
PO_4^{3-}	$KHPO_4$	50	281.8	0
		100	277.8	- 1.4
		500	281.8	0

Table 2.49 Summary of the interference effect for the 0.1 mg Cr^{6+}/l.

Interference ions	* Tolerable concentration ratio (mg/l) of [ion] / [Cr^{6+}]
Na^+, K^+, Mg^{2+}, Ca^{2+}, Mn^{2+}, Ni^{2+}, Cu^{2+}, Cd^{2+}, Pb^{2+}, Cr^{3+}, Al^{3+}, Cl^-, NO_3^-, PO_4^{3-}	≥ 5,000
Zn^{2+}, Fe^{3+}	1,000
SO_4^{2-}, Co^{2+}	500
NO_2^-	100
Fe^{2+}	5

* A concentration of anion is refered to interfere when causing a relative error of more than ± 5% with respect to the signal of the chromium(VI) alone.

2.5.4 Optimization of Sequential Determination of Chromium(VI) and Chromium(III)

Flow injection procedure for the sequential determination of Cr(VI) and Cr(III) based on the Cr-DPC system by oxidation with cerium(IV) as described in 2.5 and 2.5.1.

Preliminary conditions were set as following :

reagent R1	0.1%(w/v) DPC + 1 M HNO_3
flow rate of methanol	3.9 ml/min
flow rate of R1	3.9 ml/min
flow rate of R2	2.3 ml/min
flow rate of sample	2.6 ml/min
flow rate of H_2O	2.3 ml/min
C18 SPE column length	3 cm (i.d. = 1.5 mm)
loading time on C18 SPE column	1 min
flow through cell volume	30 µl (path length = 1 cm)
RC1 length	120 cm (i.d. = 0.5 mm)
RC2 length	150 cm (i.d. = 0.5 mm)
GBC length	2 cm (i.d.= 0.35 cm)
LED color of the detector	green
sensitivity of recorder	1000 mV
chart speed of recorder	0.5 cm/min

2.5.4.1 Effect of Cerium(IV) Concentration

Using the manifold as shown in Figure 2.28(b) ; various Ce(IV) concentration were investigated. The results are shown in Table 2.50 and Figure 2.36. A concentration of 1.2 % (w/v) cerium(IV) was chosen as giving the highest peak height and slope.

Table 2.50 Effect of cerium(IV) concentration on peak height; mean of triplicate injections.

Cr^{3+} (µg/l)	Peak height corrected for blank (mV)						
	Cerium (IV) (%w/v)						
	0.1	0.3	0.6	0.8	1.0	1.2	2.0
blank	158.7	174.6	212.3	218.3	222.2	238.1	223.4
0.1	15.9	13.9	7.1	17.1	29.8	31.8	25.8
0.25	26.6	32.9	45.6	46.4	69.4	75.4	56.4
0.5	35.7	68.7	104.0	113.9	138.9	138.9	104.0
1.0	63.5	134.9	215.1	230.2	254.0	284.5	209.1
y=a(x)+b	y=51.52 (x)+11.60	y=135.06 (x)+0.14	y=229.72 (x)-13.30	y=239.77 (x)-8.99	y=248.85 (x)+7.93	y=279.68 (x)+3.30	y=203.38 (x)+4.76
r^2	0.993	0.999	0.999	0.999	0.998	0.999	0.998

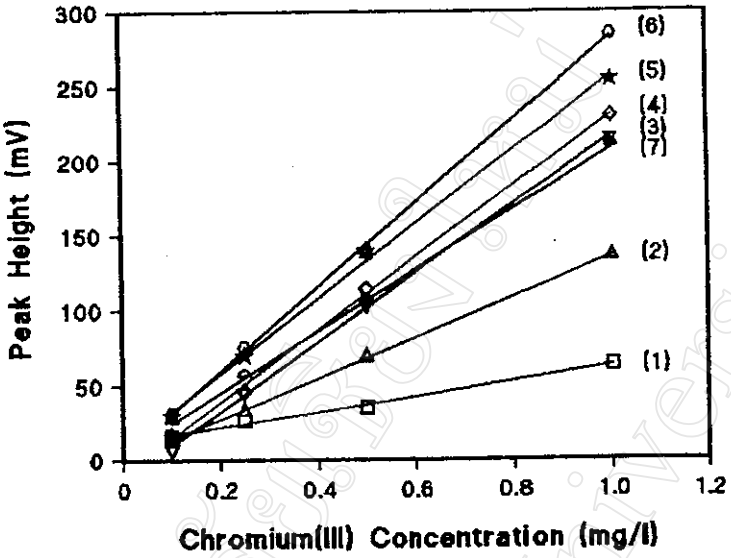

Figure 2.36 Effect of cerium(IV) concentration on peak height; Cerium(IV) concentration: (1) 0.1, (2) 0.3, (3) 0.6, (4) 0.8, (5) 1.0, (6) 1.2 and (7) 2.0 %(w/v).

2.5.4.2 Effect of H_2SO_4 Acid Concentration in the Reagent R2

Using the conditions described in 2.5.4.1, various H_2SO_4 concentrations were tried. The results are shown in Table 2.51 and Figure 2.37. It was found that decrease in the H_2SO_4 acid concentration, the peak height increased. A concentration of 0.3 M H_2SO_4 was chosen, the cerium(IV) hydroxide precipitated if the concentration was less than this, as giving the highest peak height and slope.

Table 2.51 Effect of H_2SO_4 acid concentration in the reagent R2 on peak height; mean of triplicate injections.

Cr^{3+} (mg/l)	Peak height corrected for blank (mV)			
	H_2SO_4 (M)			
	0.3	0.5	1.0	1.5
blank	236.1	215.5	239.3	248.0
0.1	47.6	34.5	14.7	7.1
0.25	103.2	74.2	27.8	6.0
0.5	186.5	127.0	46.4	11.1
1.0	361.9	234.1	67.5	27.0
y=a(x)+b	y=347.69(x) +13.99	y=219.15(x) +16.09	y=57.37(x) +12.57	y=23.73(x) +1.82
r^2	0.999	0.999	0.971	0.928

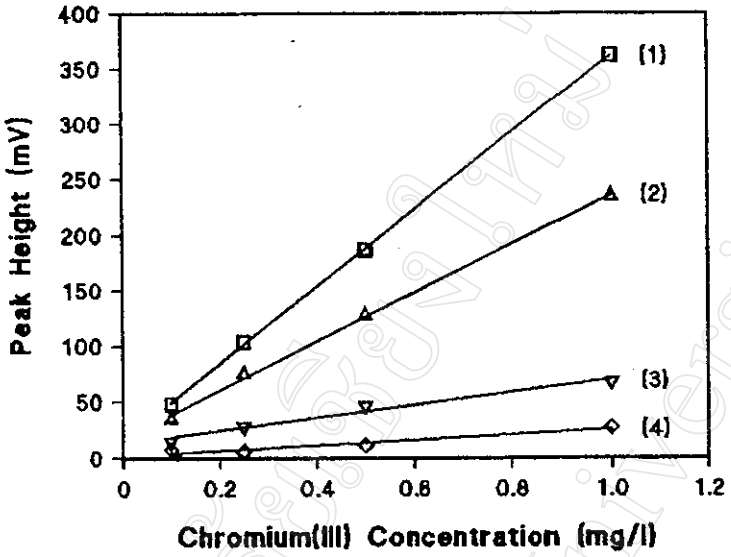

Figure 2.37 Effect of H_2SO_4 acid concentration in reagent R2 on peak height ; H_2SO_4 concentration : (1) 0.3, (2) 0.5, (3) 1.0 and (4) 1.5 M.

2.5.4.3 Effect of DPC Concentration

Using the condition described in 2.5.4.2, various DPC concentrations were performed. The results are shown in Table 2.52 and Figure 2.38. A concentration of 0.1 % (w/v) DPC was chosen as giving the highest peak height and slope.

Table 2.52 Effect of DPC concentration on peak height ; mean of triplicate injections.

Cr^{3+} (mg/l)	Peak height corrected for blank (mV)				
	DPC (% w/v)				
	0.05	0.10	0.13	0.15	0.20
blank	197.2	250.0	242.1	246.0	285.7
0.1	15.1	15.9	57.5	35.7	21.8
0.25	16.3	97.2	115.1	101.2	51.6
0.5	25.0	210.3	196.4	182.5	101.2
1.0	27.0	451.2	392.0	343.3	201.2
y=a(x)+b	y=13.95(x)+ 14.40	y=479.76(x)- 28.24	y=370.04(x) +19.11	y=336.03(x) +10.01	y=199.35(x) +1.75
r^2	0.835	0.999	0.999	0.997	0.999

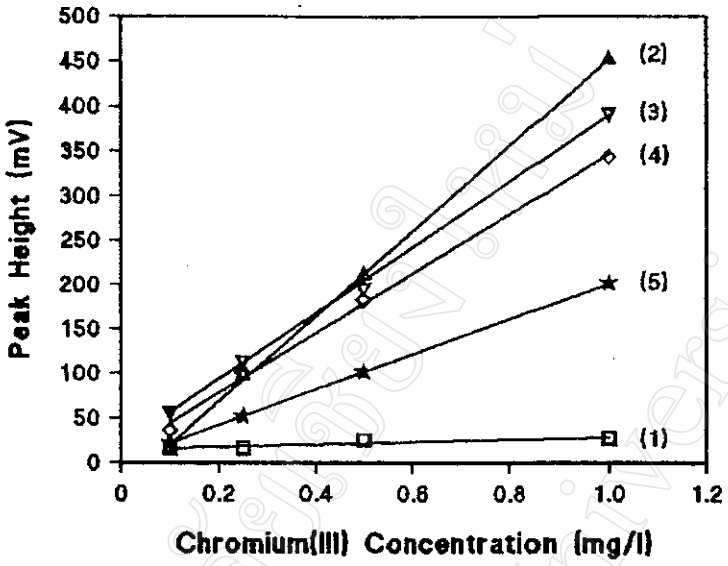

Figure 2.38 Effect of DPC concentration on peak height ; DPC concentrations : (1) 0.05, (2) 0.10, (3) 0.13, (4) 0.15 and (5) 0.20 % (w/v).

2.5.4.4 Effect of the RC1 Length

The effect of the RC1 length was studied by using the conditions described in 2.5.4.3. The results are shown in Table 2.53 and Figure 2.39. The results indicate that 120 cm of RC1 length should be used as giving the highest peak height and slope.

Table 2.53 Effect of the RC1 length on peak height ; mean of triplicate injections.

Cr^{3+} (mg/l)	Peak height corrected for blank (mV)		
	RC1 (cm)		
	50	120	200
blank	257.9	255.2	248.0
0.1	31.8	16.7	19.9
0.25	49.6	46.4	37.7
0.5	83.3	107.9	83.7
1.0	154.8	204.0	172.6
y=a(x)+b	y=137.64(x)+16.22	y=209.44(x)-3.12	y=172.82(x)-1.46
r^2	0.999	0.997	0.997

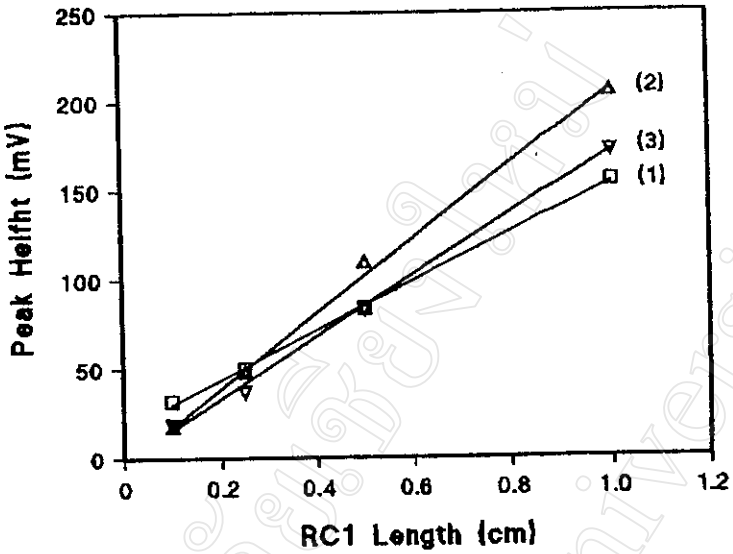

Figure 2.39 Effect of the RC1 length on peak height ; RC1 lengths : (1) 50, (2) 120 and (3) 200 cm.

2.5.4.5 Effect of the Aqueous Methanol Concentration

Using the condition described in 2.5.4.4, the eluents of various concentrations of aqueous methanol were tried. The results are shown in Table 2.54 and Figure 2.40. It was found that a concentration of 70-99.8 % (v/v) methanol should be used as giving an acceptable peak height. However, 80 % (v/v) of methanol was chosen to give a good compromise.

Table 2.54 Effect of the aqueous methanol concentration on peak height ; mean of triplicate injections.

Methanol (% v/v)	Peak height (mV)		
	Blank	0.8 mg Cr^{3+}/l	Corrected for blank
30	117.9	259.9	142.0
50	143.7	293.3	149.6
70	163.9	384.9	221.0
80	185.3	403.2	217.9
90	203.2	432.5	229.3
absolute (99.8)	234.1	447.2	213.1

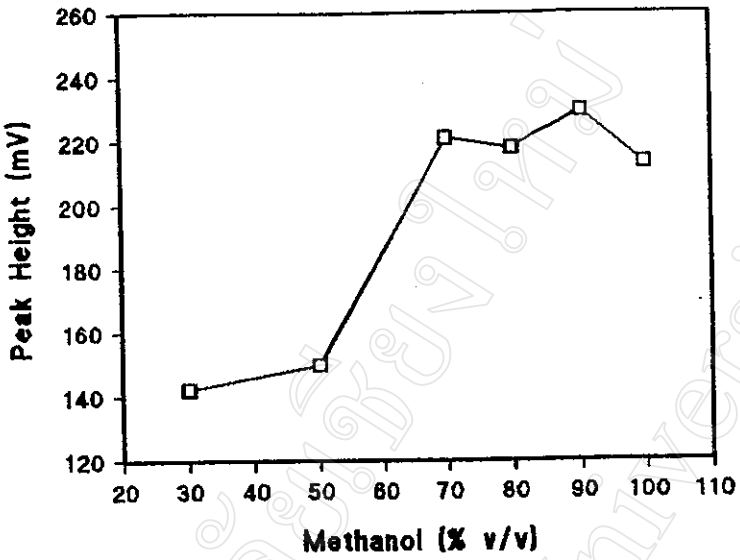

Figure 2.40 Effect of the aqueous methanol concentration on peak height ; Methanol concentrations : (1) 30, (2) 50, (3) 70, (4) 80, (5) 90 and (6) absolute (99.8) % (v/v).

2.5.4.6 Effect of pH in a Mixture of Chromium(VI) and Chromium(III)

Using the condition described in 2.5.4.6, a blank and mixture of 0.3 mg/l Cr(VI) and 0.3 mg/l Cr(III) in various pHs of H_2SO_4 acid media were tried. The results are shown in Table 2.55 and Figure 2.41. The results indicate that pH of 2.0-2.5 of a mixture of Cr(VI) an Cr(III) solution should be used as giving an acceptable peak height and blank.

Table 2.55 Effect of pH in a mixture of 0.3 mg Cr^{6+}/l and 0.3 mg Cr^{3+}/l solution ; mean of triplicate injections.

H_2SO_4 (M)	Measured pH	Peak height (mV)					
		H_2O stream			the Ce(IV) reagent stream		
		Blank	the mixture	corrected for blank	Blank	the mixture	Corrected for blank
0.001	2.6	57.5	113.9	56.4	197.6	302.8	105.2
0.005	2.1	58.7	114.3	55.6	196.4	309.5	113.1
0.01	1.8	58.3	108.3	50.0	173.4	283.7	110.3
0.05	1.3	55.6	106.4	50.8	158.7	269.8	111.1
0.10	1.2	55.6	98.4	42.8	171.4	249.2	77.8
0.15	1.1	56.8	89.3	32.5	179.4	225.0	45.6
0.20	0.9	54.8	89.3	34.5	208.3	229.4	21.1

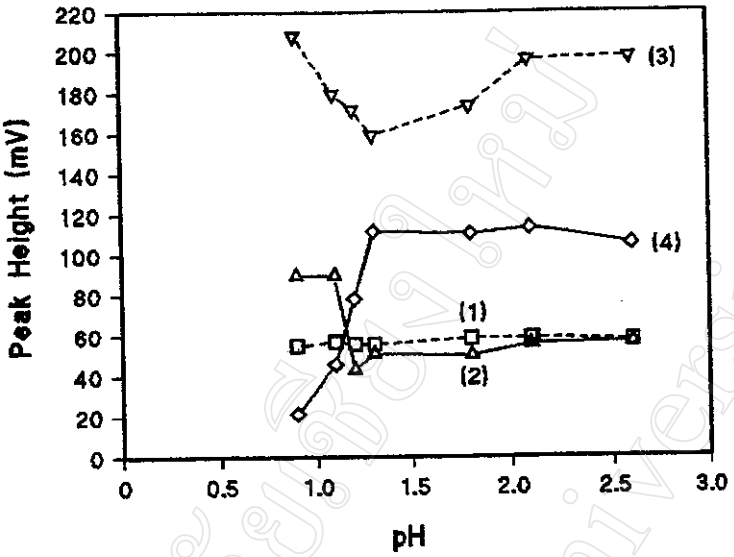

Figure 2.41 Effect of pH in a mixture of 0.3 mg Cr^{6+}/l and 0.3 mg Cr^{3+}/l solution : (1) blank, H_2O stream, (2) the mixture, H_2O stream, (3) blank, the Ce(IV) reagent stream (R2) and (4) the mixture, the Ce(IV) reagent stream.

2.5.4.7 Effect of Loading Time on Calibration Curve

Different loading time was tried. Using the conditions described in 2.5.4.6, a blank and a series of standard Cr(VI) solutions were used for calibration curve. The results are shown in Table 2.56 and Figure 2.42. It was found that decrease in loading time on C18 SPE column, the peak height decreased. In this case, 60 sec of retained time was chosen as giving an acceptable peak height. It is too slow, if the retained time higher than 1 min.

Table 2.56 Different loading time ; mean of triplicate injections.

Cr^{6+} (mg/l)	Peak height corrected for blank (mV)					
	H_2O stream			the Ce(IV) reagent stream		
	Loading time (sec)			Loading time (sec)		
	15	30	60	15	30	60
blank	72.6	69.1	67.9	113.9	130.9	154.8
0.1	30.6	31.7	32.9	19.1	15.9	40.9
0.2	51.2	69.8	85.3	32.9	38.5	75.4
0.5	164.3	194.1	242.9	68.7	95.2	153.6
1.0	328.2	415.1	515.5	105.6	162.7	269.8

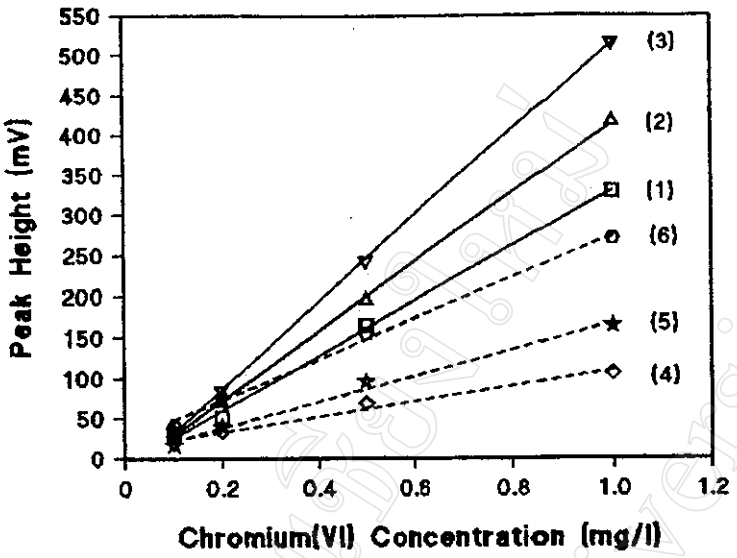

Figure 2.42 Calibration curve : Different loading time ; (1),(2),(3) 15, 30 and 60 sec, respectively using H_2O stream and (4),(5),(6) 15, 30 and 60 sec, respectively using the Ce(IV) reagent stream (R2).

In order to see if a single standard solution for calibration is possible or not. A 1.0 mg Cr^{6+}/l was tried for different loading periods. The expected µg of Cr sorbed on the column is assumed to be : loading time (x sec) × flow rate (2.6 ml/60 sec) × concentration (1 µg/ml) as summarized in Table 2.58. A curve plotted using peak height versus the µg of Cr(VI) (Figure 2.43(1)). A straight line was not obtained. This indicated that a single standard solution calibration cannot be applicable. Conventional calibration curve was made using a series of standard solutions obtained by similar calculation (Table 2.57). A similar curve was plotted (Figure 2.43(2)). A practical straigth-line was obtained.

Table 2.57 Two sets of experiments ; a single standard solution and a constant loading time.

Single standard				Conventional curve			
Time (sec)	Cr^{6+} (mg/l)	Cr^{6+} (µg)	Peak height corrected for blank (mV)	Time (sec)	Cr^{6+} (mg/l)	Cr^{6+} (µg)	Peak height corrected for blank (mV)
-	* blank	-	83.3	60	blank	-	79.4
5	1.0	0.2	23.8	60	0.1	0.3	19.1
10	1.0	0.4	161.5	60	0.3	0.8	59.5
20	1.0	0.9	257.9	60	0.5	1.3	111.1
30	1.0	1.3	318.7	60	0.8	2.1	231.4
40	1.0	1.7	390.1	60	1.0	2.4	257.9
60	1.0	2.6	444.4	60	1.2	2.9	397.6
90	1.0	3.9	464.3	60	1.4	3.4	495.2
120	1.0	5.2	402.8	60	1.6	3.9	551.6
180	1.0	7.8	341.3	60	2.0	4.8	633.7

* blank for 30, 60 and 120 sec loading periods were the same.

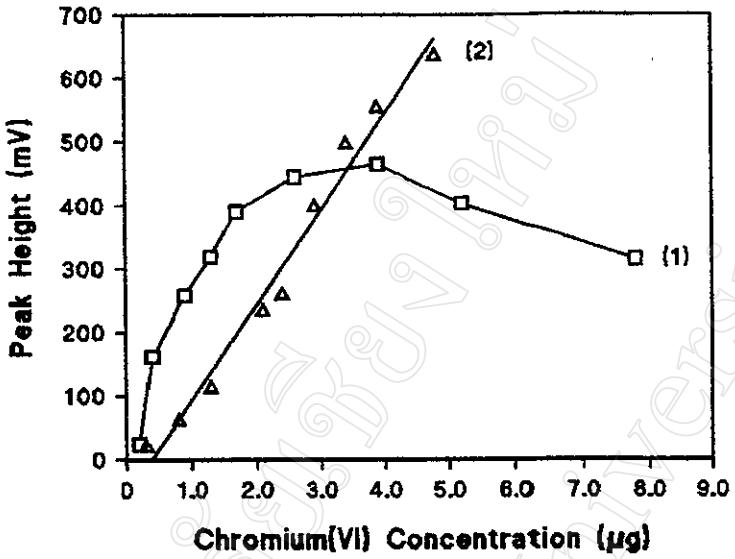

Figure 2.43 (1) a single standard and (2) conventional calibration.

2.5.4.8 Summary of the Conditions Used

The recommended FIA manifold is depicted in Figure 2.28(b) and the optimum conditions are summarized in Table 2.58.

Table 2.58 Condition for the sequential determination of chromium(VI) and chromium(III)

reagent R1	0.1 % (w/v) DPC + 1 M HNO_3
reagent R2	1.2 % (w/v) Ce(IV) + 0.3 M H_2SO_4
flow rate of methanol	3.9 ml/min
flow rate of R1	3.9 ml/min
flow rate of R2	2.3 ml/min
flow rate of sample	2.6 ml/min
flow rate of H_2O	2.3 ml/min
C18 SPE column length	3 cm (i.d.= 1.5 mm)
retained time on C18 SPE column	1 min
flow through cell volume	30 µl (path length = 1 cm)
RC1 length	120 cm (i.d.= 0.5 mm)
RC2 length	150 cm (i.d.= 0.5 mm)
GBC length	2 cm (i.d.= 0.35 cm)
LED color of colorimeter	green
sensitivity of recorder	1000 mV
chart speed of recorder	0.5 cm/min

2.5.4.9 Calibration Curve and Detection Limit

Using the optimum FIA system described in 2.5.4.8, the calibration curve and detection limit of the condition used were studied. The results are shown in Table 2.59 ,Figure 2.44 and Figure 2.45. Curve (1) in the Figure 2.45 is a plot of peak height of the signals (with respect to water stream in operation (see section 2.5.2)) versus Cr(VI) concentration, i.e. this curve is for Cr(VI) determination. Curve (2) in the Figure 2.45 is a plot of the signals (with respected to the R2 stream in operation) versus Cr(VI) concentration and the curve (3) is a plot of the signals due to the operation using the R2 stream versus Cr(III) concentration. The 3 curves were used for evaluation of the Cr(VI) and Cr(III) concentration in a mixture (see Appendix I). From the curves detection limit for each curve was calculated (Appendix J) : 0.05 mg Cr^{6+}/l, 0.04 mg Cr^{6+}/l and 0.08 mg Cr^{3+}/l respectively.

Table 2.59 Calibration curve for Cr(VI) and Cr(III) standard solution ; mean of triplicate injections.

Concentration (mg/l)		the H_2O stream peak height (mV)		the R2 reagent stream peak height (mV)	
Cr^{6+}	Cr^{3+}	mean	corrected for blank	mean	corrected for blank
blank	0	82.1	-	205.2	-
0.1	0	115.1	33.0	232.9	27.7
0.3	0	188.5	106.4	297.6	92.4
0.5	0	281.8	199.7	369.8	164.6
0.8	0	394.1	312.0	464.3	259.1
1.0	0	472.2	390.1	521.8	316.6
0	0.1	-	-	231.4	26.2
0	0.3	-	-	282.9	77.7
0	0.5	-	-	339.3	134.1
0	0.8	-	-	440.5	235.3
0	1.0	-	-	480.2	275.0

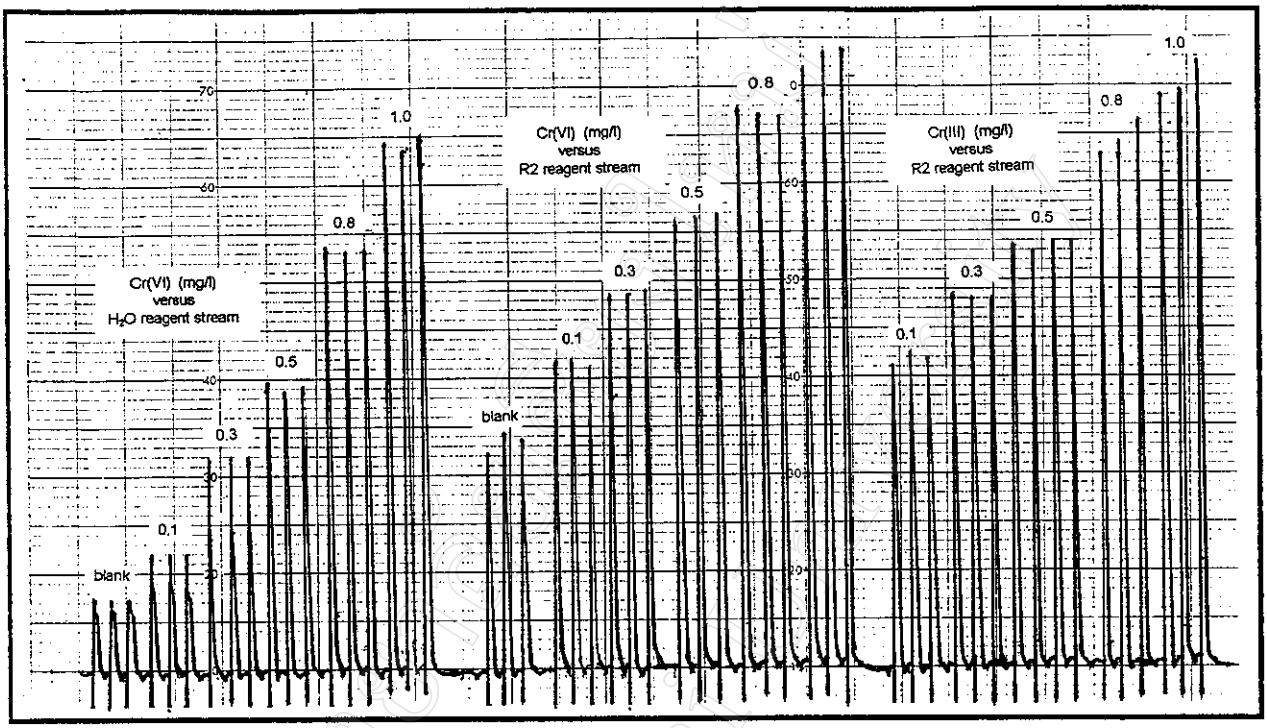

Figure 2.44 FIA signals for the chromium determination ; (a) Cr(VI), H_2O stream, (b) Cr(VI), R2 reagent stream, (c) Cr(III), R2 reagent stream.

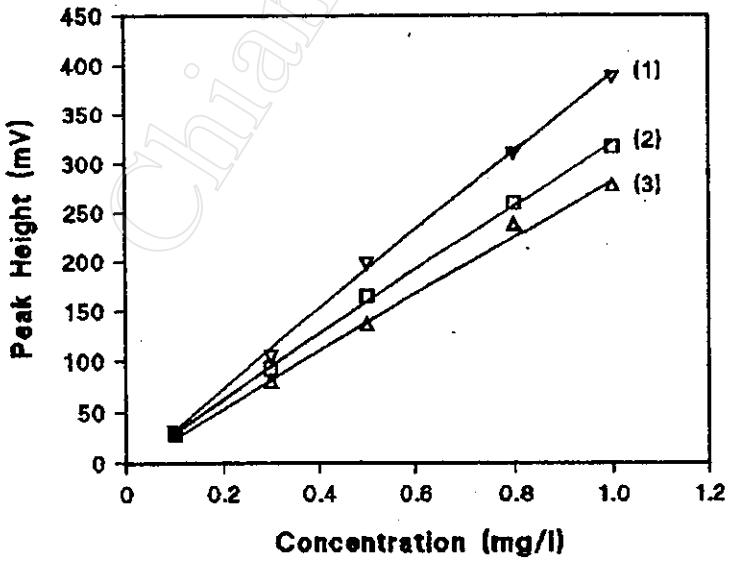

Figure 2.45 Calibration curve for chromium standards (n=3) : (1) Cr(VI), H_2O stream, (2) Cr(VI), R2 reagent stream and (3) Cr(III), R2 reagent stream (see text).

2.5.4.10 Precision

Using the optimum FIA conditions described in 2.5.4.8, 20 injections for 0.1 mg/l of standard Cr(VI) solution using H_2O stream (% RSD = 5.6) and 0.4 mg/l of standard Cr(III) solution using R2 reagent stream (% RSD = 4.2) were made. The results are shown in Table 2.60.

Table 2.60 Precision study using 0.1 mg Cr^{6+}/l (n=20) and 0.4 mg Cr^{3+}/l (n=20).

	Peak height (mV)									
	0.1 mg Cr^{6+}/l using H_2O stream					0.4 mg Cr^{3+}/l using R2 reagent stream				
	95.2	91.3	91.3	95.2	97.2	313.5	285.7	277.8	273.8	313.5
	91.3	99.2	87.3	89.3	83.3	285.7	305.6	309.5	309.5	293.7
	81.4	97.2	87.3	91.3	81.4	297.6	289.7	297.6	293.7	289.7
	83.3	83.3	91.3	91.3	89.3	285.7	285.7	277.8	289.7	277.8
mean (x)	89.9					292.7				
S.D.	5.4					12.3				
% RSD	6.0					4.2				

2.5.4.11 Determination of Chromium(VI) and Chromium(III) in Drinking Water Sample

The recommended condition described in 2.5.4.8 was applied for the determination of Cr(III) and Cr(VI) in a drinking water sample, Aura, a mineral water. The sample was spiked with different standard Cr(III) and Cr(VI) amounts. Percentage recoveries were evaluated. The results are represented in Table 2.61.

Table 2.61 Determination of Cr(VI) and Cr(III) in drinking water samples ; mean of triplicate injections.

No.	Concentration spiked (mg/l)		Peak height (mV)				* Concentration found (mg/l)		% recovery	
			H_2O stream		R2 reagent stream					
	Cr^{6+}	Cr^{3+}	Mean	Corrected for blank	Mean	Corrected for blank	Cr^{6+}	Cr^{3+}	Cr^{6+}	Cr^{3+}
1	0	0	77.4	0	241.3	0	0	0	-	-
2	0.3	0	220.2	142.8	377.8	136.5	0.3	0	100	-
3	0.3	0.1	228.2	150.8	421.8	180.5	0.3	0.2	100	200
4	0.3	0.2	230.2	152.8	467.5	226.2	0.3	0.3	100	150
5	0.3	0.3	226.2	148.8	494.1	252.8	0.3	0.3	100	100
6	0.3	0.4	222.2	144.8	531.0	289.7	0.3	0.4	100	100
7	0	0.3	79.4	0	356.0	118.7	0	0.2	-	67
8	0.1	0.3	127.0	49.6	410.7	169.4	0.1	0.3	100	100
9	0.2	0.3	177.4	100.0	452.4	211.1	0.2	0.3	100	100
10	0.3	0.3	224.2	146.8	499.2	257.9	0.3	0.4	100	133
11	0.4	0.3	257.1	179.7	536.9	295.6	0.4	0.4	100	100
									x = 100	x = 117
									SD = 0	SD = 39
									%RSD = 0	%RSD = 34

* Calculation described in Appendix I.

2.6 Determination of Calcium

2.6.1 Determination of Calcium by Using Murexide

2.6.1.1 Absorption Spectra

The absorption spectra of the solution of calcium with murexide (0.01 %w/v) in ethylenediamine buffer (pH = 11) was studied by using UV-265 Shimadzu spectrophotometer. Absorption spectra are recorded at 360-700 nm (Figure 2.46). The maximum absorption wavelength is at 543 nm of murexide and at 506 nm of Ca(II)-murexide complex.

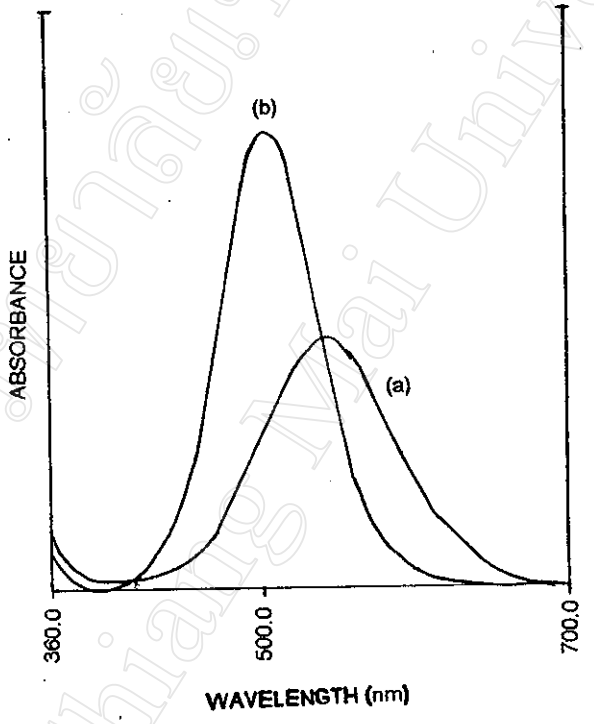

Figure 2.46 Absorption spectra of (a) murexide (using water as a reference) and (b) its calcium(II) complex (using the reagent blank as reference), buffer pH 11.

2.6.1.2 Manifold

A simple flow diagram of the system used shown in Figure 2.47 was adopted from spectrophotometric determination of calcium by flow injection analysis using murexide by Jakmunee and et.al [54].

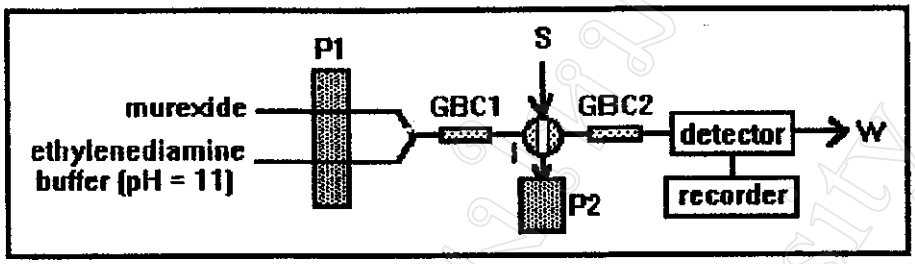

Figure 2.47 Flow diagram of the system ; P1 : peristaltic pump, P2 : aquarium pump, GBC1 and GBC2 : glass bead columns, S : sample, I : rotary injection valve and W : waste.

A sample was injected into a stream of murexide (violet) and ethylenediamine buffer (pH = 11). The red color complex was continuously monitored and recorded with a chart recorder. The complexation reaction between murexide and calcium(II) is 1:1 complexes [62] as following.

$$Ca^{2+} + Mu^{-} \rightleftharpoons Ca[Mu]^{+} \qquad (2.8)$$

(murexide) (red complex)

Preliminary conditions were used as following [54]:

ethylenediamine buffer (pH = 11)	2 M ethylenediamine + 0.17 M HCl
flow rate	4.0 ml/min
sample volume	100 μl (teflon tube)
GBC1 length	20 cm
GBC2 length	10 cm
LED color of colorimeter detector	green
sensitivity of recorder	1000 mV
chart speed of recorder	0.5 cm/min

2.6.1.3 Effect of Murexide Concentration

Using the manifold shown in Figure 2.47 and the conditions described above, various concentrations of murexide were tried. The results are shown in Table 2.62 and Figure 2.48. The results indicate that 0.03 % (w/v) of murexide should be used as giving an acceptable peak height.

Table 2.62 Effect of murexide concentration on peak height ; mean of triplicate injections.

Ca^{2+} (mg/l)	Peak height (mV) Murexide (% w/v)				
	0.005	0.01	0.02	0.03	0.04
40	300.4	239.3	80.6	45.8	0
60	308.7	261.9	129.8	50.4	0
80	310.7	261.9	146.8	79.4	10.7
100	322.6	269.1	156.0	109.1	21.0
120	324.2	274.6	173.4	111.1	31.8
140	328.6	271.0	179.8	120.2	42.5
160	336.5	269.1	185.7	122.2	48.8

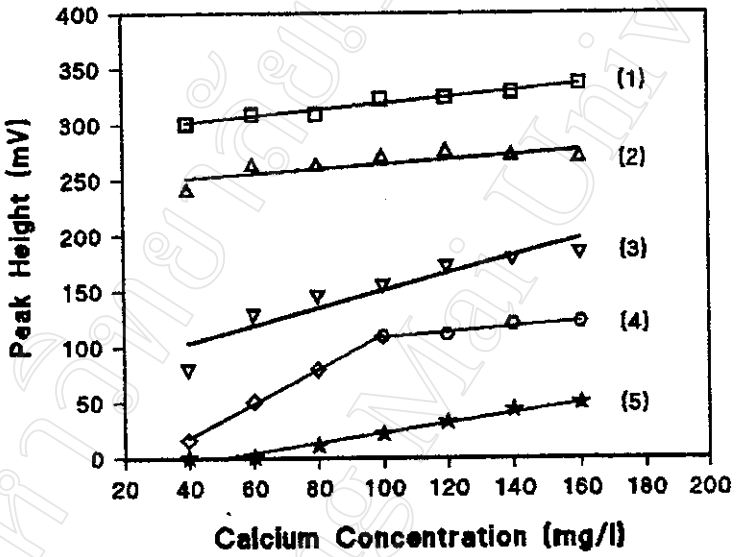

Figure 2.48 Effect of murexide concentration on peak height ; Murexide concentrations : (1) 0.005, (2) 0.01, (3) 0.02, (4) 0.03 and (5) 0.04 % (w/v).

2.6.1.4 Effect of Sample Volume

The effect of sample volume was studied, using the conditions described in 2.6.1.3. The results are shown in Table 2.63 and Figure 2.49. The results indicate that a sample volume of 100 µl should be used as its yield acceptable peak height and linear ranges , 40-120 mg/l and 120-160 mg/l.

Table 2.63 Effect of sample volume on peak height ; mean of triplicate injections.

Ca^{2+} (mg/l)	Peak height (mV)			
	Sample volume (µl)			
	100	200	250	300
40	11.9	82.1	113.1	144.8
60	35.3	137.7	164.7	179.4
80	71.4	165.5	171.8	193.3
100	95.2	177.4	179.8	201.2
120	123.0	186.5	185.3	211.1
140	131.0	191.3	196.4	207.5
160	141.7	393.7	197.2	214.3

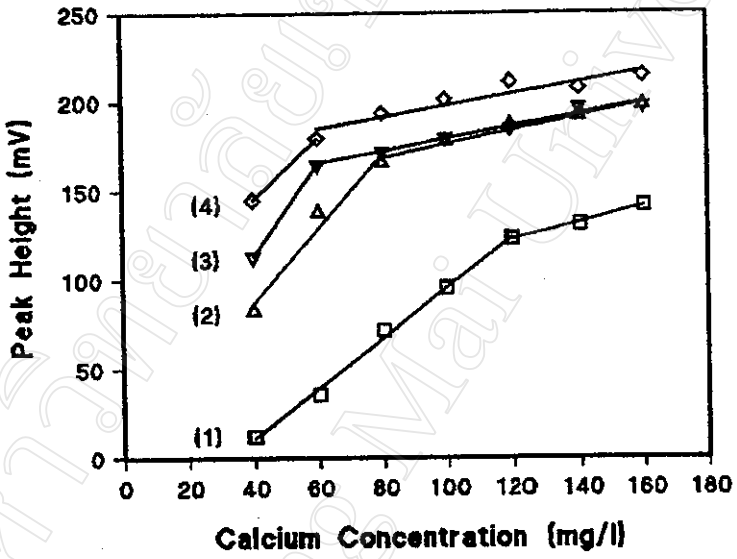

Figure 2.49 Effect of sample volume on peak height ; Sample volumes : (1) 100, (2) 200, (3) 250 and (4) 300 µl.

2.6.1.5 Effect of Flow Rates of Murexide and Ethylenediamine Buffer Streams

The effects of flow rates of murexide and ethylenediamine buffer streams were investigated, using the conditions described in 2.6.1.4. The results are shown in Table 2.64 and Figure 2.50. The results indicate that flow rate 3.3 of ml/min was chosen as giving the highest peak height.

Table 2.64 Effects of flow rates of murexide and ethylenediamine buffer streams on peak height ; mean of triplicate injections.

Flow rate (ml/min)	Peak height (mV) Ca^{2+} (mg/l)	
	80	160
2.2	99.2	163.5
3.3	103.2	176.6
4.0	96.0	162.7
4.9	101.2	137.7
7.9	89.3	129.0

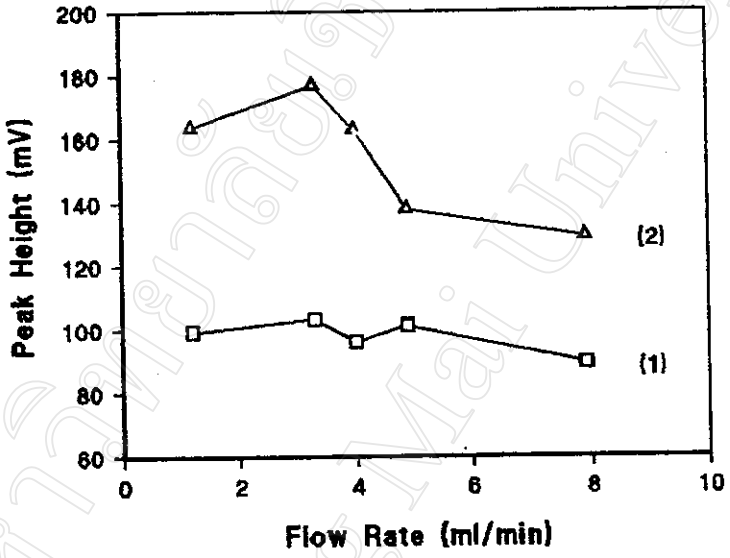

Figure 2.50 Effects of flow rates of murexide and ethylenediamine buffer streams on peak height for (1) 80 and (2) 160 mg Ca^{2+}/l.

2.6.1.6 Effect of LED Color

The effect of LED color of colorimeter was studied, using the conditions described in 2.6.1.5. The results are shown in Table 2.65 and Figure 2.51. The results indicate that the peak heights of Ca(II)-murexide complex are interfered by Mg(II)-murexide complex in this conditions. However, a green LED was chosen as giving higher peak height and more slope than a yellow color.

Table 2.65 Effect of LED color on peak height ; mean of triplicate injections.

Ca^{2+} (mg/l)	Peak height corrected for blank (mV)		Mg^{2+} (mg/l)	Peak height corrected for blank (mV)	
	LED colour			LED colour	
	green	yellow		green	yellow
blank	69.4	31.8	blank	73.4	33.7
20	23.0	15.9	20	31.8	17.9
40	38.9	25.8	40	61.5	36.5
60	64.7	40.9	60	92.1	48.4
80	83.3	55.6	80	121.0	66.3
100	105.2	68.7	100	146.8	79.4
slope	1.04	0.68	slope	1.45	0.76

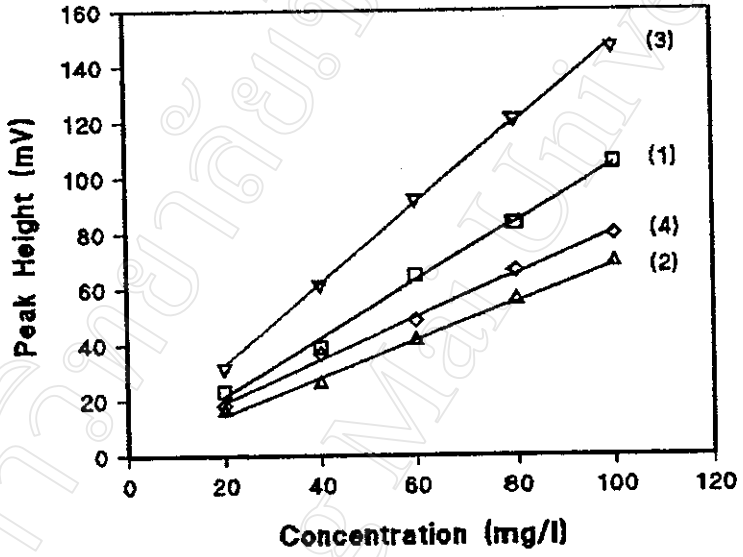

Figure 2.51 Effect of LED color on peak height (1) green , calcium, (2) yellow , calcium, (3) green , magnesium and (4) yellow , magnesium.

2.6.1.7 Effect of pH

This effect was first studied batchwise. The effect of pH of ethylenediamine buffer (pH = 9.0-12.5) on the absorption spectra of Ca(II)-murexide complex and Mg(II)-murexide complex were studied. A 50 ml solution was prepared by mixing 5 ml of 0.01 % (w/v) murexide, 10 ml of 10 M ethylenediamine, various volume (ml) of 6 M HCl and 4 ml of 8 mg Ca^{2+}/l or 8 mg Mg^{2+}/l. Absorption spectra were recorded at 360-700 nm. The results are shown in Table 2.66 and Figure 2.52. It was found that ethylenediamine buffer of pH 11.5-12.5 should be used as giving high blank corrected absorbance (A_1-A_2) and difference in the absorption maxima of Ca- and Mg-complexes is observed.

Table 2.66 Effect of pH on absorption maxima (λ) and absorbance (A).

pH	Ca(II)-murexide		Mg(II)-murexide		$/\lambda_1-\lambda_2/$ (nm)	A_1-A_2
	λ_1 (nm)	A_1	λ_2 (nm)	A_2		
9.0	506	0.406	534	1.462	28	-1.056
9.5	503	0.489	535	0.677	33	-0.188
10.0	503	0.710	538	1.106	35	-0.396
10.5	506	2.022	540	1.197	34	0.825
11.0	506	1.494	541	1.104	35	0.390
11.5	506	2.947	463	0.360	43	2.587
12.0	499	2.819	541	0.349	42	2.470
12.5	498	3.349	547	1.176	49	2.173

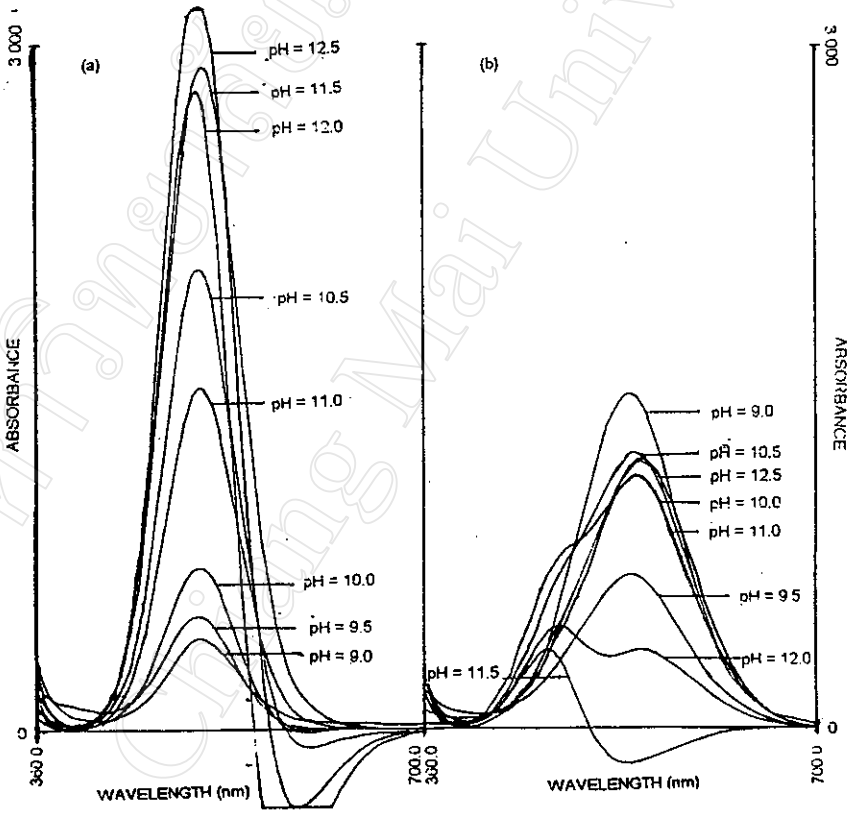

Figure 2.52 Effect of pH : (a) Ca(II)-murexide and (b) Mg(II)-murexide complexes.

Although, the pH values of 11.5-12.5 should be used for batch determination of calcium. It was re-studied for the proposed FIA method (using green LED) and the condition described in 2.6.1.6. The results are shown in Table 2.67, Figure 2.53 and Figure 2.54. It was found that pH = 9.0 (detection limit = 0.15 mol/l Ca^{2+}, described in Appendix J) to pH = 9.5 (detection limit = 0.21 mol/l Ca^{2+}) should be used as giving the lowest peak height of Mg(II)-murexide complex which interfered a peak height of Ca(II)-murexide complex and giving a good linear range of 10-120 mg Ca^{2+}/l.

Table 2.67 Calibration curves : (a) Ca(II)-murexide and (b) Mg(II)-murexide complexes of various pHs ; mean of triplicate injections.

(a) Ca(II)-murexide complex

Ca^{2+} (mg/l)	Ca^{2+} ($x10^{-3}$ mol/l)	Peak height corrected for blank (mV)				
		Various pH				
		9.0	9.5	10.5	11.5	12.0
blank	-	31.0	23.8	22.6	9.9	7.9
10	0.25	14.7	15.9	15.9	11.9	7.9
20	0.50	30.6	35.7	31.0	23.8	23.8
30	0.75	43.7	55.6	50.0	37.7	39.7
40	1.00	62.3	71.4	72.6	57.5	54.4
60	1.50	94.1	113.1	124.2	100.4	96.4
80	2.00	132.9	164.7	200.4	177.8	196.4
100	2.50	170.2	213.1	265.9	269.8	259.1
120	3.00	196.4	256.0	344.4	390.9	392.1

(b) Mg(II)-murexide complex

Mg^{2+} (mg/l)	Mg^{2+} ($x10^{-3}$ mol/l)	Peak height corrected for blank (mV)				
		Various pH				
		9.0	9.5	10.5	11.5	12.0
blank	-	31.0	23.8	22.6	9.9	7.9
10	0.41	9.5	6.0	12.3	15.1	15.9
20	0.82	15.5	9.9	21.8	32.9	31.8
30	1.23	14.7	13.9	32.9	50.4	50.8
40	1.65	18.7	25.8	44.8	78.6	72.2
60	2.47	23.4	37.7	75.8	140.1	124.2
80	3.29	32.1	50.8	109.1	232.9	165.9
100	4.11	38.5	63.5	144.8	352.0	192.5
120	4.94	42.5	75.4	188.9	490.1	207.5

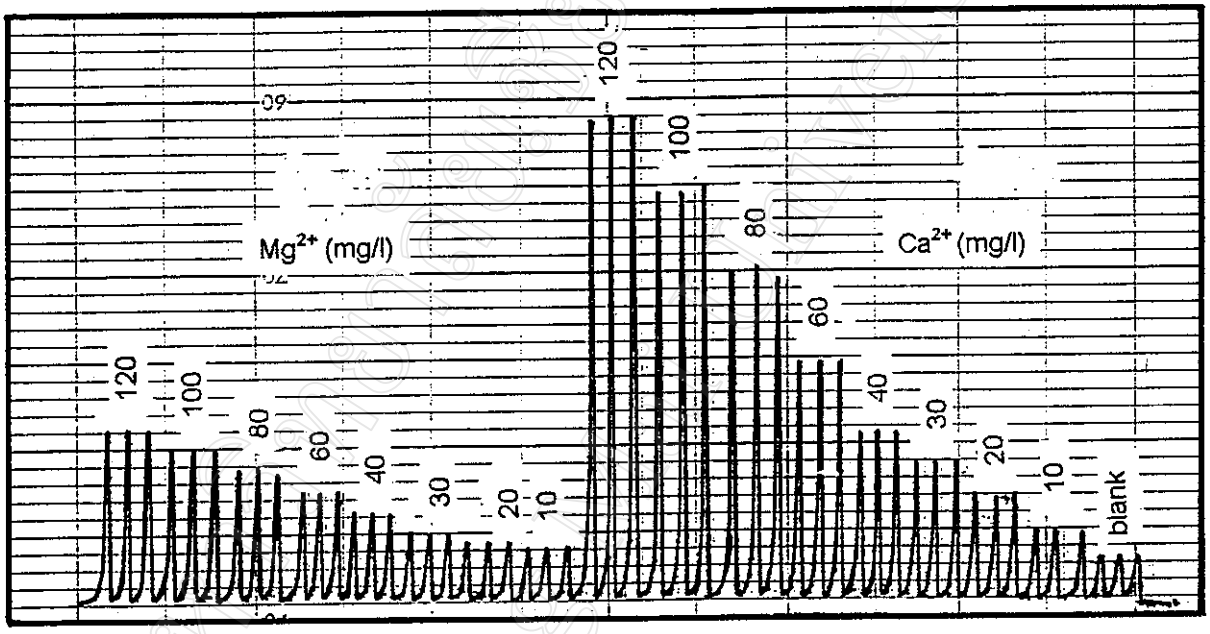

Figure 2.53 FIA signals of Ca(II)- and Mg(II)-murexide complexes using of buffer pH being 9.5.

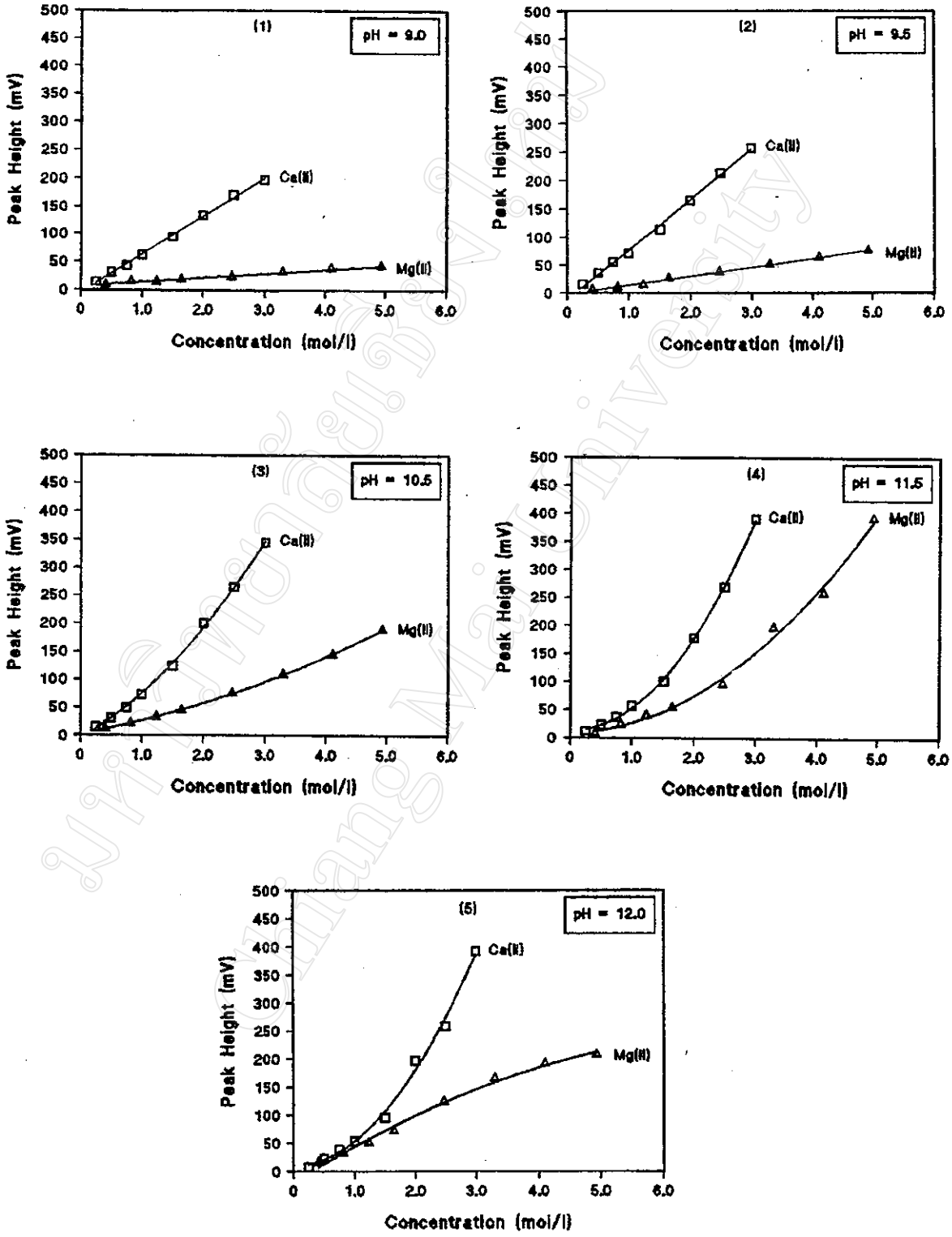

Figure 2.54 Calibration curves for Ca(II)-murexide and Mg(II)-murexide complex in different pH values; (1) pH = 9.0, (2) pH = 9.5, (3) pH = 10.5, (4) pH = 11.5 and (5) pH = 12.0.

2.6.2 Determination of Calcium by Using Calmagite

2.6.2.1 Absorption Spectra

Spectra of Ca-Calmagite, Mg-Calmagite solutions (each solution containing 40 mg/l of each metal and calmagite (2×10^{-5} %(w/v) in borate buffer, pH=10)) and the calmagite solution alone were recorded (Figure 2.55(a)). A Spectum of the reagent soluton in boric/borate buffer (pH=10) containing Calmagite (0.001 % (w/v)), $MgCl_2$ (2×10^{-5} %(w/v)) and an amount of EDTA which just turned the red to blue gave a maximum at 615 nm (Figure (2.55(b(1)). This spectrum should be due to the Calmagite absorption. When the solution was added with calcium (40 mg/l), a maximum wavelength at 540 nm was observed (Figure 2.55(b(2)). This would be due to the Mg-Calmagite complex absorption. The spectrum of the Mg-complex when using the reagent as a reference yielded a maximum at 535 nm (Figure 2.55(b(3)).

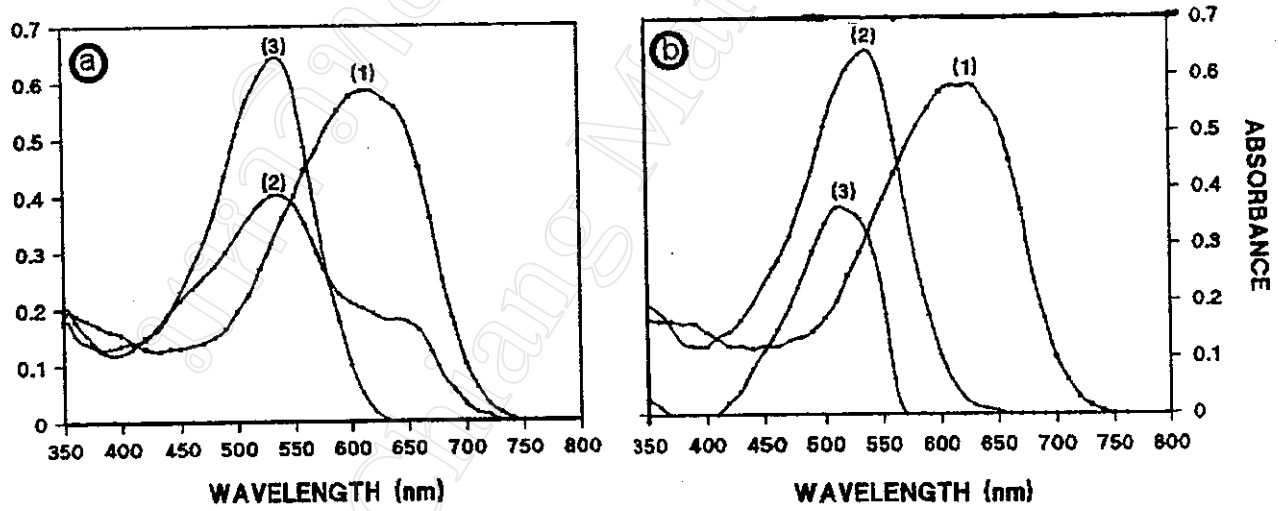

Figure 2.55 Absorption spectra : (a) vs H2O ; (1) Calmagite (pH=10) (2) Ca-Calmagite (3) Mg-Calmagite complexes; (b) : (1) the reagent in boric/borate buffer (pH=10) (Calmagite (0.001 % (w/v)), $MgCl_2$ (2×10^{-5} %(w/v)) and an amount of EDTA which just turned the red to blue), (2) Ca (40 mg/l) in the reagent, both using water as a reference and (3) the Ca solution versus the reagent as reference).

2.6.2.2 Manifold

The flow diagram of the system is shown in Figure 2.56.

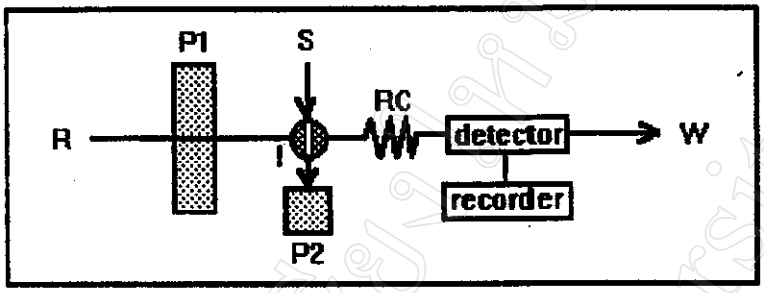

Figure 2.56 Flow diagram of the system ; R : reagent (calmagite + $MgCl_2$ + EDTA + borate buffer), S : sample, P1 : peristaltic pump, P2 : aquarium pump, I : rotary injection valve, RC : reaction coil and W : waste.

The sample was injected into a reagent stream of a mixture of calmagite, $MgCl_2$, EDTA and borate buffer (pH = 10). The red color due to the formation of Ca(II)-Mg(II)-calmagite complexes is continuously monitored at 540 nm an recorded with a chart recorder. The chemical reaction are involved :

$$\underset{\text{(reagent)}}{Mg^{*}[EDTA]} + \underset{\text{(reagent)}}{Mg^{*}[calmagite]} + \underset{\text{(reagent; excess)}}{calmagite} + \underset{\text{(sample)}}{Ca^{2+}} \longrightarrow Ca[EDTA] + Mg^{*}[calmagite] + \underset{\text{(excess)}}{calmagite} \quad (2.9)$$

$$\underset{\text{(reagent)}}{Mg^{*}[calmagite]} + \underset{\text{(sample)}}{Mg^{2+}} + \underset{\text{(excess)}}{calmagite} \longrightarrow \text{total } Mg[calmagite] \quad (2.10)$$

Preliminary conditions were set as following [56] :

concentration of EDTA	0.036% (w/v)
concentration of calmagite	0.003 % (w/v)
concentration of $MgCl_2$	0.04 % (w/v)
borate buffer (pH = 10)	0.62 % (w/v) H_3BO_3 + 0.36 % (w/v) NaOH
flow rate	3.3 ml/min
sample volume	100 µl (teflon tube)
RC length	50 cm
LED color of colorimeter	green
sensitivity of recorder	1000 mV
chart speed of recorder	0.5 cm/min

2.6.2.3 Effect of the Amount of EDTA

Using the manifold shown in Figure 2.56 and the conditions in 2.6.2.2, variuos amounts of EDTA were tried. The results are shown in Table 2.68 and Figure 2.57. 0.72 mg of EDTA was chosen. The amount was equivalent to 2 ml of EDTA (0.036%(w/v)) which turned the mixture from red to blue.

Table 2.68 Effect of the amount of EDTA on peak height ; mean of triplicate injections.

amounts of EDTA added (mg)	Ca as $CaCO_3$ (mg/l)	Peak height (mV)	Peak height corrected for blank (mV)
0.72	blank	94.5	-
	100	185.0	90.5
	300	222.4	127.9
1.44	blank	124.0	-
	100	126.0	2.0
	300	169.3	45.3
2.16	blank	102.4	-
	100	102.4	0
	300	106.3	3.9
2.88	blank	102.4	-
	100	102.4	0
	300	118.1	15.7

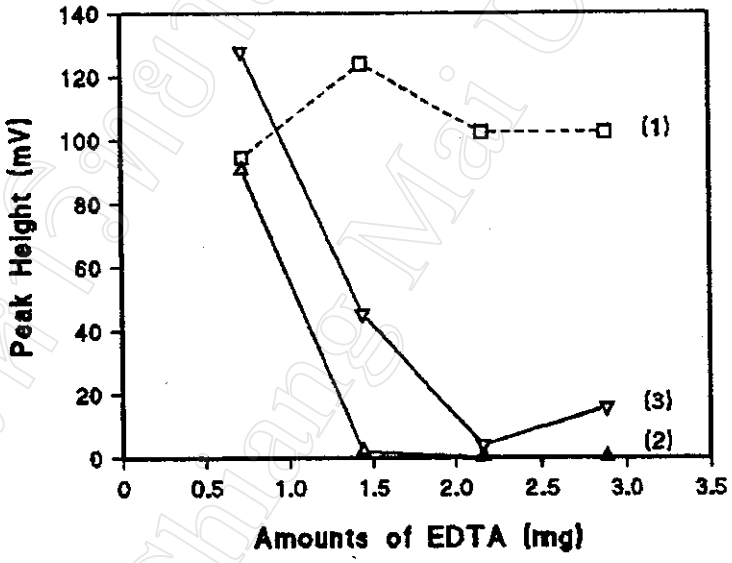

Figure 2.57 Effect of amounts of EDTA on peak height for ; (1) blank, (2) 100 and (3) 300 mg/l as $CaCO_3$ (blank subtraction).

2.6.2.4 Effect of Calmagite Concentration

Using the conditions described in 2.6.2.3, various concentrations of calmagite were used. The results are shown in Table 2.69 and Figure 2.58. The results indicate that 0.018 % (w/v) calmagite should be used as giving good linear ranges in 25-150 mg/l as $CaCO_3$ and 150-450 mg/l as $CaCO_3$ and it yields acceptable peak height.

Table 2.69 Effect of calmagite concentration on peak height ; mean of triplicate injections.

as $CaCO_3$ (mg/l)	Peak height corrected for blank (mV)					
	Calmagite (% w/v)					
	0.003	0.006	0.009	0.012	0.015	0.018
blank	94.5	169.3	118.1	57.1	17.7	7.9
25	7.9	0	27.6	2.0	2.0	0
50	47.2	74.8	90.6	15.8	7.9	2.0
100	114.2	189.0	244.1	78.7	41.3	11.8
150	141.7	293.3	362.2	181.1	90.6	39.4
200	155.5	346.5	437.0	181.5	157.5	82.7
250	165.4	374.0	488.2	358.3	209.1	124.0
300	169.3	393.7	535.4	424.4	295.3	167.3
350	181.1	405.5	567.0	494.1	340.6	226.4
400	183.1	421.3	586.6	537.4	391.7	248.0
450	185.0	433.1	606.3	574.8	421.3	295.3

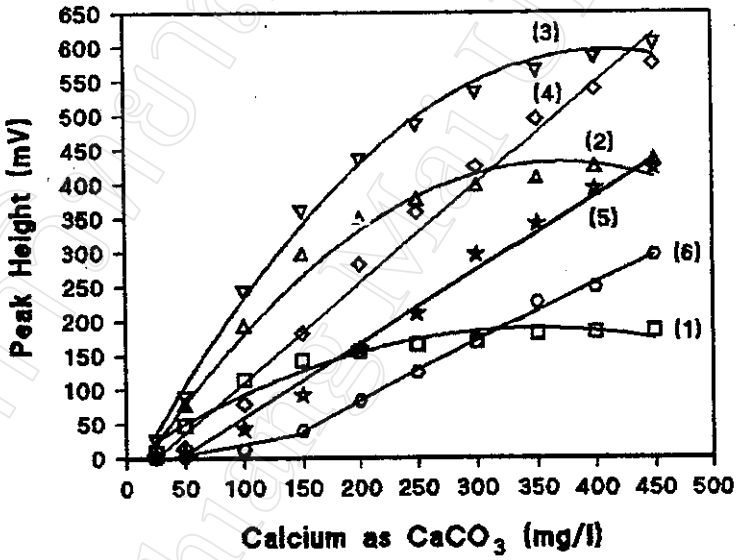

Figure 2.58 Effect of calmagite concentration on peak height ; Calmagite concentrations : (1) 0.003, (2) 0.006, (3) 0.009, (4) 0.012, (5) 0.015 and (6) 0.018 % (w/v).

2.6.2.5 Effect of $MgCl_2$ Concentration

Using the conditions described in 2.6.2.4, a blank, 100 and 400 mg/l of standard as $CaCO_3$ solutions were injected. The results are shown in Table 2.70 and Figure 2.59. The results indicate that 0.04 % (w/v) $MgCl_2$ was chosen as giving the highest peak height.

Table 2.70 Effect of $MgCl_2$ concentration on peak height ; mean of triplicate injections.

$MgCl_2$ (% w/v)	as $CaCO_3$ (mg/l)	Peak height (mV)	Peak height corrected for blank (mV)
0.02	blank	1.0	-
	100	1.0	0
	400	96.7	95.7
0.04	blank	9.8	-
	100	22.8	13.0
	400	226.4	216.6
0.06	blank	9.8	-
	100	29.5	19.7
	400	215.8	206.0
0.08	blank	9.8	-
	100	17.7	7.9
	400	175.2	165.4

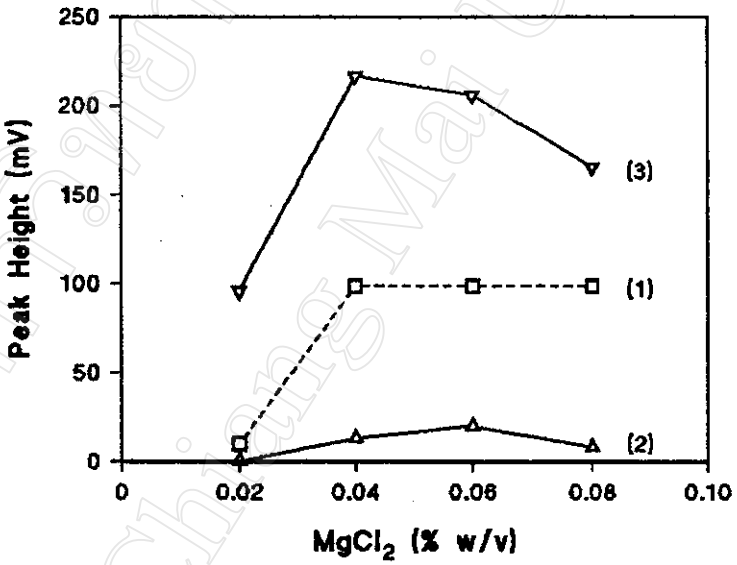

Figure 2.59 Effect of $MgCl_2$ concentration on peak height ; $MgCl_2$ concentrations : (1) blank (×10), (2) 100 and (3) 400 mg/l as $CaCO_3$.

2.6.2.6 Effect of Sample Volume

The effect of various sample volume was studied, using the conditions described in 2.6.2.5. The results are shown in Table 2.71 and Figure 2.60. It was found that 100 µl of sample volume should be used as giving good linear ranges in 25-100 mg/l as $CaCO_3$ and 100-400 mg/l as $CaCO_3$ and it yields acceptable peak height.

Table 2.71 Effect of sample volume on peak height ; mean of triplicate injections.

as $CaCO_3$ (mg/l)	Peak height corrected for blank (mV)		
	Sample volume (µl)		
	100	200	300
blank	9.84	21.7	27.6
25	3.94	7.9	15.8
50	13.8	29.5	59.1
100	31.5	104.3	192.9
150	65.0	179.1	303.2
200	104.3	253.9	385.8
250	145.7	322.8	442.9
300	190.9	376.0	488.2
350	234.3	401.6	521.7
400	285.4	433.1	549.2
450	326.8	482.3	574.8

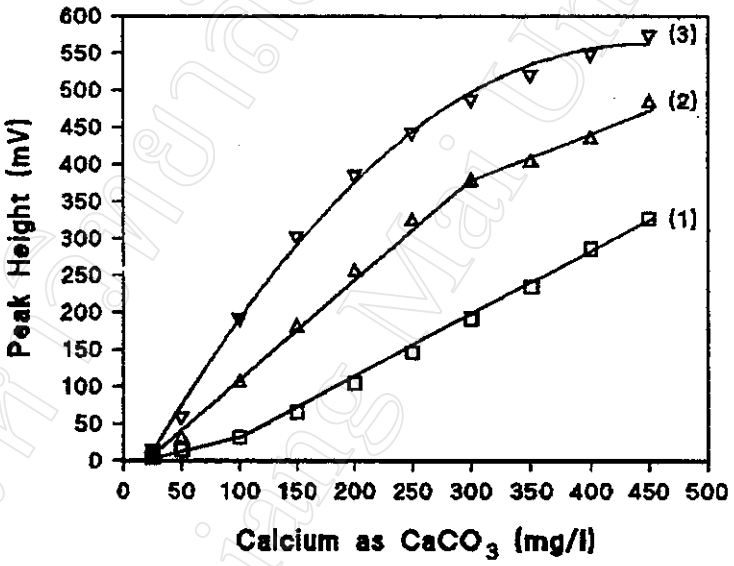

Figure 2.60 Effect of sample volume on peak height ; Sample volumes : (1) 100, (2) 200 and (3) 300 µl.

2.6.2.7 Effect of the RC Length

The effect of the RC length was studied. Using the conditions described in 2.6.2.6. The results are shown in Table 2.72 and Figure 2.61. The results indicate that 50 cm of RC length was chosen as it yields acceptable peak height and giving good linear ranges in 25-100 mg/l as $CaCO_3$ and 100-450 mg/l as $CaCO_3$.

Table 2.72 Effect of the RC length on peak height ; mean of triplicate injections.

as $CaCO_3$ (mg/l)	Peak height corrected for blank (mV)		
	RC length (cm)		
	20	50	100
blank	13.8	9.8	7.9
25	11.8	3.9	2.0
50	25.6	13.8	17.7
100	70.9	31.5	17.7
150	116.1	65.0	35.4
200	151.6	104.3	55.1
250	185.0	145.7	106.3
300	210.6	190.9	153.5
350	242.1	234.3	196.9
400	267.7	285.4	240.2
450	283.5	326.8	287.4

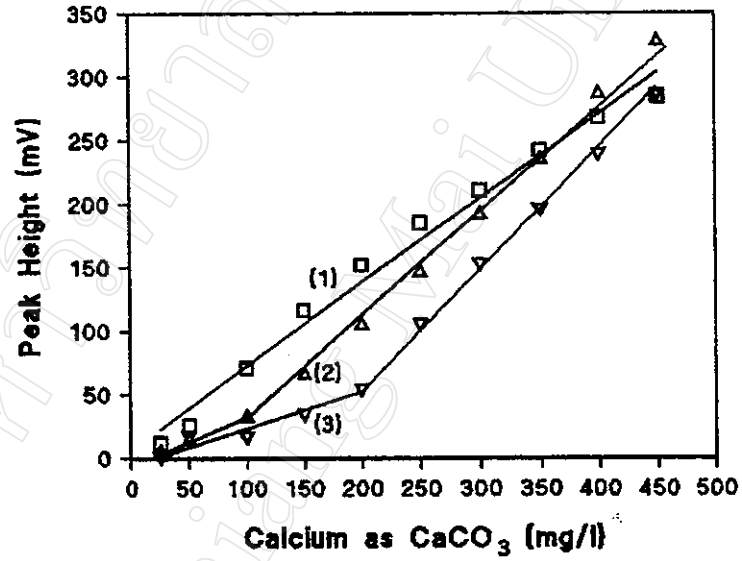

Figure 2.61 Effect of the RC length on peak height ; The RC lengths : (1) 20, (2) 50 and (3) 100 cm.

2.6.2.8 Effect of Flow Rate

The effect of flow rate was studied, using the conditions described in 2.6.2.7. The results are in Table 2.73 and Figure 2.62. The results indicate that flow rate of 3.3 ml/min should be used as it yields acceptable peak height and giving linear ranges , 25-100 mg/l as $CaCO_3$ and 100- 450 mg/l as $CaCO_3$.

Table 2.73 Effect of flow rate on peak height ; mean of triplicate injections.

as $CaCO_3$ (mg/l)	Peak height corrected for blank (mV)		
	Flow rate (ml/min)		
	1.2	3.3	7.0
blank	15.8	9.8	3.9
25	2.0	3.9	2.0
50	11.8	7.9	7.9
100	49.2	33.5	23.6
150	94.5	70.9	45.3
200	143.7	114.2	70.9
250	200.8	145.7	90.6
300	228.4	181.1	112.2
350	259.8	226.4	129.9
400	299.2	257.9	143.7
450	307.1	295.3	169.3

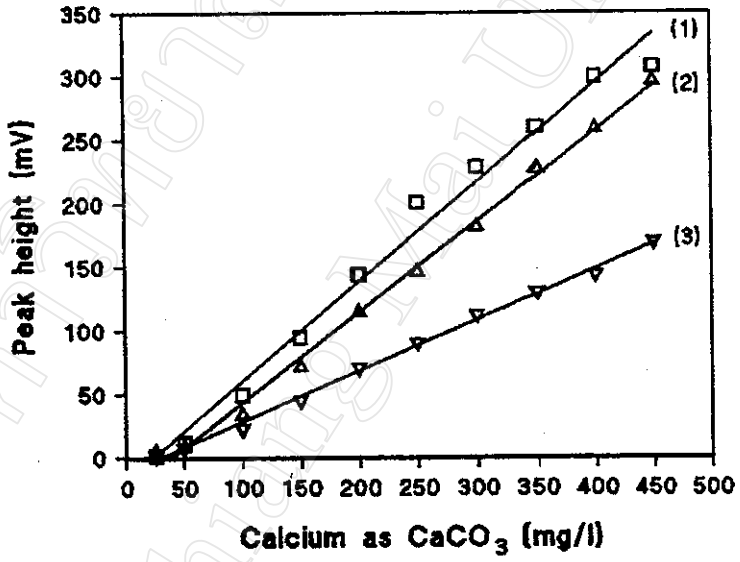

Figure 2.62 Effect of flow rate on peak height ; Flow rates : (1) 1.2, (2) 3.3 and (3) 7.0 ml/min.

2.6.2.9 Summary of the Conditions Used

The recommended FIA manifold is depicted in Figure 2.56 and the optimum conditions are summarized in Table 2.74.

Table 2.74 Conditions used for the determination of calcium by using calmagite

EDTA	0.036 % (w/v) + 2 ml (0.72 mg)
concentration of calmagite	0.018 % (w/v)
concentration of $MgCl_2$	0.04 % (w/v)
borate buffer (pH = 10)	0.62 % (w/v) H_3BO_3 + 0.36 % (w/v) NaOH
flow rate	3.3 ml/min
sample volume	100 µl (teflon tube)
RC length	50 cm
LED color of colorimeter detector	green
sensitivity of recorder	1000 mV
chart speed of recorder	0.5 cm/min

2.6.2.10 Calibration Curve and Detection Limit

Using the optimum FIA system described in 2.6.2.9. The calibration curve and detection limit of the condition used were studied. The results are shown in Table 2.75, Figure 2.63 and Figure 2.64. Linearity was obtained in the ranges of 25-100 mg/l as $CaCO_3$ ($y = 0.247(x)-5.85$, $r^2 = 0.948$) and 100-450 mg/l as $CaCO_3$ ($y = 0.840(x)-67.14$, $r^2 = 0.998$).

Table 2.75 The calibration curve for Ca; mean of triplicate injections.

as $CaCO_3$ (mg/l)	Peak height (mV)	Peak height corrected for blank (mV)
blank	11.8	-
25	13.8	2.0
50	15.8	4.0
100	31.5	19.7
150	70.9	59.1
200	108.3	96.5
250	148.8	137.0
300	202.0	190.2
350	242.1	230.3
400	283.5	271.7
450	318.9	307.1

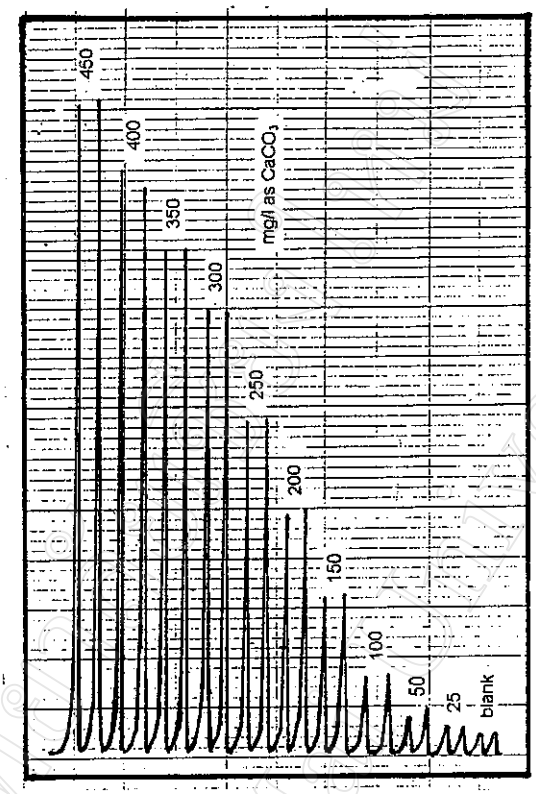

Figure 2.63 FIA signals of Ca standards.

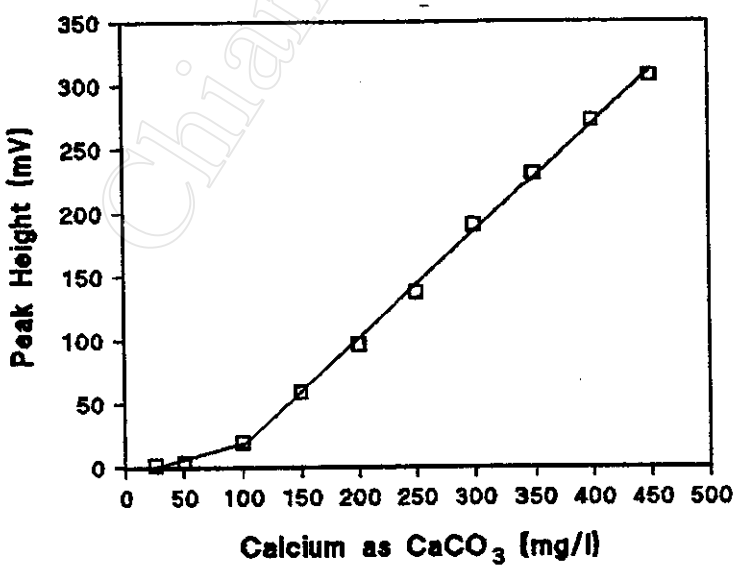

Figure 2.64 Calibration curve for Ca.

2.6.2.11 Precision

Using the optimum FIA system described in 2.6.2.9, the precision of the conditions used was determined by 12 replicate injections of 250 mg/l as $CaCO_3$. The results are shown Table 2.76. The relative standard deviation (RSD) was found to be 2.

Table 2.76 Precision study of 250 mg/l as $CaCO_3$; n = 12.

Peak height corrected for blank * (mV)				Mean (X)	SD	% RSD
148.6	144.7	146.7	144.7	144.0	2.9	2.0
143.7	138.8	143.7	139.8			
140.8	144.7	145.7	145.7			

* A blank : 12.8 mV.

2.6.2.12 Application of the Procedure for the Determination of Hardness Water Samples

The optimum FIA system was applied to the determination of hardness in water samples. The results obtained were compared to the ones obtained by the EDTA titrimetry [36] using calmagite indicator and the one obtained by the calculation method [36] (Table 2.77) and the correlation is shown in Figure 2.65.

Table 2.77 Application of the procedure for the determination of hardness of water samples.

Sample No.	Hardness found (mg/l)		
	FIA	Titration *	Calculation **
1	65	68	65
2	220	163	165
3	135	130	132
4	178	205	200
5	340	325	330
6	278	268	265

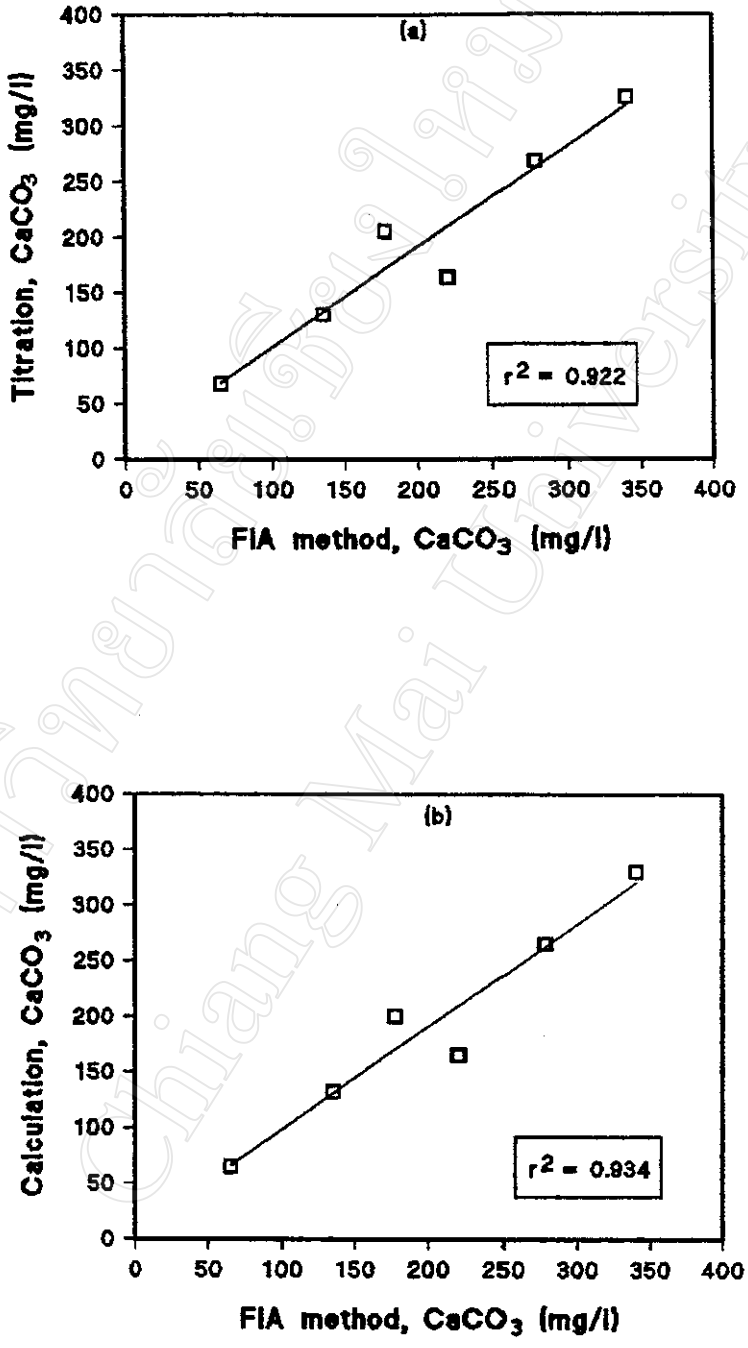

Figure 2.65 Correlation between the results obtained by the proposed method (FIA) and (a) the titrimetric method or (b) the calculation method.